

Washington University in St. Louis

Washington University Open Scholarship

All Theses and Dissertations (ETDs)

8-15-2012

The Pathophysiological Importance of Nicotinamide Phosphoribosyltransferase as a Key NAD Biosynthesis Enzyme in Metabolic Homeostasis

Myeong Jin Yoon

Washington University in St. Louis

Follow this and additional works at: <https://openscholarship.wustl.edu/etd>

Recommended Citation

Yoon, Myeong Jin, "The Pathophysiological Importance of Nicotinamide Phosphoribosyltransferase as a Key NAD Biosynthesis Enzyme in Metabolic Homeostasis" (2012). *All Theses and Dissertations (ETDs)*. 991.

<https://openscholarship.wustl.edu/etd/991>

This Dissertation is brought to you for free and open access by Washington University Open Scholarship. It has been accepted for inclusion in All Theses and Dissertations (ETDs) by an authorized administrator of Washington University Open Scholarship. For more information, please contact digital@wumail.wustl.edu.

WASHINGTON UNIVERSITY IN ST. LOUIS

Division of Biology and Biomedical Sciences

Molecular Genetics and Genomics

Dissertation Examination Committee:

Shin-ichiro Imai, Chair

Nada Abumrad

Thomas Baranski

Jeffrey Milbrandt

Kelle Moley

Jean Schaffer

The Pathophysiological Importance of Nicotinamide Phosphoribosyltransferase
as a Key NAD Biosynthesis Enzyme in Metabolic Homeostasis

by

Myeong Jin Yoon

A dissertation presented to the
Graduate School of Arts and Sciences
of Washington University in
partial fulfillment of the
requirements for the degree
of Doctor of Philosophy

August 2012

Saint Louis, Missouri

ACKNOWLEDGEMENTS

I am indebted to many individuals who have made my thesis possible. Foremost, I would like to express my sincere gratitude to my advisor Dr. Shin-ichiro Imai for the continuous support of my PhD study and research. I am very fortunate that I had an opportunity to work with him. He has been continually supportive and encouraged me with tireless devotion for science and enthusiastic efforts to discuss and plan my projects. He is the most passionate scientist I have ever seen. His passion which has become deeply rooted in me, has been inspiring and will also inspire me to continue to create new knowledge.

I would also like to show myriad thanks to my committee members. They have been a source of constructive criticism, invaluable suggestions, and constant encouragement. Especially, I would like to express special thanks to Dr. Thomas Baranski, my committee chair, for giving me invaluable advice on my general life as well as on my project. Without all their guidance and persistent help this thesis would not have been possible.

I also would like to express the deepest appreciation to my lab members, Akiko Satoh, Kathy Mills, Cindy Brace, Jun Yoshino, Sean Johnson, Liana Stein, Mitsu Yoshida, and semi-Imai lab member Fiorella Ghisays. All Imai lab members have always been more than good friends for me. They are already part of my family. Under a stimulating and fun environment that they have been providing, I have successfully overcome many difficulties and made this thesis work an unforgettable experience for me.

Lastly, I would like to pay high regards to my father and mother, sister Seung-A and her family for their endless love and sincere encouragement throughout my research

work and lifting me up during this phase of life. I owe everything to them. I doubt that I will ever be able to convey my appreciation fully to my fiancé, Yong-Jae. He has always been beside me, sharing all my happy and hard moments during my thesis research. This long journey in obtaining my PhD would not have been completed without his selfless and heartfelt support. I am truly looking forward to having my next journey with him.

TABLE OF CONTENTS

Acknowledgements	ii
Table of Contents	iv
List of Figures and Tables	vi
Chapter 1. NAMPT-mediated NAD⁺ biosynthesis and its physiological functions	1
Adipose tissue; the new central metabolic system	2
History of Nampt; from cytokine to enzyme	3
Multiple functions of NAD ⁺	8
NAD ⁺ -dependent Sirtuins; the link from NAD ⁺ to metabolic syndrome	10
Goals of this study	15
Figure Legends	17
Figures	18
References	21
Chapter 2. Nicotinamide mononucleotide, a key NAD⁺ precursor, treats the pathophysiology of diet- and age-induced diabetes	31
Abstract	32
Introduction	33
Results	35
Discussion	42
Experimental Procedures	44
Figure Legends	47
Figures	51
References	55
Supplemental Figures and legends	60
Supplemental Experimental Procedures	67
Supplemental References	72
Chapter 3. eNAMPT secretion from adipose tissue is regulated by SIRT1 through its deacetylation	74
Abstract	75
Introduction	77
Results	79
Discussion	84
Experimental Procedures	88
Figure Legends	93
Figures	97
References	101
Supplemental Figures and Legends	104
Chapter 4. eNAMPT secreted from adipose tissue regulates glucose homeostasis in mice	107

Abstract	108
Introduction	109
Results	112
Discussion	118
Experimental Procedures	123
Figure Legends	126
Figures	129
References	132
Supplemental Figures and legends	135
Supplemental Experimental Procedures	143
Chapter 5. Summary, Discussion, and Future Direction	145
Summary	146
Do NAMPT and SIRT1 compose a new feed back loop?	147
How is eNAMPT secreted?	149
Is adipose tissue the only source of eNAMPT?	152
What is the function of eNAMPT, cytokine or NAD ⁺ -biosynthetic enzyme?	154
Do gender differences affect energy metabolism via NAMPT?	156
Final comments	158
References	160

LIST OF FIGURES AND TABLES

Chapter 1.

Figure 1	NAD ⁺ biosynthesis pathway from nicotinamide	18
Figure 2	NAD ⁺ as a substrate for ADP-ribose transfer, cADP-ribose synthesis and protein lysine deacetylation	19
Table 1	Sirtuins localization and function	20

Chapter 2.

Figure 1	NMN ameliorates defects in NAMPT-mediated NAD ⁺ biosynthesis in HFD-induced diabetic mice	51
Figure 2	NMN administration improves impaired glucose tolerance in HFD-induced diabetic mice	52
Figure 3	NMN ameliorates hepatic insulin resistance and restores gene expression related to oxidative stress, inflammatory response, and circadian rhythm	53
Figure 4	NMN improves glucose and lipid homeostasis in age-induced T2D	54
Figure S1	Defects in NAMPT-mediated NAD ⁺ biosynthesis in high-fat diet-induced diabetic mice	60
Figure S2	NAD ⁺ levels and glucose-stimulated insulin secretion in HFD-fed primary islets treated with NMN	62
Figure S3	Microarray analysis of liver samples from RC, HFD, and NMN-treated HFD mice	63
Figure S4	NAMPT protein levels and the effect of NMN on metabolism in aged mice	65

Chapter 3.

Figure 1	iNAMPT acetylation status in adipose tissue regulates eNAMPT secretion	97
Figure 2	eNAMPT secretion is increased during fasting in a SIRT1 dependent manner	98

Figure 3	SIRT1 regulates eNAMPT secretion by deacetylating iNAMPT	99
Figure 4	Lysine 53 acetylation status on iNAMPT is important in regulating eNAMPT secretion and enzymatic activity	100
Figure S1	SIRT1 is expressed in both the cytoplasm and nucleus of differentiated 3T3L1 cells	104
Figure S2	Acetylation on K53 and K79 of NAMPT are identified through MS/MS analysis	105

Chapter 4

Figure 1	ANKO mice have lower plasma eNAMPT and NAD ⁺ levels in the hypothalamus and adipose tissue	129
Figure 2	ANKO mice have impaired glucose metabolism and hyperinsulinemia	130
Figure 3	NMN administration improves hyperinsulinemia and glucose metabolism in 7-8 month-old female ANKO mice compared to wild type	131
Figure S1	Female ANKO mice have normal adipose tissue morphology and gene expression profiles in the hypothalamus	135
Figure S2	Male ANKO mice have normal glucose metabolism and insulin secretion compared to wild type	137
Figure S3	Female ANKO mice exhibit increased macrophage infiltration polarized to M1 in adipose tissue compared to wild type	139
Figure S4	NMN administration to ANKO mice does not fully restore NAD levels in adipose tissue to that of WT and does not significantly alter adipose tissue macrophages	141

Chapter 1

NAMPT-mediated NAD biosynthesis and its physiological functions

Adipose tissue; the new central metabolic system

Until the identification of Leptin in 1994 ¹, adipose tissue had been considered as the organ that reserves excessive energy as fat. However, it is now well recognized that adipose tissue plays a dynamic role in metabolic regulation as a new central metabolic system. First, adipose tissue is able to sense metabolic states through its ability to perceive a large number of neuronal and hormonal signals. For example, both sympathetic and parasympathetic neurons from the central nervous system (CNS) innervate adipose tissue and regulate the activity of enzymes. Both control hormone-sensitive lipase activity in adipocytes, and this lipase activity in turn regulates glucose and lipid uptake into adipocytes in opposing ways ^{2,3}. Secondly, adipose tissue is also able to secrete various endocrine and paracrine hormones, commonly referred to as adipokines. The endocrine functions of adipokines allow the adipocytes to regulate cellular processes in peripheral tissues such as liver and pancreas, and in CNS such as the hypothalamus ⁴. Leptin, the first adipokine identified by Jeffrey M. Friedman and his colleagues, acts on receptors in the hypothalamus of the brain ¹, where it controls body weight homeostasis. This process is mediated by decreasing hunger and food consumption at least in part by inhibition of neuropeptide Y (NPY) synthesis, a very potent stimulator of feeding behavior, and by increasing energy expenditure through activation of sympathetic neurons ⁵. The paracrine effects of adipokines have an impact on neighboring adipocytes, as well as other local cell types within adipose tissue, such as immune cells. Proinflammatory cytokine tumor necrosis factor- α (TNF- α), known to be produced chiefly by activated macrophages, is secreted by enlarged adipose tissues in excess nutrient conditions, and neutralization of TNF- α showed improved insulin

sensitivity by diet-induced obesity⁶. By activating Inhibitor of κ B kinase- β (IKK) and Jun N-terminal kinases (JNKs) which inhibit the insulin signaling pathway, TNF- α increases lipolysis and decreases glucose uptake in adipose tissues⁷⁻¹⁰. TNF- α also has been recognized as a powerful driving force to activate adipose tissue macrophages (ATMs), leading to the secretion of a variety of proinflammatory cytokines from ATMs such as TNF- α itself, and setting up a feed-forward inflammatory process¹¹⁻¹³. Communicating with other tissues as aforementioned, adipose tissue affects nutrient intake, metabolism, and energy expenditure, and finally plays an important role in pathophysiology of several diseases including obesity, diabetes, cancers, and inflammatory disorders.

In this thesis, I will introduce one more communication method of adipose tissue, Nicotinamide phosphoribosyltransferase (Nampt). Nampt catalyzes the condensation of nicotinamide with 5-phosphoribosyl-1-pyrophosphate (PRPP) to yield nicotinamide mononucleotide (NMN), the rate-limiting step in nicotinamide adenine nucleotide (NAD) biosynthesis in mammals¹⁴. It is of special interest that Nampt is also secreted by adipose tissue and circulates through the body in the blood stream¹⁵. Even though at least three different functions have been assigned to extracellular Nampt (eNampt) including a cytokine-like, an insulin-mimetic, and an enzyme function that catalyzes the production of NMN, the physiological role of eNampt has been a matter of much debate. There is also little work that demonstrates how eNampt is secreted from adipocytes, and what distinguishes intracellular Nampt (iNampt) and eNampt at the molecular level. Here, in this chapter, I will briefly recapitulate the research story of Nampt and summarize its unique function in different biological contexts. In the following chapters,

I will discuss the importance of iNAMPT in metabolically active tissues on the onset of age- or diet-induced type 2 diabetes, and also explain a sophisticated mechanism of eNAMPT secretion from adipose tissue and its physiological significance on regulation of glucose metabolism.

History of Nampt; from cytokine to enzyme

Nampt was originally cloned from a human peripheral blood lymphocyte cDNA library as a presumptive cytokine shown to enhance the maturation of B cell precursors in the presence of Interleukin-7 (IL-7) and stem cell factor (SCF), therefore named as pre B cell colony-enhancing factor (PBEF)¹⁶. Seven years later, when the gene encoding the bacterial Nampt (*nadV*) was first isolated in the prokaryote *Hemophilus ducreyi*, it was found to display significant homology to the mammalian PBEF genes¹⁷. In addition, through genetic approaches, Rongvaux *et al.* also demonstrated that the mouse PBEF gave Nampt enzymatic activity and NAD-independent growth to bacteria lacking *nadV*, suggesting that PBEF had NAD biosynthesis enzymatic activity at least within the cells¹⁸. Nampt protein is expressed ubiquitously almost in all tissues, however several tissues such as pancreas and brain have relatively lower expression levels of Nampt compared to other tissues^{15,19}. It is also highly conserved, with orthologs in bacteria, invertebrate sponges, *Drosophila*, amphibians (*Xenopus*), fish, bird (chicken), and mammals^{14,17,20-22}.

Interestingly, since the report of PBEF, several papers have suggested a cytokine-like function for eNampt. First of all, when Samal and colleagues first identified PBEF, they reported that although PBEF lacks a characteristic signal peptide necessary for extracellular secretion of mature protein, the 3' untranslated region (UTR) contains

multiple TATT motifs, a characteristic of cytokines, and that it is present in conditioned medium from activated lymphocytes and COS cells ¹⁶. In line with this study, eNampt has been reported to have an important role in pro-inflammatory and immunomodulatory responses as a cytokine. *Nampt* belongs to a group of genes defined by an immune “activating signature” being widely expressed within the immune system and increased in virtually all activated immune cells including T cells, B cells, monocytes, macrophages, dendritic cells, and neutrophils ²³. eNampt was found to increase under inflammatory conditions, and recombinant forms of Nampt have been shown to exert an anti-apoptotic role on activated neutrophils. Jia *et al.* have found that eNampt/PBEF expression is upregulated by inflammatory stimuli such as lipopolysaccharide (LPS), IL-1 β , and TNF- α in neutrophils and monocytes *in vitro*, and in neutrophils harvested from critically ill patients with sepsis, a complex clinical syndrome that results from an activated systemic host inflammatory response to infection ²⁴. They have also demonstrated that eNampt inhibits neutrophil apoptosis in response to a variety of inflammatory stimuli, but this effect seems to be partially dependent on iNampt. Similarly, Li *et al.* have also demonstrated that eNampt potently blocks macrophage apoptosis induced by a number of ER stressors, a process associated with obesity and obesity-associated diseases, through IL-6/Stat3 cell-survival pathway ²⁵. Interestingly, the ability of eNampt to trigger this anti-apoptotic effect was independent of its enzymatic activity, implying a non-enzymatic mechanism presumably through an undefined eNampt receptor.

It has been also suggested that eNampt has insulin-like activity. Fukuhara *at al.* demonstrated that eNampt can directly bind to insulin receptor and activate downstream signaling cascades, resulting in similar biological effects *in vitro* and *in vivo* on

adipogenesis, cellular glucose uptake and blood glucose levels ²⁶. They also found that Nampt is enriched in the visceral fat of both humans and mice and that its plasma levels increase during the development of obesity. Therefore, they re-identified Nampt as a “new visceral fat-derived hormone” named visfatin. Although their results immediately drew significant attention in the field metabolism and diabetes research, subsequent studies have produced conflicting results regarding the physiological significance of visfatin function, and the original visfatin paper has been retracted because of concerns on the reproducibility of the results ²⁷.

Our lab has clearly reconstituted a mammalian NAD biosynthesis pathway from nicotinamide using recombinant Nampt and nicotinamide/nicotinic acid mononucleotide adenylyltransferase (Nmnat), another important enzyme in mammalian NAD biosynthesis which converts NMN to NAD, and analyzed enzymological features of this NAD biosynthetic pathway within the cells ¹⁴. By using biochemical analysis, we have demonstrated that the catalytic efficiency of NAMPT is almost 50 times lower than NMNAT even though NAMPT has very high affinity for its substrate. Consistently, overexpression of Nampt significantly increased total cellular NAD in mouse fibroblasts while increased doses of Nmnat were unable to increase NAD, suggesting that Nampt is the rate-limiting enzyme in mammalian NAD biosynthesis in the cells. The enzymological features and the crystal structures of NAMPT have also been studied extensively. Wang et al., and Kim et al., have recently resolved the crystal structure of mouse and rat NAMPT ^{28,29}. Both groups reported that functional NAMPT forms a homodimer composed of two identical subunits, both of which contribute to the active site that catalyzes the conversion of nicotinamide and phosphoribosyl-pyrophosphate to

form NMN. Although NAMPT has no substantial sequence identity to other phosphoribosyltransferase enzymes, comparison of the sequence of the rat NAMPT dimer active site with that of 13 different organisms revealed the high degree of conservation of the sequence of amino acid residues responsible for the nicotinamide (substrate) and NMN (product)-binding abilities²⁸. Most recently, we have demonstrated that NAMPT functions as an NAD biosynthetic enzyme extracellularly as well as intracellularly¹⁵. Female *Nampt*^{+/-} mice, but not male, showed moderately impaired glucose tolerance and a significant defect in glucose stimulated insulin secretion (GSIS). Interestingly, whereas tissue iNAMPT and NAD levels were reduced both in *Nampt*^{+/-} male and female mice, plasma eNAMPT and NMN, the product of the *Nampt* reaction, were reduced only in female *Nampt*^{+/-} mice, and indeed insulin secretion defects in female *Nampt*^{+/-} mice were corrected by NMN administration. These data imply that systemic NAD biosynthesis, mediated by eNAMPT, has a crucial role in controlling β cell function in pancreatic islets for the regulation of glucose homeostasis. In addition, most recently, we have observed that *Nampt*-mediated NAD biosynthesis is compromised in metabolic organs of high fat diet-induced and age-induced diabetic mice, and NMN administration improved glucose metabolism and insulin sensitivity of these mice, supporting the idea that increasing systemic NAD biosynthesis could be an effective intervention against diet- and age-induced type 2 diabetes³⁰. In these studies, we proposed that all of these effects of NMN administration on improving diet- and age-induced type 2 diabetes are mediated, at least partially, through the activity of the NAD-dependent protein deacetylase, Sirt1.

Multiple functions of NAD

NAD is one of the oldest molecules in the history of biochemistry. A century ago, pellagra, which is characterized by a darkly pigmented skin rash and the three D's of dermatitis, diarrhea, and dementia, was common among the rural poor in the southern United States. However, in 1914, Joseph Goldberger hypothesized that pellagra might be caused by a poor nutrition and discovered that substitution of corn-based diet to milk, eggs, and meat cured and prevented this disease ³¹. In 1937, Conrad Elvehjem finally identified Niasin, also known as vitamin B₃, containing nicotinamide and nicotinic acid, as the key molecule to cure pellagra ³². After a year, he also provided the evidence that this vitamin was used for synthesizing NAD ³².

NAD has been primarily known as a coenzyme that is involved in redox reactions, carrying electrons from one reaction to another. Once NAD accepts electrons from other molecules, it becomes reduced as NADH, which can be used as reducing agent to donate electron ³³. Recycling back and forth between the oxidized form (NAD) and reduced form (NADH), cells rely on NAD to maintain basic cellular reactions such as glucose and fatty acid metabolism, respiration, and photosynthesis ^{34 35}.

In addition to a coenzyme, NAD also acts as a substrate for three other classes of enzymes, ADP-ribose transferases (ARTs) or poly(ADP-ribose) polymerases (PARPs), cADP-ribose synthases, and Sirtuins (type III protein lysine deacetylases) ³³. ARTs and the more numerous, PARPs transfer the ADP-ribose group from NAD onto acceptors such as arginine, glutamic acid, or aspartic acid to create an ADP-ribosyl protein modification and/or to form the ADP-ribose polymer, referred as mono-ADP-ribosylation and poly-ADP-ribosylation, respectively ^{36,37}. Although mono-ADP-ribosylation has

been observed in many prokaryotic and eukaryotic species and in viruses, the biological functions of this reaction have been more closely characterized from bacterial toxins since mono-ADP-ribosylation is responsible for the actions of several bacterial toxins such as cholera, diphtheria, pertussis, and clostridial toxins. These toxin proteins are ARTs which modify crucial host cell target proteins like the α -subunit of heterotrimeric GTP binding proteins, the small GTPase Rho, monomeric actin and eukaryotic elongation factor 2(eEF2), resulting in permanent activation or inactivation of cell functions modulated by these protein substrates ³⁷. The mono-ADP-ribosylation reactions induced by these bacterial toxins are an important part of the pathogenic mechanisms that cause cholera, botulism and other diseases. In vertebrates, mono-ADP-ribosylation also can be applied to their own endogenous target proteins such as integrins, defensin, β -subunit of heterotrimeric G proteins, and GRP78/BiP, through which cell signaling and cellular metabolism are regulated ³⁷.

Different from mono-ADP-ribosylation, poly-ADP-ribosylation occurs in many multicellular organisms including plants and some lower unicellular eukaryotes, but is absent in prokaryotes and yeast. PARPs are mainly localized in the nucleus and involved in DNA repair and programmed cell death. For instance, in an immediate cellular response to metabolic, chemical, or radiation-induced single strand DNA breaks (SSB) damage, PARP-1 binds to SSB and begins the synthesis of poly-ADP-ribose chain as the signal for other DNA repairing enzymes such as topoisomerase I and II, NAD helicases, single-strand-break repair (SSBR) and base-excision repair (BER) factors. Strong activation of PARP-1 by DNA damage may deplete the storage of cellular NAD and induce a progressive ATP depletion, leading to apoptotic or necrotic cell death ³⁶.

cADP-ribose synthases, also known CD38 and CD157, are a pair of multifunctional ecto-enzymes which are involved in the catabolism of NAD and NADP³⁸. This reaction leads to the generation of potent intracellular Ca²⁺ mobilizing compounds such as cyclic ADP ribose (cADPR), nicotinic acid adenine dinucleotide phosphate (NADDP), and ADPR³⁹. The importance of these enzymatic pathways has been demonstrated not only in the immune system, but also in tissues and organs, such as pancreas and kidney. In innate immunity, neutrophils and dendritic cells (DCs) are critical regulators of innate and adaptive immune responses, respectively. Neutrophils and DCs obtain the capacity of directionally migrating to the site of infection through modulating cADPR-induced Ca²⁺ mobilization into the cells, suggesting that CD38 is required for the chemotaxis of neutrophils and DCs³⁹. Similarly in islet microsomes, cADPR is generated by glucose stimulation in islets and serves as a second messenger for Ca²⁺ mobilization in the endoplasmic reticulum, resulting in induction of insulin secretion⁴⁰.

NAD-dependent Sirtuins; the link from NAD to metabolic syndrome

Sirtuins are the class III histone deacetylase family, and require NAD as a cofactor to deacetylate target proteins and modify their function⁴¹. Sirtuins couple the breakdown of NAD with deacetylation and/or ADP-ribosylation on lysine residues of target proteins, and nicotinamide, acetyl-ADP-ribose, and deacetylated proteins are produced in these NAD-dependent deacetylation reactions⁴¹⁻⁴³. The first member of the Sirtuin family of proteins to be identified was the *Saccharomyces cerevisiae* NAD-dependent histone deacetylase silent information regulator 2, SIR2⁴¹. As the name

implies, the *SIR2* gene was originally discovered as one of the genes that encode a chromatin-silencing complex, which represses gene transcription in the coding region of chromosomes as well as telomeres and ribosomal DNA (rDNA) repeats⁴⁴⁻⁴⁷. Subsequent work showed that Sir2 was necessary and sufficient to prolong the replicative lifespan of budding yeast by reducing the number of extrachromosomal rDNA circles⁴⁸. Sir2 orthologous genes in the nematode *Caenorhabditis elegans* (*sir-2.1*) and in the fruit fly *Drosophila melanogaster* (*Sir2*) also function to increase lifespan⁴⁹⁻⁵¹.

Numerous target proteins, including histones and a variety of transcription factors and co-activators, have already been reported for Sirtuins in different species, and these roles of Sirtuins are also conserved in mammals. In mammals, seven sirtuin family members, SIRT1 through SIRT7, have been identified. SIRT1, SIRT6, and SIRT7 are mainly localized in the nucleus of most cell types and regulate metabolism at multiple levels⁵², even though SIRT1 is reported to be also localized in cytoplasm depending on cell cycle and developmental stage⁵³⁻⁵⁶. SIRT2 is mostly found in the cytoplasm, whereas SIRT3, SIRT4, and SIRT5 are primarily localized in mitochondria⁵². In addition to deacetylase activity, SIRT4 and SIRT6 were reported to function as ADP-ribosyltransferases, even though SIRT6 also can act as a deacetylase⁵².

The most-studied member of the mammalian sirtuin family is SIRT1, which was originally described to deacetylate histones but soon after was also shown to deacetylate other protein targets in almost all tissues. The first-described non-histone target is p53, which is deacetylated and repressed upon DNA damage or oxidative stress, resulting in impaired apoptosis^{57,58}. Peroxisome-activated receptor- γ co-activator 1 α (PGC1 α), which is a transcriptional co-regulator that governs mitochondrial biogenesis and activity,

is also deacetylated and activated by SIRT1 during exercise or fasting, resulting in upregulation of the transcription of genes responsible for mitochondrial biogenesis and fatty acid oxidation in skeletal muscle ⁵⁹⁻⁶¹. In addition, SIRT1 regulates hepatic metabolism at multiple levels. First of all, SIRT1 orchestrates the activity of an array of transcription factors that can alter hepatic glucose output during fasting. SIRT1 deacetylates and activates PGC1 α , PPAR α , and FOXO1, which induces the expression of genes whose products are involved in gluconeogenesis, fatty acid oxidation, and mitochondrial biogenesis ^{59,62,63}. SIRT1 also deacetylates and inhibits STAT3, which normally acts as a transcriptional repressor of gluconeogenic genes ⁶⁴. Secondly, SIRT1 can induce the liver to shut off lipid and cholesterol synthesis and storage, and activates lipolysis pathways to supply the fasting organism with energy. Deacetylation of sterol regulatory element binding protein 1 (SREBP1) by SIRT1 results in targeting of SREBP1 for ubiquitination and proteasomal degradation, which inhibits the expression of lipogenic and cholesterol synthesis genes ^{65,66}. SIRT1 also promotes reverse cholesterol transport by deacetylating and activating the oxysterol receptor (LXR α) ⁶⁷, and promotes the cholesterol catabolic pathway by deacetylating and activating nuclear bile acid receptor (FXR) ⁶⁸.

SIRT1 also plays a crucial role in counteracting many features of metabolic syndrome. SIRT1 has an inhibitory effect on adipocyte differentiation and fat tissue accumulation by inhibiting the activity of PPAR γ , the master regulator of adipogenesis ⁶⁹. SIRT1 also augments insulin secretion in response to glucose in pancreatic β cells by repressing the transcription of uncoupling protein 2 (UCP2) ^{54,70}. SIRT1 achieves this effect on UCP2 expression by directly binding to and repressing UCP2 gene transcription

in pancreatic β cells ⁷⁰. By deacetylating FOXO1 in response to oxidative stress caused by hyperglycemia, SIRT1 also mediates protection against hyperglycemia-induced toxicity and failure of pancreatic β cells ⁷¹. In the brain, SIRT1 acts in pro-opiomelanocortin (POMC) neurons in the hypothalamus to regulate energy expenditure and body weight ⁷²⁻⁷⁴. Additionally, SIRT1 activity in neurons that express steidogenic factor 1 (SF1) has a protective role against the development of insulin resistance in skeletal muscle in response to a high-fat diet through the mediating anti-diabetic effects of the neuropeptide orexin A ⁷⁵.

Different from SIRT1, SIRT2 is mainly found in cytoplasm. SIRT2 deacetylates tubulin ⁷⁶, but the relevance of this is unclear. More importantly, SIRT2 also deacetylates partitioning defective 3 homologue (PAR3), which, in turn, decreases the activity of the cell polarity to control the protein atypical protein kinase C (aPKC), thereby changing myelin formation of Schwann cells ⁷⁷. In addition, SIRT2 may have roles in metabolic homeostasis by deacetylating phosphoenolpyruvate carboxykinase (PEPCK), which is involved in gluconeogenesis, and thereby preventing its ubiquitylation-dependent degradation ⁷⁸. SIRT2 also deacetylates and inactivates FOXO1, resulting in inhibition of adipocyte differentiation ⁷⁹.

SIRT3 functions in mitochondria as a metabolic sensor by regulating adaptive responses to changes in available energy. In response to fasting, SIRT3 protein levels and activity are upregulated in the liver and in turn acetylate several mitochondrial proteins. These acetylated proteins include long-chain acyl-coenzyme A dehydrogenase (LCAD), a key enzyme in the fatty acid oxidation pathway ⁸⁰, and 3-hydroxy-3-methylglutaryl CoA synthase 2 (HMGCS2), the rate-limiting enzyme in the synthesis of

the ketone β -hydroxybutyrate⁸¹, which increases their enzymatic activity. By-products of lipid oxidation such as acetate and the ketone body β -hydroxybutyrate are exported from the liver and used for energy production in other peripheral tissues. SIRT3 also deacetylates acetyl-CoA synthetase (AceCS) in peripheral tissues to generate acetyl-CoA from acetate, which can be consumed in the TCA cycle^{82,83}. Another link between SIRT3 and the adaptive response to fasting is the regulation of the urea cycle, which clears away ammonia produced by protein breakdown during conditions of energy limitation. SIRT3 promotes the urea cycle by deacetylating and activating ornithine transcarbamoylase⁸⁴.

SIRT3 is also essential for calorie restriction-mediated reduction in oxidative stress. During calorie restriction, SIRT3 activates superoxide dismutase 2, a key mitochondrial antioxidant enzyme that converts reactive oxygen species (ROS) such as superoxide (O_2^-) into hydrogen peroxide (H_2O_2)⁸⁵. Moreover, calorie restriction induces SIRT3-mediated deacetylation of isocitrate dehydrogenase 2 (IDH2) in various tissues including inner ear cells, and in turn increases the ratio of reduced to oxidized glutathione, thus attenuating ROS generation⁸⁶. As a result, calorie restriction protects against age-associated hearing loss in a SIRT3-dependent manner⁸⁶. These results suggest that SIRT3 might be an important factor for the beneficial aspects of calorie restriction. Indeed, in the absence of SIRT3, the reduction in oxidative stress normally observed during calorie restriction is lost^{85,86}.

In contrast to the other sirtuins which all have deacetylase activities, SIRT4 only seems to have NAD-dependent ADP-ribosyl transferase activity. SIRT4 ADP-ribosylates glutamate dehydrogenase (GDH) and inhibits its activity, thereby blocking

amino acid-induced insulin secretion ⁴². SIRT4 also regulates fatty acid oxidation in hepatocytes and myocytes, and short hairpin RNA (shRNA)-mediated knockdown of *Sirt4* in the liver increases fatty acid oxidation ⁸⁷. The only target described for SIRT5 is carbamoyl phosphate synthetase 1 (CPS1). By deacetylating it, SIRT5 activates ammonia detoxification through the urea cycle ⁸⁸. Interestingly, SIRT3 and SIRT5 regulate different steps in the urea cycle, to clear away ammonia and prevent its toxic effects in conditions of nutrient limitation.

SIRT6 is mainly involved in processes related to chromatin and regulates several pathways of cellular metabolism. It can regulate chromatin by acting as a co-repressor, deacetylating lysine 9 of histone H3 at NF- κ B signaling, which results in suppression of NF- κ B activity and inhibition of apoptosis and cellular senescence ^{89,90}. SIRT6 also has a key role in glucose homeostasis through co-repression of HIF-1 α that encodes glycolytic enzymes in the liver and skeletal muscle ⁹¹. SIRT7, probably the least studied of the sirtuins, localizes to the nucleolus and activates RNA polymerase I transcription ^{92,93}. SIRT7 whole body KO mice develop inflammatory cardiomyopathy and die prematurely ⁹³.

Goals of this study

Based on current understanding on NAD biosynthesis via NAMPT and its effects on regulating metabolism through multiple NAD-dependent enzymes including sirtuins, several important questions arise. First, I want to understand the physiological functions of NAMPT. Is NAMPT expression and/or activity changed under pathophysiological conditions such as in diet-induced diabetic or aged animal models? If so, in which tissues

does this occur, and does this result in a deleterious metabolic phenotype in the animal? Would this metabolic phenotype be related to the NAD biosynthetic activity of NAMPT? Can it be reversible with inducing NAD biosynthesis by NMN administration? Secondly, I am interested in the function of eNAMPT especially secreted from adipose tissues. Is eNAMPT not released from cell death, but positively secreted from adipocytes? If so, when is its secretion increased or decreased? Would any post-translational modification be involved in eNAMPT secretion? If there is any, which protein is related in this and what is the detailed molecular mechanism? Lastly, what is the physiological importance of eNAMPT secreted from adipose tissue? Using a genetically engineered mouse model, adipose tissue-specific Nampt KO (ANKO) mice, we will try to present evidence demonstrating that NAMPT in adipose tissues systemically regulates glucose homeostasis.

Figure Legends

Figure 1. NAD biosynthesis pathway from nicotinamide.

The rate-limiting step in mammalian NAD biosynthesis from nicotinamide is the transfer of a phosphoribosyl residue from 5-phosphoribosyl-1-pyrophosphate (PRPP) to nicotinamide catalyzed by nicotinamide phosphoribosyltransferase (NAMPT) to produce nicotinamide mononucleotide (NMN), which is then converted to nicotinamide adenine dinucleotide (NAD) by nicotinamide mononucleotide adenylyltransferase (NMNAT).

ATP; adenosine triphosphate, PPI; inorganic pyrophosphate

Figure 2. NAD as a substrate for ADP-ribose transfer, cADP-ribose synthesis and protein lysine deacetylation.

ADP-ribose transferases (ARTs) and poly(ADP-ribose) polymerases (PARPs) transfer ADP-ribose from NAD as a protein modification with production of nicotinamide. In the case of PARPs, the ADP-ribose acceptor, X, can also be ADP-ribose, forming poly(ADP-ribose). cADP-ribose synthases cyclize the ADP-ribose moiety of NAD with production of nicotinamide. These enzymes also hydrolyze cADP-ribose. Sirtuins use the ADP-ribose moiety of NAD to accept the acetyl modification of a protein lysine, forming deacetylated protein and nicotinamide. After acetyl-group rearrangement, a mixture of 2' and 3' O-acetyl-ADP-ribose are produced.

Figure 1

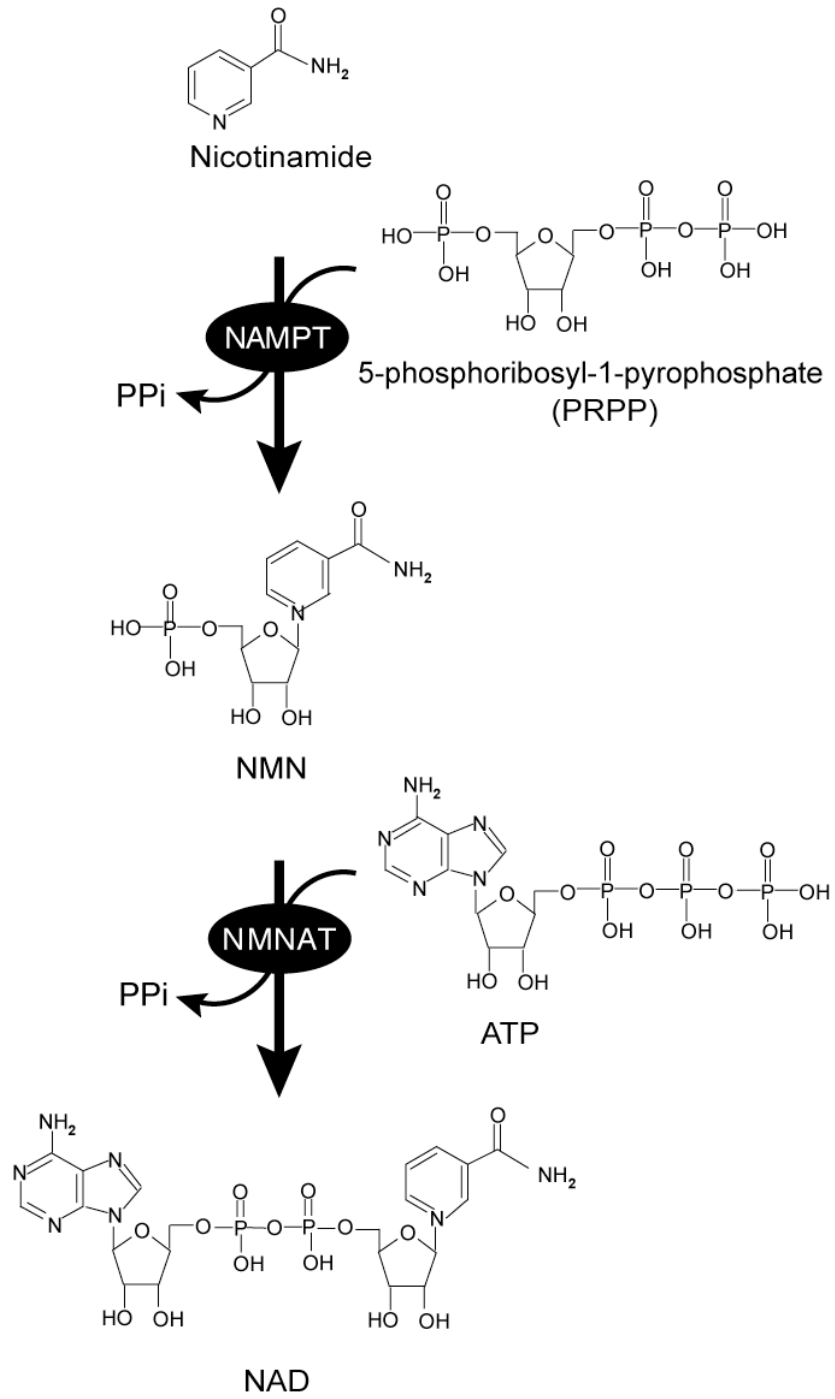


Figure 2

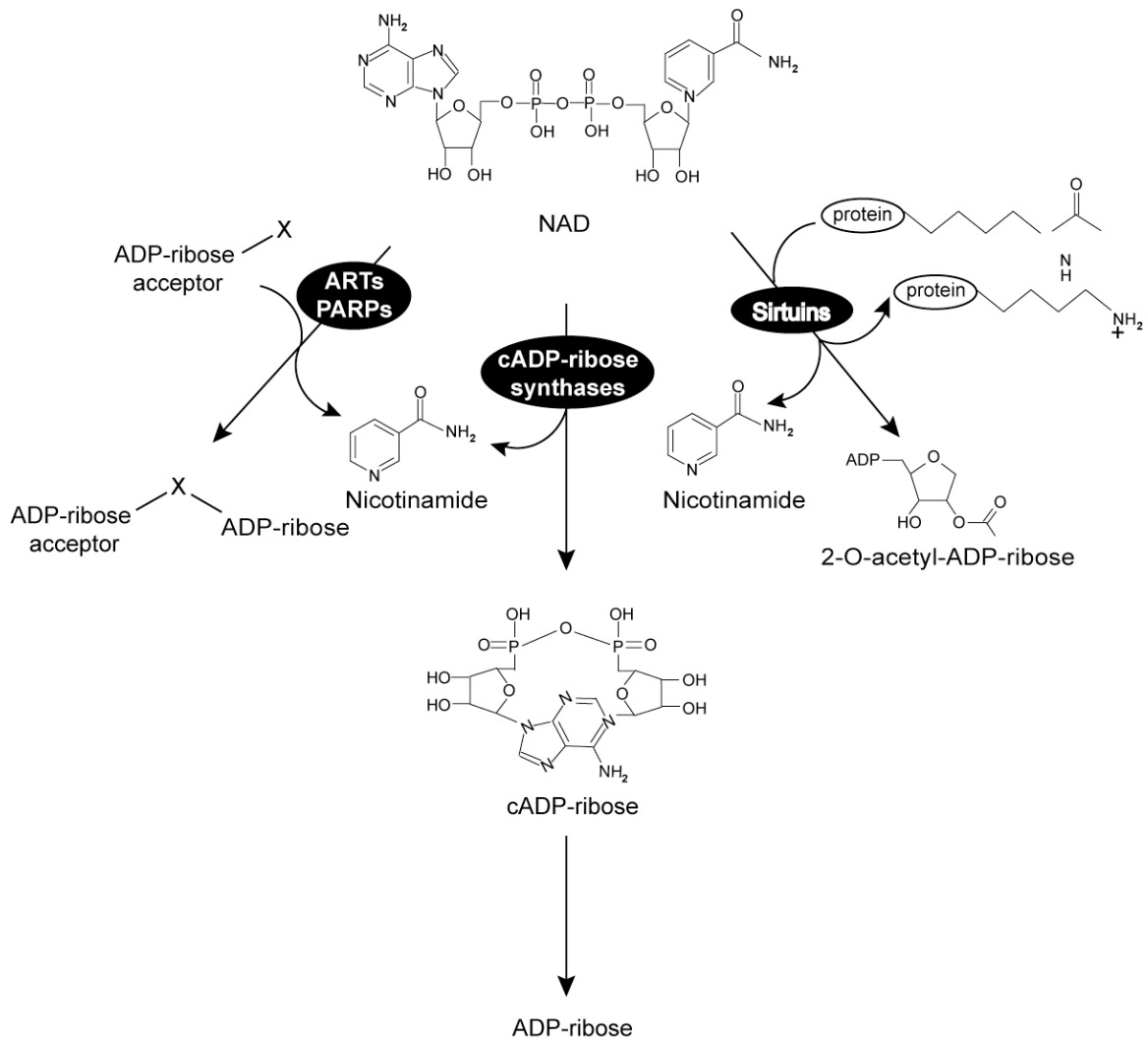


Table 1

Sirtuin localization and function

Sirtuin	Enzymatic activity	Subcellular localization	Function
SIRT1	Deacetylation	Nuclues,Cytosol	Glucose production (liver) Cholesterol regulation (liver) Fatty acid mobilization (WAT) Fatty acid oxidation (skeletal muscle) Insulin secretion (pancreatic β cells) Energy expenditure (brain) Insulin sensitivity (brain) Stress resistance and apoptosis
SIRT2	Deacetylation	Cytosol	Tubulin deacetylation Myelin formation (Schwann cells) Glucose production (liver) Differentiation (adipocytes)
SIRT3	Deacetylation	Mitochondria	Mitochondrial protein deacetylation Ammonia detoxification Oxitative stress
SIRT4	ADP-ribosylation	Mitochondria	Amino acid-induced insulin secretion (pancreatic β cells) Fatty acid oxidation (hepatocytes & myocytes)
SIRT5	Deacetylation	Mitochondria	Ammonia detoxification
SIRT6	Deacetylation ADP-ribosylation	Nucleus	Base excision repair Glycolysis (liver & skeletal muscle) Apoptosis & cellular senescence
SIRT7	Unknown	Nucleolus	RNA polymerase I transcription

WAT; white adipose tissue

REFERENCES

1. Zhang, Y., *et al.* Positional cloning of the mouse obese gene and its human homologue. *Nature* **372**, 425-432 (1994).
2. Bamshad, M., Song, C.K. & Bartness, T.J. CNS origins of the sympathetic nervous system outflow to brown adipose tissue. *Am J Physiol* **276**, R1569-1578 (1999).
3. Bartness, T.J. & Bamshad, M. Innervation of mammalian white adipose tissue: implications for the regulation of total body fat. *Am J Physiol* **275**, R1399-1411 (1998).
4. Lago, F., Gomez, R., Gomez-Reino, J.J., Dieguez, C. & Gualillo, O. Adipokines as novel modulators of lipid metabolism. *Trends Biochem Sci* **34**, 500-510 (2009).
5. Williams, K.W., Scott, M.M. & Elmquist, J.K. From observation to experimentation: leptin action in the mediobasal hypothalamus. *Am J Clin Nutr* **89**, 985S-990S (2009).
6. Uysal, K.T., Wiesbrock, S.M., Marino, M.W. & Hotamisligil, G.S. Protection from obesity-induced insulin resistance in mice lacking TNF-alpha function. *Nature* **389**, 610-614 (1997).
7. Yin, M.J., Yamamoto, Y. & Gaynor, R.B. The anti-inflammatory agents aspirin and salicylate inhibit the activity of I(kappa)B kinase-beta. *Nature* **396**, 77-80 (1998).
8. Cai, D., *et al.* Local and systemic insulin resistance resulting from hepatic activation of IKK-beta and NF-kappaB. *Nat Med* **11**, 183-190 (2005).
9. Hirosumi, J., *et al.* A central role for JNK in obesity and insulin resistance. *Nature* **420**, 333-336 (2002).

10. Tuncman, G., *et al.* Functional in vivo interactions between JNK1 and JNK2 isoforms in obesity and insulin resistance. *Proc Natl Acad Sci U S A* **103**, 10741-10746 (2006).
11. De Taeye, B.M., *et al.* Macrophage TNF-alpha contributes to insulin resistance and hepatic steatosis in diet-induced obesity. *Am J Physiol Endocrinol Metab* **293**, E713-725 (2007).
12. Suganami, T., Nishida, J. & Ogawa, Y. A paracrine loop between adipocytes and macrophages aggravates inflammatory changes: role of free fatty acids and tumor necrosis factor alpha. *Arterioscler Thromb Vasc Biol* **25**, 2062-2068 (2005).
13. Weisberg, S.P., *et al.* Obesity is associated with macrophage accumulation in adipose tissue. *J Clin Invest* **112**, 1796-1808 (2003).
14. Revollo, J.R., Grimm, A.A. & Imai, S. The NAD biosynthesis pathway mediated by nicotinamide phosphoribosyltransferase regulates Sir2 activity in mammalian cells. *J Biol Chem* **279**, 50754-50763 (2004).
15. Revollo, J.R., *et al.* Nampt/PBEF/Visfatin regulates insulin secretion in beta cells as a systemic NAD biosynthetic enzyme. *Cell Metab* **6**, 363-375 (2007).
16. Samal, B., *et al.* Cloning and characterization of the cDNA encoding a novel human pre-B-cell colony-enhancing factor. *Mol Cell Biol* **14**, 1431-1437 (1994).
17. Martin, P.R., Shea, R.J. & Mulks, M.H. Identification of a plasmid-encoded gene from *Haemophilus ducreyi* which confers NAD independence. *J Bacteriol* **183**, 1168-1174 (2001).
18. Rongvaux, A., *et al.* Pre-B-cell colony-enhancing factor, whose expression is up-regulated in activated lymphocytes, is a nicotinamide phosphoribosyltransferase, a

- cytosolic enzyme involved in NAD biosynthesis. *Eur J Immunol* **32**, 3225-3234 (2002).
19. Kitani, T., Okuno, S. & Fujisawa, H. Growth phase-dependent changes in the subcellular localization of pre-B-cell colony-enhancing factor. *FEBS Lett* **544**, 74-78 (2003).
 20. McGlothlin, J.R., *et al.* Molecular cloning and characterization of canine pre-B-cell colony-enhancing factor. *Biochem Genet* **43**, 127-141 (2005).
 21. Muller, W.E., *et al.* Increased gene expression of a cytokine-related molecule and profilin after activation of *Suberites domuncula* cells with xenogeneic sponge molecule(s). *DNA Cell Biol* **18**, 885-893 (1999).
 22. Fujiki, K., Shin, D.H., Nakao, M. & Yano, T. Molecular cloning and expression analysis of the putative carp (*Cyprinus carpio*) pre-B cell enhancing factor. *Fish Shellfish Immunol* **10**, 383-385 (2000).
 23. Shaffer, A.L., *et al.* Signatures of the immune response. *Immunity* **15**, 375-385 (2001).
 24. Jia, S.H., *et al.* Pre-B cell colony-enhancing factor inhibits neutrophil apoptosis in experimental inflammation and clinical sepsis. *J Clin Invest* **113**, 1318-1327 (2004).
 25. Li, Y., *et al.* Extracellular Nampt promotes macrophage survival via a nonenzymatic interleukin-6/STAT3 signaling mechanism. *J Biol Chem* **283**, 34833-34843 (2008).
 26. Fukuhara, A., *et al.* Visfatin: a protein secreted by visceral fat that mimics the effects of insulin. *Science* **307**, 426-430 (2005).
 27. Fukuhara, A., *et al.* Retraction. *Science* **318**, 565 (2007).

28. Wang, T., *et al.* Structure of Nampt/PBEF/visfatin, a mammalian NAD⁺ biosynthetic enzyme. *Nat Struct Mol Biol* **13**, 661-662 (2006).
29. Kim, M.K., *et al.* Crystal structure of visfatin/pre-B cell colony-enhancing factor 1/nicotinamide phosphoribosyltransferase, free and in complex with the anti-cancer agent FK-866. *J Mol Biol* **362**, 66-77 (2006).
30. Yoshino, J., Mills, K.F., Yoon, M.J. & Imai, S. Nicotinamide mononucleotide, a key NAD(+) intermediate, treats the pathophysiology of diet- and age-induced diabetes in mice. *Cell Metab* **14**, 528-536 (2011).
31. Bollet, A.J. Politics and pellagra: the epidemic of pellagra in the U.S. in the early twentieth century. *Yale J Biol Med* **65**, 211-221 (1992).
32. Elvehjem, C.A., Madden, R.J., Strong, F.M. & Wolley, D.W. The isolation and identification of the anti-black tongue factor. 1937. *J Biol Chem* **277**, e22 (2002).
33. Belenky, P., Bogan, K.L. & Brenner, C. NAD⁺ metabolism in health and disease. *Trends Biochem Sci* **32**, 12-19 (2007).
34. Heineke, D., *et al.* Redox Transfer across the Inner Chloroplast Envelope Membrane. *Plant Physiol* **95**, 1131-1137 (1991).
35. Rich, P.R. The molecular machinery of Keilin's respiratory chain. *Biochem Soc Trans* **31**, 1095-1105 (2003).
36. Schreiber, V., Dantzer, F., Ame, J.C. & de Murcia, G. Poly(ADP-ribose): novel functions for an old molecule. *Nat Rev Mol Cell Biol* **7**, 517-528 (2006).
37. Corda, D. & Di Girolamo, M. Functional aspects of protein mono-ADP-ribosylation. *EMBO J* **22**, 1953-1958 (2003).

38. Malavasi, F., *et al.* CD38 and CD157 as receptors of the immune system: a bridge between innate and adaptive immunity. *Mol Med* **12**, 334-341 (2006).
39. Malavasi, F., *et al.* Evolution and function of the ADP ribosyl cyclase/CD38 gene family in physiology and pathology. *Physiol Rev* **88**, 841-886 (2008).
40. Johnson, J.D., *et al.* Suppressed insulin signaling and increased apoptosis in CD38-null islets. *Diabetes* **55**, 2737-2746 (2006).
41. Imai, S., Armstrong, C.M., Kaeberlein, M. & Guarente, L. Transcriptional silencing and longevity protein Sir2 is an NAD-dependent histone deacetylase. *Nature* **403**, 795-800 (2000).
42. Haigis, M.C., *et al.* SIRT4 inhibits glutamate dehydrogenase and opposes the effects of calorie restriction in pancreatic beta cells. *Cell* **126**, 941-954 (2006).
43. Schwer, B., *et al.* Neural sirtuin 6 (Sirt6) ablation attenuates somatic growth and causes obesity. *Proc Natl Acad Sci U S A* **107**, 21790-21794 (2010).
44. Klar, A.J., Fogel, S. & Macleod, K. MAR1-a Regulator of the HMa and HMalpha Loci in SACCHAROMYCES CEREVISIAE. *Genetics* **93**, 37-50 (1979).
45. Smith, J.S. & Boeke, J.D. An unusual form of transcriptional silencing in yeast ribosomal DNA. *Genes Dev* **11**, 241-254 (1997).
46. Gottlieb, S. & Esposito, R.E. A new role for a yeast transcriptional silencer gene, SIR2, in regulation of recombination in ribosomal DNA. *Cell* **56**, 771-776 (1989).
47. Bryk, M., *et al.* Transcriptional silencing of Ty1 elements in the RDN1 locus of yeast. *Genes Dev* **11**, 255-269 (1997).
48. Sinclair, D.A. & Guarente, L. Extrachromosomal rDNA circles--a cause of aging in yeast. *Cell* **91**, 1033-1042 (1997).

49. Tissenbaum, H.A. & Guarente, L. Increased dosage of a sir-2 gene extends lifespan in *Caenorhabditis elegans*. *Nature* **410**, 227-230 (2001).
50. Viswanathan, M. & Guarente, L. Regulation of *Caenorhabditis elegans* lifespan by sir-2.1 transgenes. *Nature* **477**, E1-2 (2011).
51. Rogina, B. & Helfand, S.L. Sir2 mediates longevity in the fly through a pathway related to calorie restriction. *Proc Natl Acad Sci U S A* **101**, 15998-16003 (2004).
52. Houtkooper, R.H., Pirinen, E. & Auwerx, J. Sirtuins as regulators of metabolism and healthspan. *Nat Rev Mol Cell Biol* **13**, 225-238 (2012).
53. Tanno, M., Sakamoto, J., Miura, T., Shimamoto, K. & Horio, Y. Nucleocytoplasmic shuttling of the NAD⁺-dependent histone deacetylase SIRT1. *J Biol Chem* **282**, 6823-6832 (2007).
54. Moynihan, K.A., *et al.* Increased dosage of mammalian Sir2 in pancreatic beta cells enhances glucose-stimulated insulin secretion in mice. *Cell Metab* **2**, 105-117 (2005).
55. Chen, I.Y., *et al.* Histone H2A.z is essential for cardiac myocyte hypertrophy but opposed by silent information regulator 2alpha. *J Biol Chem* **281**, 19369-19377 (2006).
56. Rosenberg, M.I. & Parkhurst, S.M. *Drosophila* Sir2 is required for heterochromatic silencing and by euchromatic Hairy/E(Spl) bHLH repressors in segmentation and sex determination. *Cell* **109**, 447-458 (2002).
57. Vaziri, H., *et al.* hSIR2(SIRT1) functions as an NAD-dependent p53 deacetylase. *Cell* **107**, 149-159 (2001).
58. Luo, J., *et al.* Negative control of p53 by Sir2alpha promotes cell survival under stress. *Cell* **107**, 137-148 (2001).

59. Rodgers, J.T., *et al.* Nutrient control of glucose homeostasis through a complex of PGC-1alpha and SIRT1. *Nature* **434**, 113-118 (2005).
60. Lagouge, M., *et al.* Resveratrol improves mitochondrial function and protects against metabolic disease by activating SIRT1 and PGC-1alpha. *Cell* **127**, 1109-1122 (2006).
61. Gerhart-Hines, Z., *et al.* Metabolic control of muscle mitochondrial function and fatty acid oxidation through SIRT1/PGC-1alpha. *EMBO J* **26**, 1913-1923 (2007).
62. Daitoku, H., *et al.* Silent information regulator 2 potentiates Foxo1-mediated transcription through its deacetylase activity. *Proc Natl Acad Sci U S A* **101**, 10042-10047 (2004).
63. Rodgers, J.T. & Puigserver, P. Fasting-dependent glucose and lipid metabolic response through hepatic sirtuin 1. *Proc Natl Acad Sci U S A* **104**, 12861-12866 (2007).
64. Nie, Y., *et al.* STAT3 inhibition of gluconeogenesis is downregulated by SirT1. *Nat Cell Biol* **11**, 492-500 (2009).
65. Ponugoti, B., *et al.* SIRT1 deacetylates and inhibits SREBP-1C activity in regulation of hepatic lipid metabolism. *J Biol Chem* **285**, 33959-33970 (2010).
66. Walker, A.K., *et al.* Conserved role of SIRT1 orthologs in fasting-dependent inhibition of the lipid/cholesterol regulator SREBP. *Genes Dev* **24**, 1403-1417 (2010).
67. Li, X., *et al.* SIRT1 deacetylates and positively regulates the nuclear receptor LXR. *Mol Cell* **28**, 91-106 (2007).

68. Kemper, J.K., *et al.* FXR acetylation is normally dynamically regulated by p300 and SIRT1 but constitutively elevated in metabolic disease states. *Cell Metab* **10**, 392-404 (2009).
69. Picard, F., *et al.* Sirt1 promotes fat mobilization in white adipocytes by repressing PPAR-gamma. *Nature* **429**, 771-776 (2004).
70. Bordone, L., *et al.* Sirt1 regulates insulin secretion by repressing UCP2 in pancreatic beta cells. *PLoS Biol* **4**, e31 (2006).
71. Kitamura, Y.I., *et al.* FoxO1 protects against pancreatic beta cell failure through NeuroD and MafA induction. *Cell Metab* **2**, 153-163 (2005).
72. Cakir, I., *et al.* Hypothalamic Sirt1 regulates food intake in a rodent model system. *PLoS One* **4**, e8322 (2009).
73. Satoh, A., *et al.* SIRT1 promotes the central adaptive response to diet restriction through activation of the dorsomedial and lateral nuclei of the hypothalamus. *J Neurosci* **30**, 10220-10232 (2010).
74. Ramadori, G., *et al.* SIRT1 deacetylase in POMC neurons is required for homeostatic defenses against diet-induced obesity. *Cell Metab* **12**, 78-87 (2010).
75. Ramadori, G., *et al.* SIRT1 deacetylase in SF1 neurons protects against metabolic imbalance. *Cell Metab* **14**, 301-312 (2011).
76. North, B.J., Marshall, B.L., Borra, M.T., Denu, J.M. & Verdin, E. The human Sir2 ortholog, SIRT2, is an NAD⁺-dependent tubulin deacetylase. *Mol Cell* **11**, 437-444 (2003).

77. Beirowski, B., *et al.* Sir-two-homolog 2 (Sirt2) modulates peripheral myelination through polarity protein Par-3/atypical protein kinase C (aPKC) signaling. *Proc Natl Acad Sci U S A* **108**, E952-961 (2011).
78. Jiang, W., *et al.* Acetylation regulates gluconeogenesis by promoting PEPCK1 degradation via recruiting the UBR5 ubiquitin ligase. *Mol Cell* **43**, 33-44 (2011).
79. Jing, E., Gesta, S. & Kahn, C.R. SIRT2 regulates adipocyte differentiation through FoxO1 acetylation/deacetylation. *Cell Metab* **6**, 105-114 (2007).
80. Hirschey, M.D., *et al.* SIRT3 regulates mitochondrial fatty-acid oxidation by reversible enzyme deacetylation. *Nature* **464**, 121-125 (2010).
81. Shimazu, T., *et al.* SIRT3 deacetylates mitochondrial 3-hydroxy-3-methylglutaryl CoA synthase 2 and regulates ketone body production. *Cell Metab* **12**, 654-661 (2010).
82. Hallows, W.C., Lee, S. & Denu, J.M. Sirtuins deacetylate and activate mammalian acetyl-CoA synthetases. *Proc Natl Acad Sci U S A* **103**, 10230-10235 (2006).
83. Schwer, B., Bunkenborg, J., Verdin, R.O., Andersen, J.S. & Verdin, E. Reversible lysine acetylation controls the activity of the mitochondrial enzyme acetyl-CoA synthetase 2. *Proc Natl Acad Sci U S A* **103**, 10224-10229 (2006).
84. Hallows, W.C., *et al.* Sirt3 promotes the urea cycle and fatty acid oxidation during dietary restriction. *Mol Cell* **41**, 139-149 (2011).
85. Qiu, X., Brown, K., Hirschey, M.D., Verdin, E. & Chen, D. Calorie restriction reduces oxidative stress by SIRT3-mediated SOD2 activation. *Cell Metab* **12**, 662-667 (2010).

86. Someya, S., *et al.* Sirt3 mediates reduction of oxidative damage and prevention of age-related hearing loss under caloric restriction. *Cell* **143**, 802-812 (2010).
87. Nasrin, N., *et al.* SIRT4 regulates fatty acid oxidation and mitochondrial gene expression in liver and muscle cells. *J Biol Chem* **285**, 31995-32002 (2010).
88. Nakagawa, T., Lomb, D.J., Haigis, M.C. & Guarente, L. SIRT5 Deacetylates carbamoyl phosphate synthetase 1 and regulates the urea cycle. *Cell* **137**, 560-570 (2009).
89. Michishita, E., *et al.* SIRT6 is a histone H3 lysine 9 deacetylase that modulates telomeric chromatin. *Nature* **452**, 492-496 (2008).
90. Kawahara, T.L., *et al.* SIRT6 links histone H3 lysine 9 deacetylation to NF-kappaB-dependent gene expression and organismal life span. *Cell* **136**, 62-74 (2009).
91. Zhong, L., *et al.* The histone deacetylase Sirt6 regulates glucose homeostasis via Hif1alpha. *Cell* **140**, 280-293 (2010).
92. Ford, E., *et al.* Mammalian Sir2 homolog SIRT7 is an activator of RNA polymerase I transcription. *Genes Dev* **20**, 1075-1080 (2006).
93. Vakhrusheva, O., *et al.* Sirt7 increases stress resistance of cardiomyocytes and prevents apoptosis and inflammatory cardiomyopathy in mice. *Circ Res* **102**, 703-710 (2008).

Chapter 2.
Nicotinamide mononucleotide,
a key NAD⁺ precursor,
treats the pathophysiology of
diet- and age-induced diabetes

ABSTRACT

Type 2 diabetes (T2D) has become an epidemic in our modern lifestyle, likely due to calorie-rich diets overwhelming our adaptive metabolic pathways. One such pathway is mediated by nicotinamide phosphoribosyltransferase (NAMPT), the rate-limiting enzyme in mammalian NAD^+ biosynthesis, and the NAD^+ -dependent protein deacetylase SIRT1. Here we show that NAMPT-mediated NAD^+ biosynthesis is severely compromised in metabolic organs by high-fat diet (HFD). Strikingly, nicotinamide mononucleotide (NMN), a product of the NAMPT reaction and a key NAD^+ intermediate, ameliorates glucose intolerance by restoring NAD^+ levels in HFD-induced T2D mice. NMN also enhances hepatic insulin sensitivity and restores gene expression related to oxidative stress, inflammatory response, and circadian rhythm, partly through SIRT1 activation. Furthermore, NAD^+ and NAMPT levels show significant decreases in multiple organs during aging, and NMN improves glucose intolerance and lipid profiles in age-induced T2D mice. These findings provide critical insights into a novel intervention against diet- and age-induced T2D.

INTRODUCTION

Recent studies have raised an interesting possibility that various physiological mechanisms that mediate metabolic adaptation have evolved in response to nutritionally scarce conditions such as famine and drought (Lazar, 2005). In our modern, sedentary lifestyle with calorie-rich diets, such adaptive mechanisms could be seriously overwhelmed, causing an epidemic of obesity and T2D worldwide (Yach et al., 2006). In mammals, one such mechanism comprises NAMPT-mediated NAD^+ biosynthesis and the NAD^+ -dependent protein deacetylase SIRT1 (Haigis and Sinclair, 2010; Houtkooper et al., 2010; Imai, 2010; Imai and Guarente, 2010). NAMPT-mediated NAD^+ biosynthesis and SIRT1 together play critical roles in regulating a variety of biological processes that include metabolism, stress response, cellular differentiation, and circadian rhythm, and also mediating adaptive responses to limited energy intake, such as fasting and diet restriction (Imai, 2010). For example, in skeletal muscle, both nutritional deprivation and exercise increase *Nampt* expression through the activation of AMP-activated protein kinase (AMPK), enhancing NAD^+ biosynthesis and SIRT1 activity (Canto et al., 2010; Costford et al., 2010; Fulco et al., 2008). In pancreatic b cells, both NAMPT-mediated NAD^+ biosynthesis and SIRT1 regulate glucose-stimulated insulin secretion (GSIS) in response to glucose availability (Moynihan et al., 2005; Revollo et al., 2007). Additionally, in the liver and white adipose tissue (WAT), NAMPT and SIRT1 comprise a novel transcriptional-enzymatic feedback loop for the regulation of circadian rhythm, a powerful effector for metabolism (Nakahata et al., 2009; Ramsey et al., 2009).

How nutritional and environmental perturbations affect the system dynamics of this NAMPT/ NAD^+ /SIRT1-driven adaptive, systemic regulatory network, named the

“NAD World” (Imai, 2010), still remains unclear. Here we show that HFD and aging compromise NAMPT-mediated NAD⁺ biosynthesis, contributing to the pathogenesis of T2D. Importantly, we also provide evidence that promoting NAD⁺ biosynthesis by using nicotinamide mononucleotide (NMN), a product of the NAMPT reaction and a key NAD⁺ intermediate, could be a novel intervention against diet- and age-induced T2D.

RESULTS

To examine the connection between NAMPT-mediated NAD⁺ biosynthesis and T2D, wild-type B6 male and female mice at 3-6 months of age were fed a HFD containing 42% calories from fat. Both males and females developed overt diabetes after 3.5 and 6 months, respectively. In these mice, we found that NAMPT protein levels were significantly reduced in the liver and WAT, but not in skeletal muscle, compared to regular chow (RC)-fed control mice (Figures 1A, S1A, and S1B). Consistent with these decreases in NAMPT levels, NAD⁺ levels were also significantly reduced in the liver and WAT, but not in skeletal muscle (Figures 1B and S1C), indicating that there is an underlying defect in NAD⁺ biosynthesis in the liver and WAT of HFD-induced diabetic mice.

Based on these findings, we hypothesized that the defect in NAMPT-mediated NAD⁺ biosynthesis could be ameliorated by administering NMN to diabetic mice. To test this idea, we initially examined how NMN administration influences NAD⁺ biosynthesis in the liver, pancreas, and WAT. NMN was immediately utilized and converted to NAD⁺ within 15 min, resulting in significant increases in NAD⁺ levels over 60 min (Figures 1C and S1D). We also observed a mild increase (~5-fold) in nicotinamide riboside (NR) levels compared to the ~15-fold increase of NMN, implying that a part of NMN might be converted to NR to get into the liver (Figure S1E). We further confirmed that NMN enhanced NAD⁺ biosynthesis in mouse primary hepatocytes in a dose-dependent manner (Figure 1D). NMN was also able to overcome NAD⁺ deficits caused by a potent NAMPT inhibitor FK866 (Hasmann and Schemainda, 2003) but unable to alleviate the NAD⁺ reduction due to the inhibition of nicotinamide/nicotinic

acid mononucleotide adenylyltransferases (NMNATs) by their potent inhibitor gallotannin (Berger et al., 2005) (Figures 1E and S1F). These results demonstrate the effectiveness and specificity of NMN at stimulating NAD⁺ biosynthesis *in vivo* and *in vitro*.

Given these findings, we administered NMN at a dose of 500 mg/kg body weight/day intraperitoneally to HFD-fed male and female diabetic mice for 10 and 7 consecutive days, respectively. No overt abnormalities or changes in body weight were detected during this time (data not shown). NMN administration successfully restored NAD⁺ levels in the liver and WAT of diabetic mice, and even in diabetic skeletal muscle, a moderate but significant increase in NAD⁺ was detected (Figure 1B). These results demonstrate the efficacy of NMN treatment in ameliorating the underlying defect in NAD⁺ biosynthesis in HFD-induced diabetes.

Strikingly, NMN administration completely normalized impaired glucose tolerance in diabetic female mice (Figure 2A). Whereas plasma insulin levels during intraperitoneal glucose tolerance tests (IPGTTs) did not differ before and after NMN treatment, insulin tolerance was significantly improved in these females (Figures 2B and 2C). In diabetic males, NMN did improve impaired glucose tolerance, but the effect was milder compared to the females (Figure 2D). Different from females, GSIS in males was enhanced at 15- and 30-min time points in IPGTTs after NMN administration (Figure 2E). Using primary pancreatic islets isolated from diabetic males, we also confirmed that both NAD⁺ levels and GSIS were enhanced by NMN (Figure S2). On the other hand, insulin tolerance remained unchanged in males (Figures 2F), suggesting that NMN exerts its major effects on different target tissues between males and females. Although the

reason for this sex difference is currently unclear, these results demonstrate that NMN treatment can ameliorate impaired glucose tolerance by improving either insulin sensitivity or insulin secretion in HFD-induced diabetic mice.

Given that NMN administration restored normal NAD⁺ levels in diabetic livers (Figure 1B) and also that the liver is known to have a major effect on insulin sensitivity in mice (Home and Pacini, 2008), we examined whether NMN improves hepatic insulin sensitivity in diabetic females. We first assessed phosphorylation status of AKT, a downstream kinase in insulin signaling, in diabetic livers with or without NMN treatment. Clear increases in AKT phosphorylation were detected in NMN-treated diabetic mice, indicating that hepatic insulin sensitivity is improved by NMN treatment (Figure 3A). We next compared gene expression profiles between RC-fed, HFD-fed, and NMN-treated HFD-fed livers. We also performed the parametric analysis of gene set enrichment (PAGE) (Kim and Volsky, 2005) using these gene expression data and GO gene sets. Interestingly, the biological pathways and genes related to oxidative stress, inflammatory response, immune response, and lipid metabolism, all of which are known to contribute to hepatic insulin resistance (Mattson, 2009; Shoelson et al., 2006), were affected by HFD and reversed by NMN (Figures 3B and S3A). For example, pathways related to glutathione S-transferases, which play an important role in the protection from lipid peroxidation products and thereby the maintenance of hepatic insulin sensitivity (Mattson, 2009), were suppressed by HFD and restored by NMN (Figure 3B, GO:0004364 and GO: 0016765). Indeed, expression levels of the glutathione S-transferase alpha 2 gene (*Gsta2*) were significantly reduced by HFD and recovered by NMN (Figures 3C). *Gsta1* and *Gsta4* also showed the same directions of changes (12.3

and 6.18 for the sum of Z ratio, respectively), although their false discovery rates did not reach statistical significance (data not shown). Pathways related to damage, inflammatory, and immune responses were induced by HFD and suppressed by NMN (Figure 3B, GO:0006952, GO:0006954, GO:0009611, GO:0006955, and GO:0009605). Consistent with these pathway alterations, expression levels of the interleukin 1b gene (*Il1b*) and the S100 calcium binding protein A8 and A9 genes (*S100a8* and *S100a9*), which are all direct NF- κ B target genes and play important roles in hepatic insulin resistance (Nemeth et al., 2009; Nov et al., 2010), were significantly up-regulated by HFD and down-regulated by NMN (Figures 3C and S3A). Other genes that showed significant changes by both HFD and NMN, such as *Lipin1* (Croce et al., 2007) and pyruvate dehydrogenase kinase 4 (*Pdk4*) (Jeoung and Harris, 2008), have also been connected to insulin resistance. It should also be noted that expression of genes related to circadian rhythm (*Dbp*, *Dec1*, and *Rev-erb-a*) were altered by HFD and reversed by NMN (Figures 3C). The genes regulated by DBP, such as *Cyp2a5* and *Rgs16*, also showed similar expression profiles (Figure 3C and S3A). These findings provide strong support for the importance of NAMPT-mediated NAD⁺ biosynthesis in the connection between circadian rhythm and metabolic disorders (Ramsey et al., 2009).

To elucidate what transcription factors mediate expression changes by HFD and NMN, biological network analysis was performed using the shortest path and the transcription regulation (TR) algorithms (Figure S3B). We noticed that transcription factors that formed relatively large hubs in the deduced network, such as c-Myc, NF- κ B, PPAR γ , and p53, are all reported targets of SIRT1 (Figure S3C), implying that SIRT1 might be one of the mediators for the observed gene expression changes. Given that NF-

kB is regulated by SIRT1-mediated deacetylation (Yeung et al., 2004) and plays a critical role in hepatic insulin resistance (Shoelson et al., 2006), we analyzed acetylation status of NF-kB in livers from each experimental condition (Figure 3D). Consistent with changes in NAD⁺ levels and NF-kB target gene expression, levels of acetylated p65, a component of NF-kB, increased by HFD and decreased considerably by NMN, suggesting that SIRT1 activity is suppressed by HFD and restored by NMN.

Because both inflammatory cytokines and oxidative stress are linked to hepatic insulin resistance (Evans et al., 2005; Peraldi and Spiegelman, 1998), we also tested whether TNF- α and menadione can affect NAMPT-mediated NAD⁺ biosynthesis and cause similar gene expression changes *in vitro*. Interestingly, whereas both reagents were able to significantly reduce NAMPT and NAD⁺ levels in primary hepatocytes, only TNF- α showed gene expression patterns similar to those in HFD-fed diabetic livers (Figure 3E, 3F, S3D, and data not shown). This TNF- α -mediated decrease in NAD⁺ levels was ameliorated by NMN (Figure 3F). In TNF- α /NMN-treated primary hepatocytes, NMN was able to restore the *Gsta2* expression to a similar level observed in HFD-fed, NMN-treated livers, and its effect was abrogated by EX527, a potent SIRT1-specific inhibitor, further confirming that SIRT1 is at least one of the mediators for the effect of NMN (Figure 3G).

In addition to calorie-rich diets, aging is one of the greatest risk factors for developing T2D (Moller et al., 2003). We found that NAD⁺ levels showed significant decreases in the pancreas, WAT, and skeletal muscle and also the same trend with a much larger variation in the liver in old mice, compared to those in young mice (Figure 4A). NAMPT protein levels also decreased in those tissues (Figures S4A and S4B). Based on

these findings, we speculated that NMN treatment might also be effective in age-induced T2D models. We screened RC wild-type B6 males and females at 15-26 months of age and found ~15% of males diabetic (>200 mg/dl at 2-hr time point in IPGTTs). To these aged, naturally occurring diabetic male mice, we intraperitoneally administered the same dose of NMN. Surprisingly, just one dose of NMN normalized impaired glucose tolerance (Figure 4B). In these mice, GSIS at 15- and 30-min time points during IPGTTs were higher after NMN treatment, although the difference did not reach statistical significance (Figure 4C). This is consistent with the results in HFD-induced diabetic male mice (Figure 2E). Importantly, NMN did not convey any significant effects to aged non-diabetic male mice (Figures S4C and S4D), indicating that NMN treatment is effective for age-induced diabetic individuals and does not negatively affect glucose homeostasis in non-diabetic individuals. Because females proved difficult to naturally develop T2D, we fed aged female mice a HFD for 7 weeks. Unlike younger females, aged females were very susceptible to HFD and developed severe diabetes within this time frame. In these aged, diabetic females, 11 consecutive injections of NMN completely normalized severely impaired glucose tolerance (Figure 4D). Qualitatively consistent with this improvement, their respiratory quotient (RQ) showed a significant increase after NMN treatment, implicating better glucose utilization, although their oxygen consumption did not change (Figure S4E). Rectal body temperature also decreased, which might be explained by a significant shift in energy utilization from fat to glucose (Figure S4F). Furthermore, hyperlipidemia induced by HFD was also corrected by NMN (Figure 4E). Thus, these results support the efficacy of NMN to significantly improve impaired glucose tolerance in age-induced T2D, as well as in HFD-

induced T2D.

DISCUSSION

The results presented in this study demonstrate that NAMPT-mediated NAD^+ biosynthesis is compromised by HFD and aging, contributing to the pathogenesis of T2D. We also provide proof of the concept that promoting NAD^+ biosynthesis by administering NMN, a key NAD^+ intermediate, can be an effective intervention to treat the pathophysiology of diet- and age-induced T2D (Figure S4G). In both diabetic models, NMN administration dramatically ameliorated impaired glucose tolerance by restoring normal NAD^+ levels and enhancing either insulin sensitivity or insulin secretion, supporting our conclusion that underlying defects in NAMPT-mediated NAD^+ biosynthesis play an important role in the pathogenesis of diet- and age-induced T2D. Although the short-term NMN administration was unable to achieve a significant improvement of fasted glucose levels, NMN is still effective at normalizing multiple metabolic pathways, such as oxidative stress, inflammatory response and circadian rhythm, and GSIS, in T2D. Whereas how NMN is transported into cells currently remains unknown, metabolic tissues and organs seem to utilize NMN and convert it to NAD^+ efficiently. Therefore, an adequate and consistent supply of this key NAD^+ intermediate must be critical to maintain normal hepatic insulin sensitivity and GSIS in pancreatic β cells. To assess beneficial and possible adverse effects of NMN more comprehensively, we are currently conducting long-term NMN supplementation experiments in different dietary conditions.

Inflammation and/or oxidative stress caused by hepatosteatosis or aging appear to trigger the reduction in NAMPT-mediated NAD^+ biosynthesis and contribute to the pathogenesis of T2D. Given that NMN is capable of reversing changes in gene

expression related to oxidative stress, inflammatory response, and circadian rhythm, NAMPT-mediated NAD^+ biosynthesis regulates homeostatic, protective mechanisms against nutritional perturbations, such as HFD. Our results also indicate that SIRT1 is at least one of the mediators for these beneficial effects of NMN on hepatic insulin sensitivity. In addition to SIRT1, there might be other NAD^+ -sensitive or NAD^+ -consuming factors that also contribute to the effects of NMN. For example, other sirtuin family members (SIRT2-7) also likely play some roles in the metabolic effects of NMN. Particularly, the functions of mitochondrial sirtuins (SIRT3-5) might be affected by deficits in NAMPT-mediated NAD^+ biosynthesis, potentially resulting in the mitochondrial dysfunction observed in T2D (Lowell and Shulman, 2005). The sex difference that we observed in this study is also interesting. Given that estrogen signaling is critical for the regulation of hepatic insulin sensitivity and GSIS (Meyer et al., 2011), estrogen might play a role in the effects of NMN under HFD feeding. Further investigation will be required to identify detailed mechanisms for the efficacy of NMN.

Our results provide an interesting implication that NMN supplementation might also be effective in human T2D patients if they have defects in NAMPT-mediated NAD^+ biosynthesis. Because NMN is an endogenous compound, this is rather a nutraceutical approach to T2D. Nonetheless, it will be of great interest to examine whether the effects of NMN are synergistic with those of small chemical SIRT1 activators (Milne et al., 2007), particularly in aged, diabetic individuals. Taken together, we anticipate that long-term NMN administration might be a highly effective way to sustain enhanced SIRT1 activity in tissues and organs where NAMPT-mediated NAD^+ biosynthesis is compromised and to combat against the disconcerting epidemic of T2D.

EXPERIMENTAL PROCEDURES

Animal Experimentation

For the HFD-induced T2D model, mice at 3-6 months of age were fed a HFD containing 42% of the total calories from fat (TD88137; Harlan Taklad). We defined diabetes as mice having fasted blood glucose levels > 120 mg/dl or blood glucose levels at 2-hr time point in IPGTTs \geq 200 mg/dl. To obtain age-induced diabetic mice, we screened male and female mice at 15-26 months of age following the criteria. For NMN treatment, we intraperitoneally administered NMN (Sigma) at the dose of 500 mg/kg body weight/day as indicated in the text and figure legends. This dose was determined in our previous studies (Revollo et al., 2007; Ramsey et al., 2008). All animal studies were approved by the Washington University Animal Studies Committee. Details are available in the Supplemental Experimental Procedure.

NAD⁺ and NMN measurements

NAD⁺ and NMN levels were determined using a HPLC system (Shimadzu) with a Supelco LC-18-T column (15cm x 4.6cm; Sigma) and a Hypercarb column (15cm x 4.6cm; Thermo Scientific), respectively. Details are available in the Supplemental Experimental Procedure.

Primary hepatocyte isolation

Primary hepatocytes were isolated from mice by hepatic portal collagenase perfusion and cultured in DMEM as described previously (Grimm et al., 2011). For treatments with NMN, enzyme inhibitors (FK866, gallotannin, EX527), TNF- α , and menadione,

hepatocytes were cultured in DMEM containing 1.0% FBS and each reagent or their combinations as indicated in the text.

Microarrays

Total RNA was isolated from frozen liver samples of RC, HFD, and NMN-treated HFD mice and used for Illumina Mouse Ref 8 whole genome microarrays (version 2). Details are available in the Supplemental Experimental Procedure.

Quantitative Real-Time PCR

Real-time PCR was performed using the 7900HT Fast Real-Time PCR System (Applied Biosystems). Relative expression levels were determined based on the CT values and normalized to CT values for the Gapdh gene. P values for the differences of CT values were calculated using one-way ANOVA with the Fisher's PLSD test.

Detection of acetylated NF- κ B p65

Nuclear extracts were prepared from frozen liver samples as previously described (Rodgers and Puigserver, 2007). 100 mg of liver nuclear extract were analyzed by Western blotting with an anti-acetyl NF- κ B p65 (Lys310) antibody (Cell Signaling Technology). The same blot was re-probed with anti-NF- κ B p65 antibody (Santa Cruz). Signals were visualized using the ECL Plus detection system (Amersham).

Statistical Analyses

Differences between two groups were assessed using Student's paired or unpaired *t* test.

Comparisons among several groups were performed using one-way ANOVA with the Fisher's PLSD *post-hoc* test. P values of less than 0.05 were considered statistically significant.

FIGURE LEGENDS

Figure 1. NMN ameliorates defects in NAMPT-mediated NAD⁺ biosynthesis in HFD-induced diabetic mice. (A) NAMPT protein levels in the liver, WAT, and skeletal muscle. Female mice were fed a RC or a HFD for 6-8 months. NAMPT levels were normalized to ACTIN (liver) or TUBULIN (WAT and skeletal muscle) (n=4 to 5 mice per group). (B) Tissue NAD⁺ levels in the liver, WAT, and skeletal muscle from RC, HFD, and NMN-treated HFD mice (n=5 to 13 mice per group). NMN (500mg/kg body weight/day) was given intraperitoneally to HFD-fed female mice for 7 consecutive days. (C) Changes in NMN and NAD⁺ levels in the liver after administering a single dose of NMN to B6 mice (n=3 to 5 mice for each time point). (D and E) Intracellular NAD⁺ levels in mouse primary hepatocytes. Cells were treated with NMN at the indicated concentrations (D), or with enzyme inhibitors [500 nM FK866 or 100 mM gallotannin (GTN)] in the presence or absence of 100 mM NMN (E), for 4 hrs (n=3 per group). Data were analyzed by Student's unpaired *t* test (A) and one-way ANOVA with the Fisher's PLSD *post-hoc* test (B, D, E). All values are presented as mean ± SEM. **P* < 0.05; ***P* < 0.01; ****P* < 0.001.

Figure 2. NMN administration improves impaired glucose tolerance in HFD-induced diabetic mice. (A and D) Glucose tolerance in HFD female (A) and male mice (D) before and after NMN treatment (n=10 for females, and n=6 for males). IPGTTs were conducted with the same individuals before (closed circles) and after (open circles) NMN. NMN (500mg/kg body weight/day) was administered to female and male mice for 7 and 10 consecutive days, respectively. The areas under each glucose tolerance

curve are presented next to the glucose tolerance curves. (**B** and **E**) Plasma insulin levels in female (**B**) and male (**E**) mice during IPGTTs before and after NMN treatment ($n=10$ for females, and $n=6$ for males). (**C** and **F**) Insulin tolerance in HFD female (**C**) and male (**F**) mice before and after NMN treatment ($n=10$ for females, and $n=6$ for males). ITTs were performed before (closed circles) and after (open circles) NMN. ITTs were conducted several days before or after IPGTTs. The areas under each insulin tolerance curve are presented next to the insulin tolerance curves. Data were analyzed by Student's paired t test. All values are presented as mean \pm SEM. * $P < 0.05$; ** $P < 0.01$; *** $P < 0.001$.

Figure 3. NMN ameliorates hepatic insulin resistance and restores gene expression related to oxidative stress, inflammatory response, and circadian rhythm. (**A**) The phosphorylation status of AKT in HFD and NMN-treated HFD female livers ($n=3$ mice per group). Signal levels of phosphorylated AKT were normalized to total AKT protein levels. (**B**) Biological pathways that were altered by HFD and reversed by NMN in female livers. Parametric analysis of gene-set enrichment (PAGE) was performed to identify pathways that were significantly up-regulated (red) or down-regulated (blue) by either HFD or NMN using our microarray data ($n=4$ mice for each condition). Twenty top pathways are listed following the sum of the absolute values of Z scores between two comparisons. (**C**) Quantitative RT-PCR results for representative genes related to oxidative stress, inflammatory response, circadian rhythm, and metabolism ($n=4$ to 5 mice per group). *Gsta2*, glutathione S-transferase alpha 2; *Il1b*, interleukin 1 beta; *Pdk4*, pyruvate dehydrogenase kinase isozyme 4; *Dbp*, D site of albumin promoter (albumin D-

box) binding protein; *Dec1*, deleted in esophageal cancer 1. (D) Acetylation status of NF-kB p65 in RC, HFD, and NMN-treated HFD livers. Two independent sets of mice were used for this analysis, and numbers below each panel represent normalized ratios of acetylated to total p65 levels. (E-G) The effects of TNF-a on NAMPT-mediated NAD⁺ biosynthesis and gene expression in mouse primary hepatocytes. Cells were treated with 50 ng/ml TNF-a for 72 hrs and given indicated reagents for 6 hrs prior to harvesting for measurements. (E) NAMPT protein levels were normalized to ACTIN (n=3 per group). (F) TNF-a-treated cells were given 100 mM NMN prior to NAD⁺ measurements (n=3-6 per group). (G) TNF-a-treated cells were cultured with NMN or NMN plus 40 mM EX527 and examined for *Gsta2* expression (n=6-9 per group). Data were analyzed by Student's unpaired *t* test (A, E). Differences in Ct values or NAD⁺ levels were analyzed with one-way ANOVA with the Fisher's PLSD *post-hoc* test (D, F, G). All values are presented as mean ± SEM. *P < 0.05; **P < 0.01; ***P < 0.001.

Figure 4. NMN improves glucose and lipid homeostasis in age-induced T2D. (A) NAD⁺ levels in metabolic tissues between young and old mice. Pancreas, liver, WAT, and skeletal muscle were collected from young (n=5-11) and old (n=5-15) mice at 3-6 and 25-31 months of age, respectively. (B) Glucose tolerance in aged, naturally occurring diabetic male mice before (closed circles) and after (open circles) a single dose of NMN (500 mg/kg body weight) (n=11). The areas under each glucose tolerance curve are presented next to the glucose tolerance curves. (C) Plasma insulin levels were measured during IPGTTs (n=5). (D and E) Glucose tolerance (D) and lipid levels (E) in aged HFD female mice before (closed circles) and after (open circles) NMN (n=5).

Fasted plasma samples were collected from the same mice and subjected to the measurements of cholesterol (Chol), triglycerides (TG), and non-esterified free fatty acids (FFA). Data were analyzed by Student's unpaired *t* test (**A**), paired *t* test (**B-D**), and one-way ANOVA with the Fisher's PLSD *post-hoc* test (**E**). All values are presented as mean \pm SEM. *P < 0.05; **P < 0.01; ***P < 0.001.

Figure 1

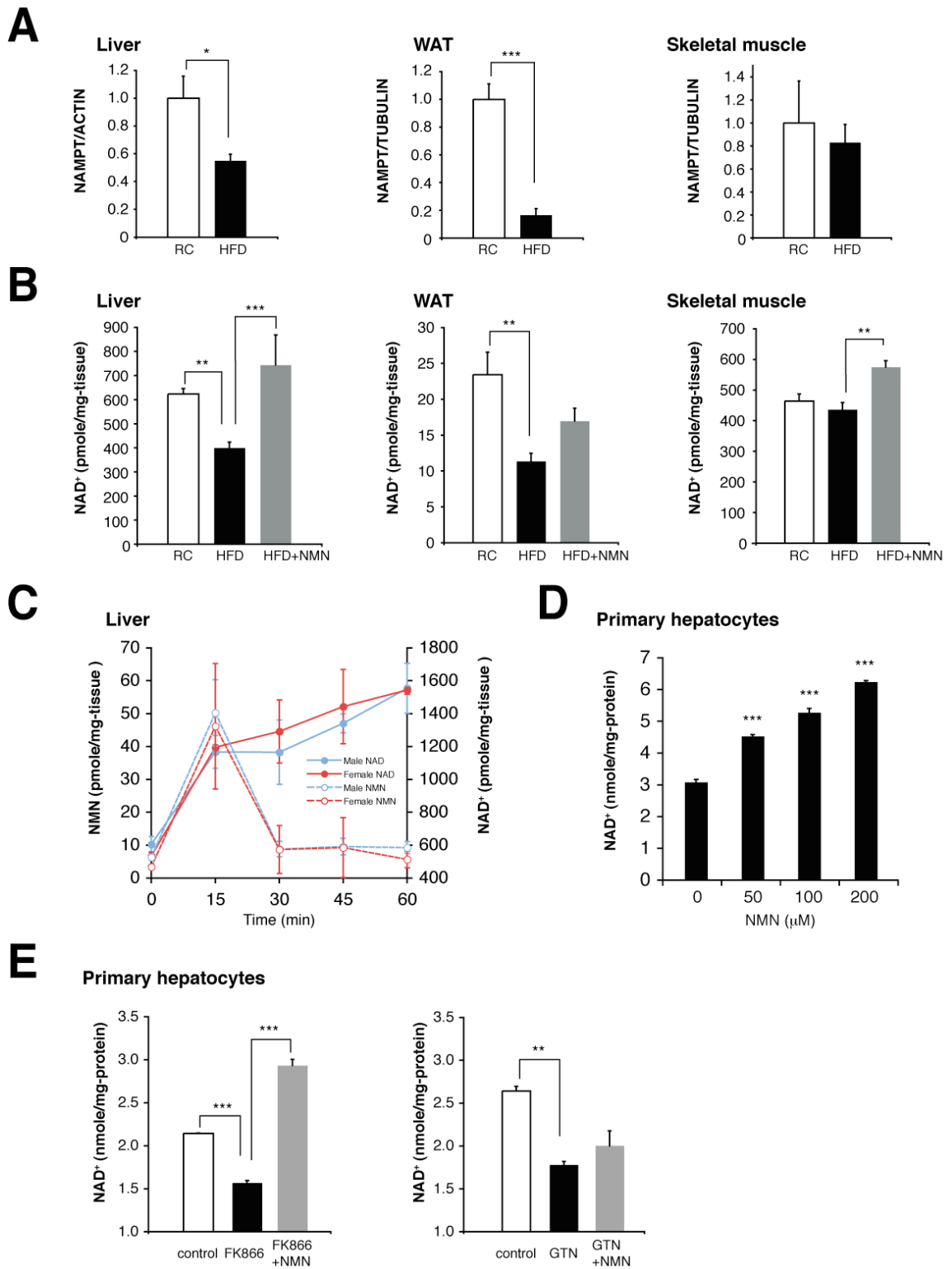


Figure 2

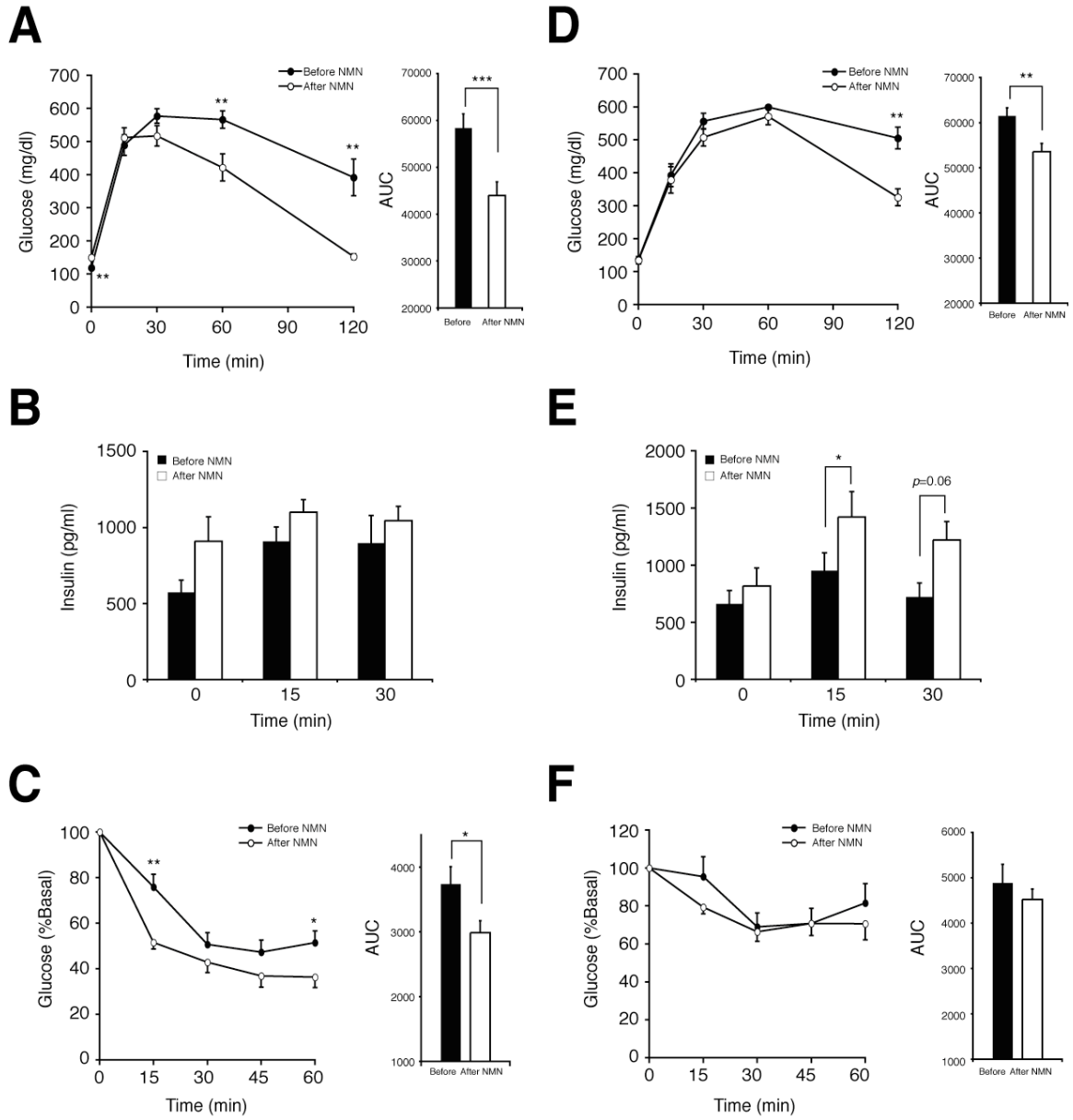


Figure 3

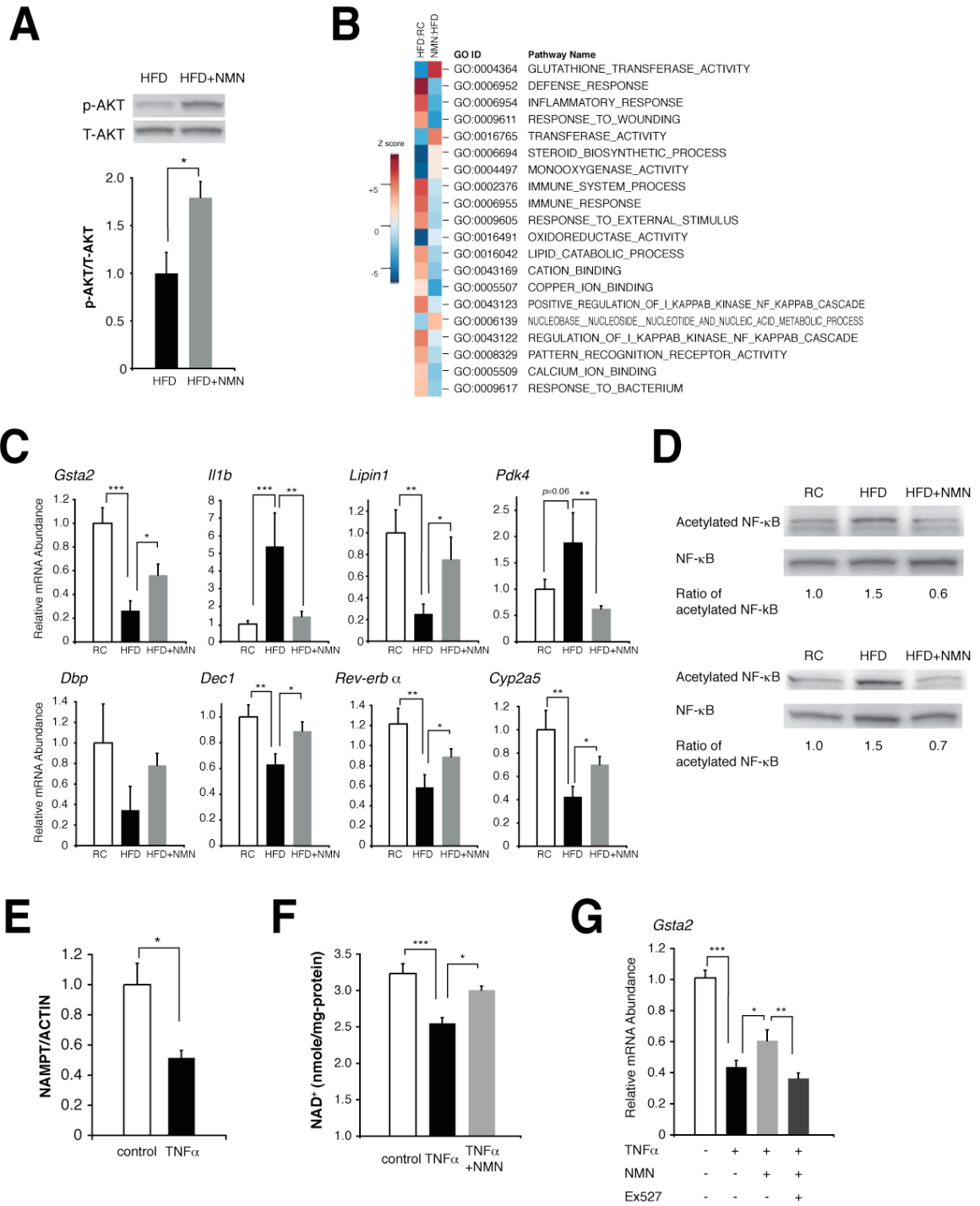
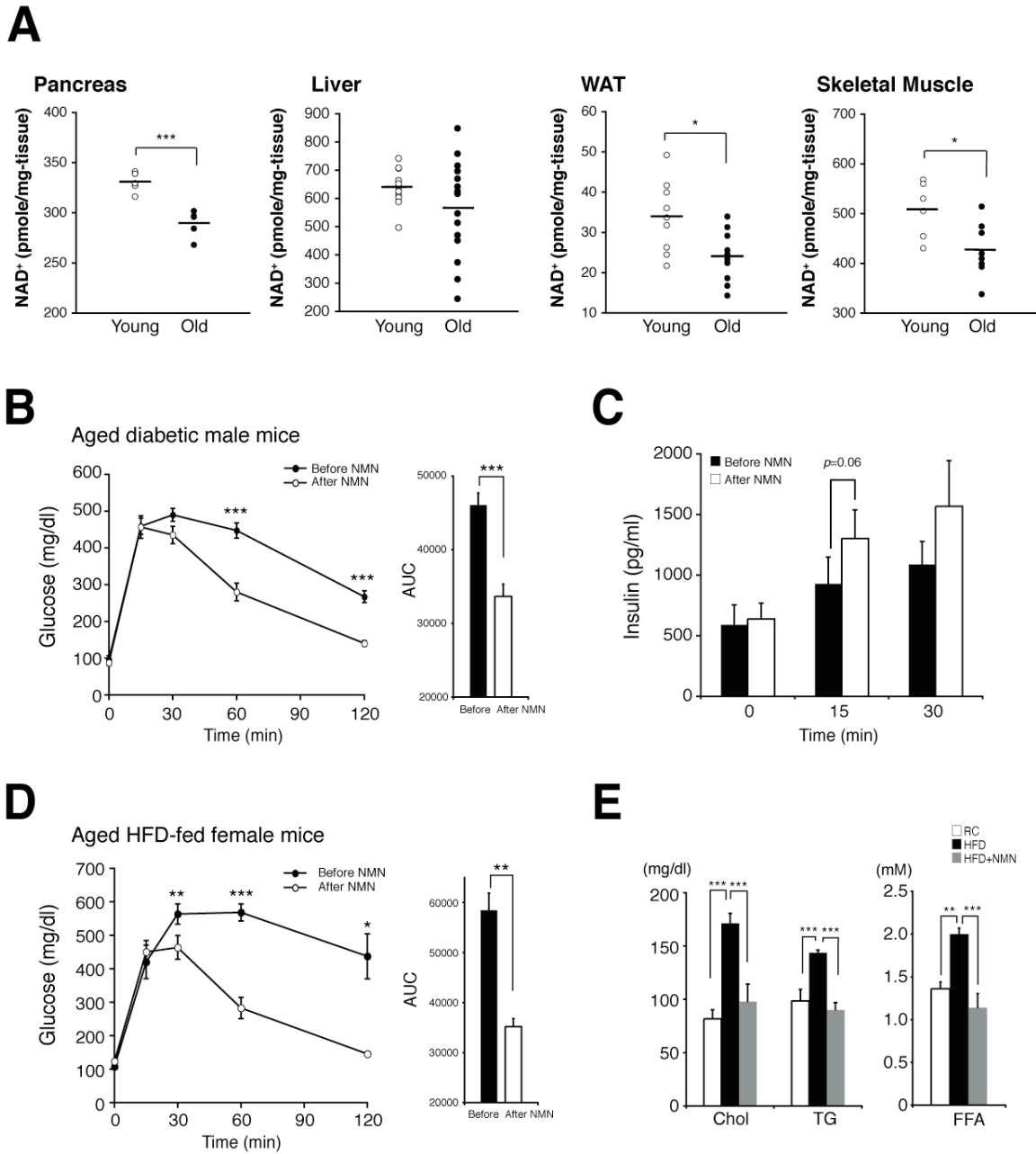


Figure 4



REFERENCES

- Berger, F., Lau, C., Dahlmann, M., and Ziegler, M. (2005). Subcellular compartmentation and differential catalytic properties of the three human nicotinamide mononucleotide adenylyltransferase isoforms. *J. Biol. Chem.* 280, 36334-36341.
- Canto, C., Jiang, L.Q., Deshmukh, A.S., Matak, C., Coste, A., Lagouge, M., Zierath, J.R., and Auwerx, J. (2010). Interdependence of AMPK and SIRT1 for metabolic adaptation to fasting and exercise in skeletal muscle. *Cell Metab.* 11, 213-219.
- Costford, S.R., Bajpeyi, S., Pasarica, M., Albarado, D.C., Thomas, S.C., Xie, H., Church, T.S., Jubrias, S.A., Conley, K.E., and Smith, S.R. (2010). Skeletal muscle NAMPT is induced by exercise in humans. *Am. J. Physiol. Endocrinol. Metab.* 298, E117-126.
- Croce, M.A., Eagon, J.C., LaRiviere, L.L., Korenblat, K.M., Klein, S., and Finck, B.N. (2007). Hepatic lipin 1beta expression is diminished in insulin-resistant obese subjects and is reactivated by marked weight loss. *Diabetes* 56, 2395-2399.
- Evans, J.L., Maddux, B.A., and Goldfine, I.D. (2005). The molecular basis for oxidative stress-induced insulin resistance. *Antioxid. Redox Signal.* 7, 1040-1052.
- Fulco, M., Cen, Y., Zhao, P., Hoffman, E.P., McBurney, M.W., Sauve, A.A., and Sartorelli, V. (2008). Glucose restriction inhibits skeletal myoblast differentiation by activating SIRT1 through AMPK-mediated regulation of Nampt. *Dev. Cell* 14, 661-673.
- Grimm, A.A., Brace, C.S., Wang, T., Stormo, G.D., and Imai, S.I. (2011). A nutrient-sensitive interaction between Sirt1 and HNF-1alpha regulates Crp expression. *Aging Cell* 10, 305-317.
- Haigis, M.C., and Sinclair, D.A. (2010). Mammalian sirtuins: biological insights and disease relevance. *Annu. Rev. Pathol.* 5, 253-295.

Hasmann, M., and Schemainda, I. (2003). FK866, a highly specific noncompetitive inhibitor of nicotinamide phosphoribosyltransferase, represents a novel mechanism for induction of tumor cell apoptosis. *Cancer Res.* 63, 7436-7442.

Home, P.D., and Pacini, G. (2008). Hepatic dysfunction and insulin insensitivity in type 2 diabetes mellitus: a critical target for insulin-sensitizing agents. *Diabetes Obes. Metab.* 10, 699-718.

Houtkooper, R.H., Canto, C., Wanders, R.J., and Auwerx, J. (2010). The secret life of NAD⁺: an old metabolite controlling new metabolic signaling pathways. *Endocr. Rev.* 31, 194-223.

Imai, S. (2010). "Clocks" in the NAD World: NAD as a metabolic oscillator for the regulation of metabolism and aging. *Biochim. Biophys. Acta* 1804, 1584-1590.

Imai, S., and Guarente, L. (2010). Ten years of NAD-dependent SIR2 family deacetylases: implications for metabolic diseases. *Trends Pharmacol. Sci.* 31, 212-220.

Jeoung, N.H., and Harris, R.A. (2008). Pyruvate dehydrogenase kinase-4 deficiency lowers blood glucose and improves glucose tolerance in diet-induced obese mice. *Am. J. Physiol. Endocrinol. Metab.* 295, E46-54.

Kim, S.Y., and Volsky, D.J. (2005). PAGE: parametric analysis of gene set enrichment. *BMC Bioinformatics* 6, 144.

Lazar, M.A. (2005). How obesity causes diabetes: not a tall tale. *Science* 307, 373-375.

Lowell, B.B., and Shulman, G.I. (2005). Mitochondrial dysfunction and type 2 diabetes. *Science* 307, 384-387.

Mattson, M.P. (2009). Roles of the lipid peroxidation product 4-hydroxynonenal in obesity, the metabolic syndrome, and associated vascular and neurodegenerative

disorders. *Exp. Gerontol.* 44, 625-633.

Meyer, M.R., Clegg, D.J., Prossnitz, E.R., and Barton, M. (2011). Obesity, insulin resistance and diabetes: sex differences and role of oestrogen receptors. *Acta Physiol (Oxf)* Epub on Feb 1.

Milne, J.C., Lambert, P.D., Schenk, S., Carney, D.P., Smith, J.J., Gagne, D.J., Jin, L., Boss, O., Perni, R.B., Vu, C.B., Bemis, J.E., Xie, R., Disch, J.S., Ng, P.Y., Nunes, J.J., Lynch, A.V., Yang, H., Galonek, H., Israelian, K., Choy, W., Iffland, A., Lavu, S., Medvedik, O., Sinclair, D.A., Olefsky, J.M., Jirousek, M.R., Elliott, P.J., and Westphal, C.H. (2007). Small molecule activators of SIRT1 as therapeutics for the treatment of type 2 diabetes. *Nature* 450, 712-716.

Moller, N., Gormsen, L., Fuglsang, J., and Gjedsted, J. (2003). Effects of ageing on insulin secretion and action. *Horm Res* 60, 102-104.

Moynihan, K.A., Grimm, A.A., Plueger, M.M., Bernal-Mizrachi, E., Ford, E., Cras-Meneur, C., Permutt, M.A., and Imai, S. (2005). Increased dosage of mammalian Sir2 in pancreatic b cells enhances glucose-stimulated insulin secretion in mice. *Cell Metab.* 2, 105-117.

Nakahata, Y., Sahar, S., Astarita, G., Kaluzova, M., and Sassone-Corsi, P. (2009). Circadian control of the NAD⁺ salvage pathway by CLOCK-SIRT1. *Science* 324, 654-657.

Nemeth, J., Stein, I., Haag, D., Riehl, A., Longerich, T., Horwitz, E., Breuhahn, K., Gebhardt, C., Schirmacher, P., Hahn, M., Ben-Neriah, Y., Pikarsky, E., Angel, P., and Hess, J. (2009). S100A8 and S100A9 are novel nuclear factor kappa B target genes during malignant progression of murine and human liver carcinogenesis. *Hepatology* 50,

1251-1262.

Nov, O., Kohl, A., Lewis, E.C., Bashan, N., Dvir, I., Ben-Shlomo, S., Fishman, S., Wueest, S., Konrad, D., and Rudich, A. (2010). Interleukin-1beta may mediate insulin resistance in liver-derived cells in response to adipocyte inflammation. *Endocrinology* 151, 4247-4256.

Peraldi, P., and Spiegelman, B. (1998). TNF-alpha and insulin resistance: summary and future prospects. *Mol. Cell. Biochem.* 182, 169-175.

Ramsey, K.M., Mills, K.F., Satoh, A., and Imai, S. (2008). Age-associated loss of Sirt1-mediated enhancement of glucose-stimulated insulin secretion in β cell-specific Sirt1-overexpressing (BESTO) mice. *Aging Cell* 7, 78-88.

Ramsey, K.M., Yoshino, J., Brace, C.S., Abrassart, D., Kobayashi, Y., Marcheva, B., Hong, H.K., Chong, J.L., Buhr, E.D., Lee, C., Takahashi, J.S., Imai, S., and Bass, J. (2009). Circadian Clock Feedback Cycle Through NAMPT-Mediated NAD⁺ Biosynthesis. *Science* 324, 651-654.

Revollo, J.R., Körner, A., Mills, K.F., Satoh, A., Wang, T., Garten, A., Dasgupta, B., Sasaki, Y., Wolberger, C., Townsend, R.R., Milbrandt, J., Kiess, W., and Imai, S. (2007). Nampt/PBEF/visfatin regulates insulin secretion in β cells as a systemic NAD biosynthetic enzyme. *Cell Metab.* 6, 363-375.

Rodgers, J.T., and Puigserver, P. (2007). Fasting-dependent glucose and lipid metabolic response through hepatic sirtuin 1. *Proc. Natl. Acad. Sci. USA* 104, 12861-12866.

Shoelson, S.E., Lee, J., and Goldfine, A.B. (2006). Inflammation and insulin resistance. *J. Clin. Invest.* 116, 1793-1801.

Yach, D., Stuckler, D., and Brownell, K.D. (2006). Epidemiologic and economic

consequences of the global epidemics of obesity and diabetes. *Nat. Med.* 12, 62-66.

Yeung, F., Hoberg, J.E., Ramsey, C.S., Keller, M.D., Jones, D.R., Frye, R.A., and Mayo, M.W. (2004). Modulation of NF- κ B-dependent transcription and cell survival by the SIRT1 deacetylase. *EMBO J.* 23, 2369-2380.

Figure S1

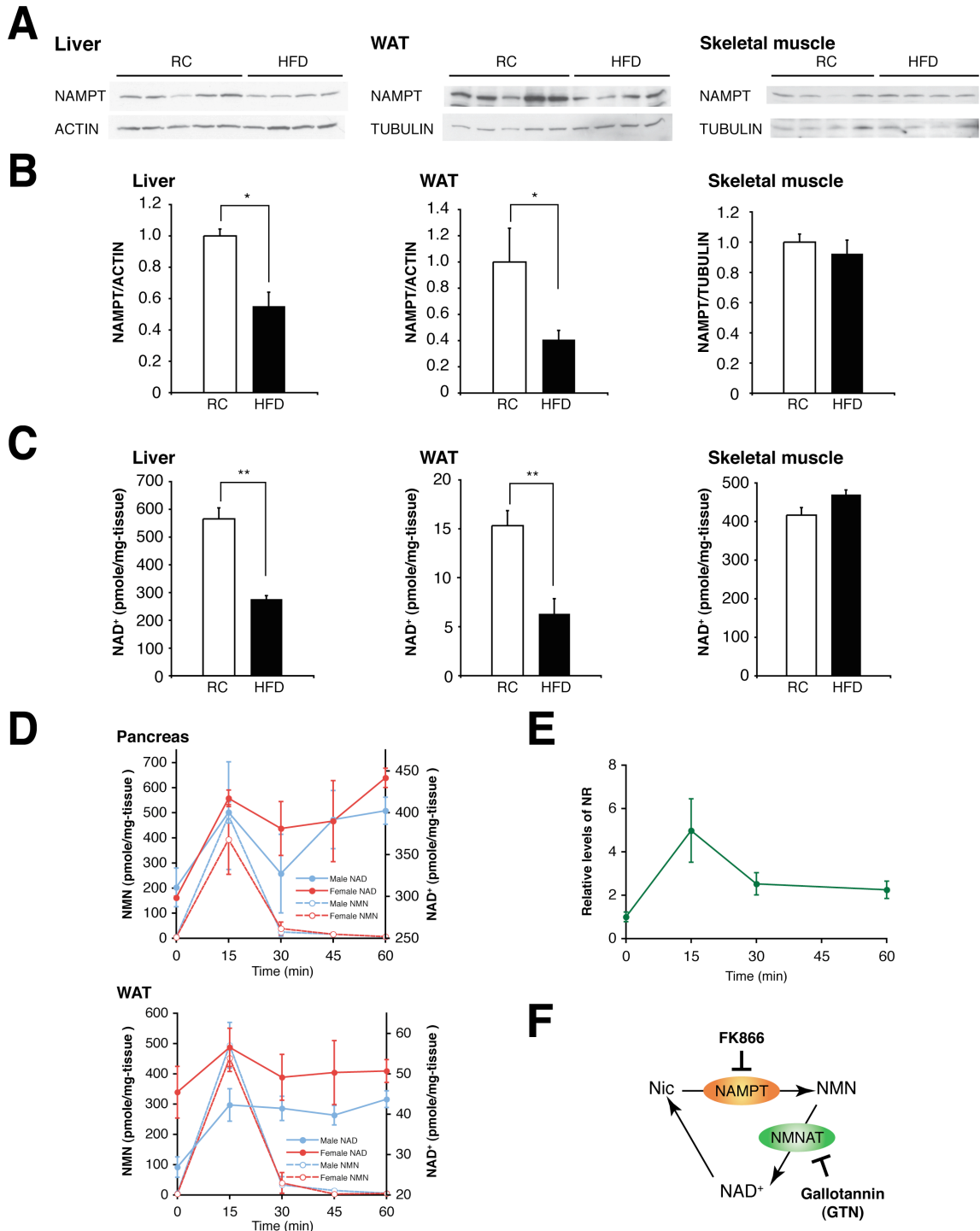


Figure S1. Defects in NAMPT-mediated NAD⁺ biosynthesis in high-fat diet-induced diabetic mice. (A) Western blots of NAMPT in the liver, white adipose tissue (WAT),

and skeletal muscle in RC and HFD female mice. **(B and C)** Levels of NAMPT **(B)** and NAD⁺ **(C)** in the liver, WAT, and skeletal muscle were measured in RC and HFD male mice. Mice at 3-6 months of age were fed a RC or a HFD for at least 3.5 months. NAMPT protein levels in RC and HFD mice were normalized to ACTIN (liver and WAT) or TUBULIN (skeletal muscle) (n=3-5 mice per group). NAD⁺ levels were measured by HPLC (n=4-9 mice per group). **(D)** Changes in NMN and NAD⁺ levels in the pancreas and WAT after NMN administration (500mg/kg body weight) (n=3 to 6 mice for each time point). **(E)** Relative nicotinamide riboside (NR) levels in liver extracts prepared from NMN-administered B6 female mice. Relative levels were assessed by the selected reaction monitoring (SRM) mode in LC/MS/MS (n=3 mice for each time point). **(F)** A diagram of the NAMPT-mediated NAD⁺ biosynthetic pathway. Nicotinamide (Nic) is the major precursor for NAD⁺ biosynthesis in mammals. NAMPT catalyzes the conversion of Nic to NMN as the rate-limiting enzyme in this pathway. Nicotinamide/nicotinic acid mononucleotide adenylyltransferase (NMNAT) converts NMN into NAD⁺. Enzyme inhibitors (FK866 and gallopamine) of the pathway are indicated. Data were analyzed by Student's unpaired *t* test. All values are presented as mean ± SEM. **P* < 0.05; ***P* < 0.01.

Figure S2

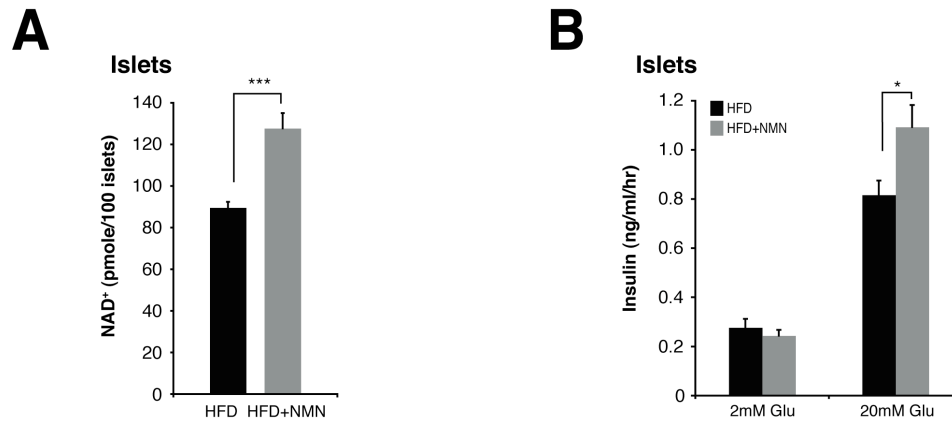


Figure S2. NAD⁺ levels and glucose-stimulated insulin secretion in HFD-fed primary islets treated with NMN. Primary islets isolated from HFD male mice were incubated in the presence or absence of 100 μ M NMN for 24 hrs prior to NAD⁺ measurement (**A**, n=6 islet groups from 4-6 mice) or glucose stimulation (**B**, n=18 islet groups from 8-12 mice). Data were analyzed by Student's unpaired *t* test. All values are presented as mean \pm SEM. **P* < 0.05; ****P* < 0.001.

Figure S3

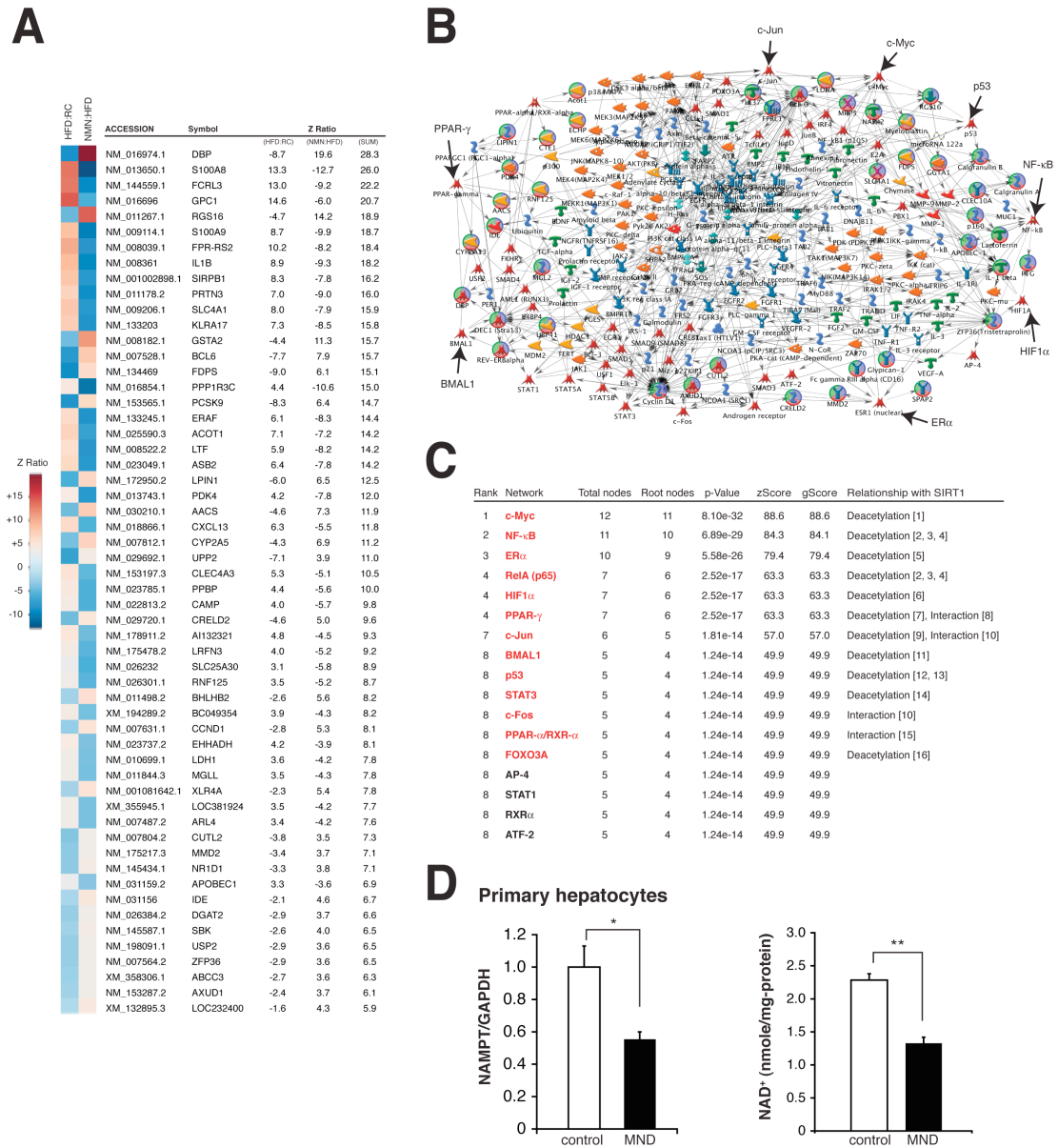


Figure S3. Microarray analysis of liver samples from RC, HFD, and NMN-treated HFD mice. (A) Gene expression data from microarrays were subjected to Z score transformation, and Z ratios were calculated. Genes were filtered based on false

discovery rates calculated by the Rank Product Analysis for the differences in expression levels between two conditions (RC vs HFD [HFD:RC] or HFD vs NMN-treated HFD [NMN:HFD]). Genes that showed their false discovery rates (FDR) less than 5% were selected and ordered based on the sum of the absolute numbers of Z ratios, a parameter that reflects the extent of the alterations between HFD feeding and NMN treatment. **(B)** The network was generated using the shortest path algorithm in the MetaCore program (GeneGo). **(C)** The transcription regulation (TR) algorithm was applied to identify transcription factors that likely cause gene expression changes detected by our microarray analyses. The total numbers of nodes were determined, and the probabilities of those links represented by zScore and gScore, and their p-values were calculated based on hypergeometric distribution. The resultant transcription factors were ranked by p-values. Transcription factors showing large total numbers of nodes (red) are all SIRT1 targets.

- ¹ J. Yuan, K. Minter-Dykhouse, and Z. Lou, *J Cell Biol.* 185 (2), 203 (2009).
- ² F. Yeung, J. E. Hoberg, C. S. Ramsey et al., *EMBO J.* 23 (12), 2369 (2004).
- ³ J. H. Lee, M. Y. Song, E. K. Song et al., *Diabetes* 58 (2), 344 (2009).
- ⁴ X. D. Yang, E. Tajkhorshid, and L. F. Chen, *Mol Cell Biol.* 30 (9), 2170 (2010).
- ⁵ M. Y. Kim, E. M. Woo, Y. T. Chong et al., *Mol Endocrinol.* 20 (7), 1479 (2006).
- ⁶ J. H. Lim, Y. M. Lee, Y. S. Chun et al., *Mol Cell* 38 (6), 864 (2010).
- ⁷ L. Han, R. Zhou, J. Niu et al., *Nucleic Acids Res.* (2010).
- ⁸ F. Picard, M. Kurtev, N. Chung et al., *Nature* 429 (6993), 771 (2004).
- ⁹ J. Zhang, S. M. Lee, S. Shannon et al., *J Clin Invest.* 119 (10), 3048 (2009).
- ¹⁰ R. Zhang, H. Z. Chen, J. J. Liu et al., *J Biol Chem.* 285 (10), 7097 (2010).
- ¹¹ Y. Nakahata, M. Kaluzova, B. Grimaldi et al., *Cell* 134 (2), 329 (2008).
- ¹² J. Luo, A. Y. Nikolaev, S. Imai et al., *Cell* 107 (2), 137 (2001).
- ¹³ H. Vaziri, S. K. Dessain, E. Ng Eaton et al., *Cell* 107 (2), 149 (2001).
- ¹⁴ Y. Nie, D. M. Erion, Z. Yuan et al., *Nat Cell Biol.* 11 (4), 492 (2009).
- ¹⁵ A. Purushotham, T. T. Schug, Q. Xu et al., *Cell Metab.* 9 (4), 327 (2009)
- ¹⁶ M. C. Motta, N. Divecha, M. Lemieux et al., *Cell* 116 (4), 551 (2004).

(D) The effects of menadione, an oxidative stress-inducing reagent, on NAMPT protein and NAD⁺ levels. Primary hepatocytes were treated with 20 μM menadione (MND) for 5 hrs. Data were analyzed by Student's unpaired *t* test. All values are presented as mean ± SEM. **P* < 0.05; ***P* < 0.01.

Figure S4

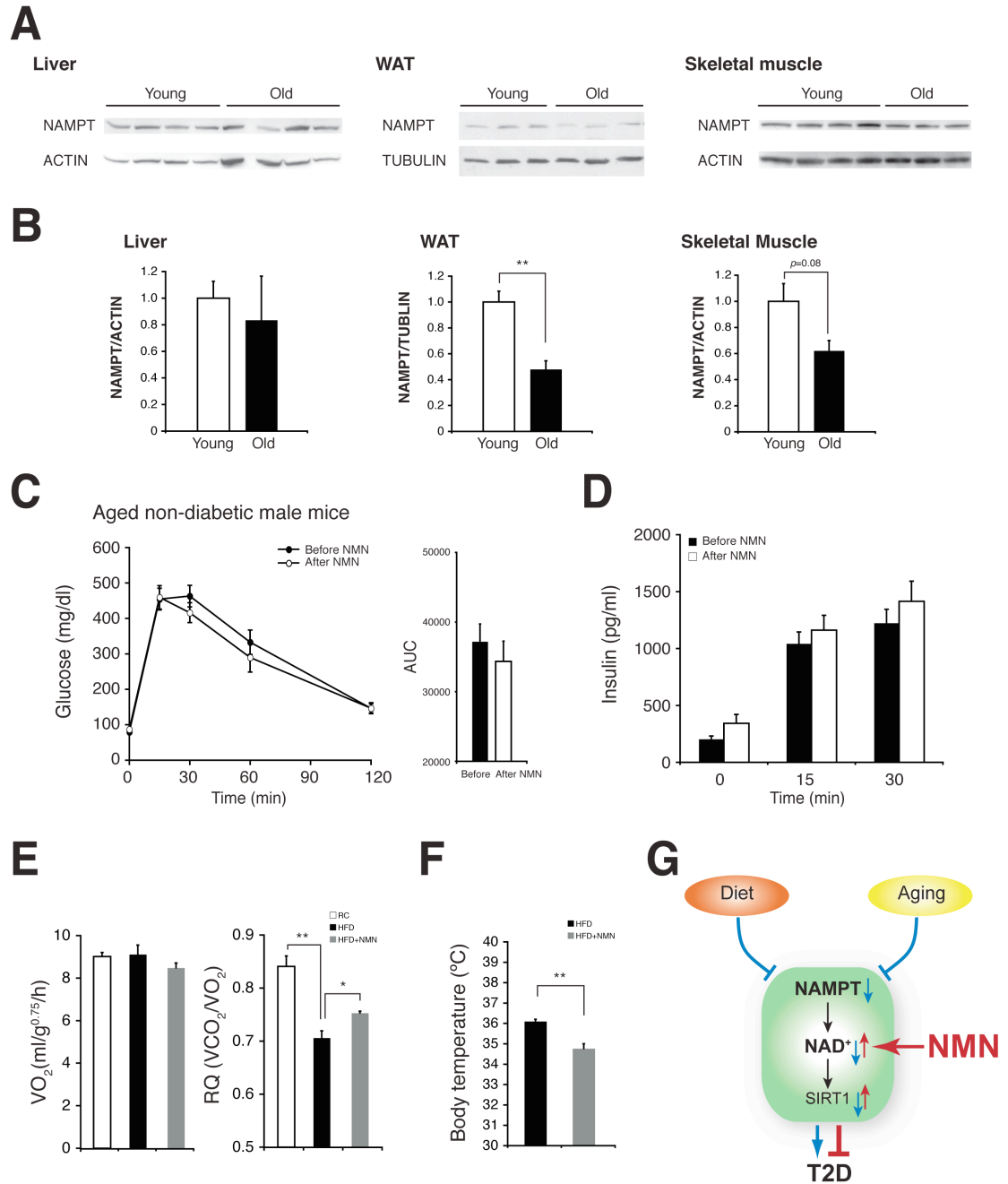


Figure S4. NAMPT protein levels and the effect of NMN on metabolism in aged mice. (A and B) Western blots of NAMPT in the liver, WAT, and skeletal muscle

between young and old mice. NAMPT protein levels were normalized to ACTIN (liver and skeletal muscle) or TUBULIN (WAT) (**B**, n= 3-4 mice per group). (**C**) Glucose tolerance in aged, non-diabetic male mice before (closed circles) and after (open circles) a single dose of NMN (n=7). The areas under each glucose tolerance curve are presented next to the glucose tolerance curves. (**D**) Plasma insulin levels were measured during IPGTTs for non-diabetic mice (n=6-7). (**E** and **F**) Indirect calorimetry over a 12-hr period (7:00 pm-7:00 am) and body temperature in HFD females. Female mice at 10-11 months of age were fed HFD for 8 weeks and treated with NMN. Oxygen consumption (VO_2), respiratory quotient (RQ) (**E**, n=3 independent measurements, 2 mice per measurement), and rectal body temperature (**F**, n=6 per group) were measured before and after NMN. Data were analyzed by Student's paired or unpaired *t* test. All values are presented as mean \pm SEM. **P* < 0.05; ***P* <0.01. (**G**) A model for the effect of NMN against diet- and age-induced T2D. NAMPT-mediated NAD^+ biosynthesis is compromised by HFD or aging, contributing to the pathogenesis of T2D. NMN restores the defects in NAMPT-mediated NAD^+ biosynthesis and treats the pathophysiology of T2D.

SUPPLEMENTAL EXPERIMENTAL PROCEDURES

Animal Experimentation

Wild-type C57BL/6J mice were bred in our laboratory or purchased from Jackson Laboratories. Mice were maintained on a regular chow (RC) (PicoLab 5053 Rodent Diet 20; Lab Diets) *ad libitum*. In HFD feeding experiments, fasted glucose levels and glucose tolerance were assessed at 3 and 6 months after starting a HFD. To obtain age-induced diabetic mice, we screened male and female mice at 15-26 months of age following the same criteria. For IPGTTs, mice were fasted for 15 hrs, and 50% dextrose (2g/kg body weight) was injected intraperitoneally. Blood was collected from the tail vein at 0, 15, 30, 60, and 120 min. Blood glucose levels were measured by the Accu-Chek II glucometer (Roche Diagnosis), and plasma insulin levels were determined using the Singulex Erenna immunoassay system at the Washington University Core Laboratory for Clinical Studies. For insulin tolerance tests, mice were fasted for 4 hrs before they were injected with human insulin (0.75 U kg⁻¹ body weight; Lilly). Blood glucose levels were measured at 0, 15, 30, 45, and 60 min after insulin injection. For lipid levels, cholesterol and triglycerides were measured using reagents from Thermo Electron Corporation (Waltham, MA), while non-esterified free fatty acid levels were measured using reagents from Wako (Richmond, VA) in the Washington University Animal Model Research Core associated with the Nutrition Obesity Research Center (NORC) and the Diabetes Research and Training Center (DRTC).

Western blotting

40-100 µg of whole tissue extracts were analyzed by Western blotting. Anti-

PBEF/NAMPT (Bethyl Laboratories), anti-NAMPT (Revollo et al., 2004), anti-tubulin (Santa Cruz), anti-actin (Calbiochem), anti-phospho-AKT (Ser473), and anti-AKT (Cell Signaling Technology) antibodies were used as primary antibodies. Horseradish peroxidase-conjugated anti-rabbit IgG (Amersham and Cell Signaling Technology) and anti-mouse IgG (Amersham) antibodies were used as secondary antibodies. Signals were visualized using the ECL detection system (Amersham).

NAD⁺ and NMN measurements by HPLC

Frozen tissues or cultured cells were extracted in perchloric acid and neutralized in K₂CO₃ on ice as described previously (Ramsey et al., 2009). For NAD⁺ measurement, the HPLC was run at a flow rate of 1 ml/min with 100% buffer A from 0-5 min, a linear gradient to 95% buffer A/5% buffer B (100% methanol) from 5-6 min, 95% buffer A/5% buffer B from 6-11 min, a linear gradient to 85% buffer A/15% buffer B from 11-13 min, 85% buffer A/15% buffer B from 13-23 min, and a linear gradient to 100% buffer A from 23-24 min. For NMN measurement, the HPLC was run at a flow rate of 1 ml/min with 100% buffer A from 0-5 min, a linear gradient to 60% buffer A/40% buffer B from 5-10 min, 60% buffer A/40% buffer B from 10-32.5 min, a linear gradient to 100% buffer A from 32.5-35 min. NAD⁺ and NMN were usually eluted at 11 min and 20 min, respectively. NAD⁺ and NMN levels were quantitated based on the peak area compared to a standard curve and normalized to weights of frozen tissues, protein content of primary hepatocytes, or to the number of primary islets. The NAD⁺ measurements in primary islets were conducted in triplicates of islets pooled from two or three individual mice and repeated twice. NAD⁺ and NMN fractions from HPLC were further analyzed

and confirmed by LC/MS/MS.

Mass spectrometry analysis of nicotinamide riboside (NR)

Liquid chromatography-tandem mass spectrometry (LC/MS/MS) was performed with a Shimadzu 10A HPLC system (Shimadzu Scientific Instruments, Columbia, MD) coupled to a TSQ Quantum Ultra triple quadrupole mass spectrometer (Thermo Finnigan, San Jose, USA) in the positive mode. NR was separated with the above HPLC system with a Hypercarb column. The mobile phase was composed of 0.1% trifluoroacetic acid (TFA) in water (buffer A) and 0.1% TFA in 100% acetonitrile (buffer B). The LC was run at a flow rate of 0.6 ml/min with 95% buffer A/5% buffer B from 0-0.2 min, a linear gradient to 50% buffer A/50% buffer B from 0.2-5 min. The column was kept at 50% buffer A/50% buffer B until 6.0 min, reverted to 95% buffer A/5% buffer B by 6.1 min, and re-equilibrated until 11.0 min. NR in liver extracts was detected using the selected reaction monitoring (SRM) mode. Two transitions were used; m/z 255 \rightarrow 123 (quantification) and m/z 255 \rightarrow 106 (confirmation). Relative NR levels were quantitated based on the peak area and normalized to that at 0 min time point.

Islet isolation and *in vitro* insulin secretion analysis

Islets were isolated from HFD-fed mice as described previously (Revollo et al., 2007). For treatments with NMN, islets were cultured for 24 hrs in RPMI media containing 100 μ M NMN.

Micorarrays and bioinformatic analyses

For individual genes, raw microarray data were subjected to Z score transformation, and Z ratios were calculated as described previously (Cheadle et al., 2003). False discovery rates for the differences in expression levels between two conditions (RC-fed vs HFD-fed or HFD-fed vs NMN-treated HFD-fed livers) were calculated using the Rank Product Analysis (Hong et al., 2006). We identified genes whose expression levels were significantly altered between two conditions with the false discovery rate (FDR) less than 5%. The genes filtered by the Rank Product Analysis were ordered based on the sum of the absolute numbers of Z ratios, a parameter that reflects the extent of the alterations between HFD feeding and NMN treatment. For the Parametric Analysis of Gene Set Enrichment (PAGE) analysis, GO biological process and GO molecular function gene sets (GO gene sets; http://www.broad.mit.edu/gsea/msigdb/msigdb_index.html) were used with our microarray data, and Z scores were calculated for each gene set, as previously described (Kim and Volsky, 2005). All data were analyzed by the R statistical software package (available at www.bioconductor.org). For the biological network analysis, the shortest path algorithm was used to deduce possible networks based on our microarray results using the MetaCore program (version 6.3) (GeneGo). We also applied the transcription regulation (TR) algorithm to identify transcription factors that likely cause gene expression changes detected by our microarray analyses. The total numbers of nodes were determined, and the probabilities of those links represented by zScore and gScore and their p-values were calculated based on hypergeometric distribution. The resultant transcription factors were ranked by p-values.

Indirect calorimetry measurements

Metabolic parameters were measured using an Oxymax indirect calorimetry system (Columbus Instruments, Columbus, OH) (Bernal-Mizrachi et al., 2002). Two mice were housed per chamber with a 12-h light/ 12-h dark cycle in an ambient temperature of 23-25°C. VO_2 and VCO_2 were determined under Oxymax system settings as follows: air flow, 1.6 l/min; sample flow, 0.5 l/min; reference settling time, 2 min; and measuring time, 0.5 min. The system was calibrated against a standard gas mixture to measure O_2 consumed (VO_2 , ml/g^{0.75}/h) and CO_2 generated (VCO_2 , ml/g^{0.75}/h). Oxygen consumption (VO_2) and respiratory quotient (RQ; VCO_2/VO_2) were evaluated over a 12-h period.

SUPPLEMENTAL REFERENCES

Bernal-Mizrachi, C., Weng, S., Li, B., Nolte, L.A., Feng, C., Coleman, T., Holloszy, J.O., and Semenkovich, C.F. (2002). Respiratory uncoupling lowers blood pressure through a leptin-dependent mechanism in genetically obese mice. *Arterioscler. Thromb. Vasc. Biol.* 22, 961-968.

Cheadle, C., Vawter, M.P., Freed, W.J., and Becker, K.G. (2003). Analysis of microarray data using Z score transformation. *J. Mol. Diagn.* 5, 73-81.

Hong, F., Breitling, R., McEntee, C.W., Wittner, B.S., Nemhauser, J.L., and Chory, J. (2006). RankProd: a bioconductor package for detecting differentially expressed genes in meta-analysis. *Bioinformatics* 22, 2825-2827.

Kim, S.Y., and Volsky, D.J. (2005). PAGE: parametric analysis of gene set enrichment. *BMC Bioinformatics* 6, 144.

Ramsey, K.M., Yoshino, J., Brace, C.S., Abrassart, D., Kobayashi, Y., Marcheva, B., Hong, H.K., Chong, J.L., Buhr, E.D., Lee, C., Takahashi, J.S., Imai, S., and Bass, J. (2009). Circadian Clock Feedback Cycle Through NAMPT-Mediated NAD⁺ Biosynthesis. *Science* 324, 651-654.

Revollo, J.R., Grimm, A.A., and Imai, S. (2004). The NAD biosynthesis pathway mediated by nicotinamide phosphoribosyltransferase regulates Sir2 activity in mammalian cells. *J. Biol. Chem.* 279, 50754-50763.

Revollo, J.R., Körner, A., Mills, K.F., Satoh, A., Wang, T., Garten, A., Dasgupta, B., Sasaki, Y., Wolberger, C., Townsend, R.R., Milbrandt, J., Kiess, W., and Imai, S. (2007). Nampt/PBEF/visfatin regulates insulin secretion in β cells as a systemic NAD

biosynthetic enzyme. *Cell Metab.* 6, 363-375.

Chapter 3.

**eNAMPT secretion from adipose tissue
is regulated by SIRT1 through its deacetylation**

ABSTRACT

Nicotinamide phosphoribosyltransferase (NAMPT) is the rate-limiting enzyme in the NAD biosynthesis pathway in mammals. Interestingly, NAMPT has intra- and extracellular forms (iNAMPT and eNAMPT, respectively), and eNAMPT is secreted from adipose tissue as one of the adipokines. However, the mechanism underlying the regulation of eNAMPT secretion has not been fully understood yet. Here, we have demonstrated that deacetylation on NAMPT by SIRT1 controls its secretion from adipocytes. iNAMPT is acetylated in both brown and white adipose tissues, and the level of acetylation of iNAMPT is decreased during fasting when Sirtuins are activated. We also found that enhancement of eNAMPT secretion under low glucose culture condition in differentiated brown and white adipocytes is completely inhibited by nicotinamide (NAM), an inhibitor of SIRTs, suggesting that deacetylation by SIRTs is required to induce eNAMPT secretion by low glucose stimulus. Consistently, eNAMPT levels in the blood were enhanced after 48 hours fasting in WT but not in Sirt1 KO mice, and iNAMPT acetylation levels are decreased while eNAMPT secretion is increased in differentiated adipocytes by SIRT1 overexpression. In addition, iNAMPT physically interacts with SIRT1 in differentiated adipocytes, and this interaction is enhanced under a low-glucose culture condition, suggesting that SIRT1 deacetylates iNAMPT by direct interaction and increases eNAMPT secretion. We have found five acetylation sites on iNAMPT and only 4 out of 5 were deacetylated. SIRT1 is responsible for deacetylating lysine 53, which results in both increased enzymatic activity and secretion of eNAMPT. These results strongly support the notion that eNAMPT secretion is controlled by SIRT1-mediated deacetylation. Taken together, our results indicate a novel feedback loop

regulating systemic NAD biosynthesis through SIRT1 and eNAMPT and provide important insight into therapeutic and preventive intervention for metabolic diseases such as type 2 diabetes.

INTRODUCTION

Over the past decade, an accumulating body of evidence suggests that the biosynthesis of nicotinamide adenine dinucleotide (NAD), an essential coenzyme and important currency for cellular energy metabolism, plays a critical role in the regulation of diverse biological processes through key NAD-consuming mediators, including poly-ADP-ribose polymerases (PARPs), CD38/157 ectoenzymes, and sirtuins¹. In mammals, NAD can be synthesized from four different substrates: two different forms of vitamin B₃, namely, nicotinamide and nicotinic acid, tryptophan, and nicotinamide riboside (NR)². Among them, nicotinamide is predominantly used to synthesize NAD in mammals³. The NAD biosynthesis starting from nicotinamide is catalyzed by two key enzymes: nicotinamide phosphoribosyltransferase (NAMPT) and nicotinamide mononucleotide adenylyltransferase (NMNAT)⁴. NAMPT, the rate-limiting enzyme in this NAD biosynthetic pathway, catalyzes the conversion of nicotinamide and 5-phosphoribosyl-pyrophosphate to nicotinamide mononucleotide (NMN), a key NAD intermediate. NMN, in turn, is adenylated by NMNAT to NAD⁴.

NAMPT is a unique enzyme that has an ancient origin and an interesting research history. NAMPT was originally identified as the product of the gene that confers the capability of synthesizing NAD from nicotinamide, called *NadV*, in the bacteria *Haemophilus ducreyi*⁵. Surprisingly, a set of genes encoding NAMPT and NMNAT homologues has been found even in some bacteriophages⁶. The biochemical and structural features of NAMPT have been extensively studied by our and other groups, clearly demonstrating that this protein belongs to a dimeric class of type II phosphoribosyltransferases^{7,8}. Interestingly, NAMPT has two different forms in

mammals: intra- and extracellular NAMPT (iNAMPT and eNAMPT, respectively). eNAMPT was previously identified as pre-B cell colony-enhancing factor (PBEF), a presumptive cytokine that enhances the maturation of B cell precursors in the presence of interleukin-7 (IL-7) and stem cell factor (SCF)⁹, and visfatin, a visceral fat-derived adipokine that was once proposed to exert an insulin-mimetic function by binding to the insulin receptor¹⁰. Neither function of PBEF and visfatin has been confirmed to date. Indeed, we have clearly demonstrated that NAMPT functions as an intra- and extracellular NAD biosynthetic enzyme and that eNAMPT does not exert insulin-mimetic effects both *in vitro* and *in vivo*^{4,11}. However, the physiological relevance and function of eNAMPT has still been controversial. For instance, a number of studies implicate that eNAMPT might function as a proinflammatory cytokine, although the enzymatic activity still appears to be required in some cases¹²⁻¹⁵. Additionally, because NAMPT does not have a cleavable signal sequence⁹, whether eNAMPT is positively secreted or passively produced due to cell lysis or cell death has been a significant debate.

Here we show that the secretion and the enzymatic activity of eNAMPT are regulated by SIRT1, the mammalian sirtuin family NAD-dependent deacetylase, in adipose tissues in response to glucose availability. Deacetylation of iNAMPT at lysine 53, a residue located close to the catalytic sites at the cleft of the NAMPT dimer, predisposes the protein to secretion and enhances its enzymatic activity in adipose tissues. These findings open a new possibility that adipose tissue functions as a critical modulator for systemic NAD biosynthesis through the NAD/SIRT1-dependent regulation of the secretion and the enzymatic activity of eNAMPT.

RESULTS

Acetylation levels of iNAMPT affect the secretion of eNAMPT

We have previously demonstrated that fully differentiated brown and white adipocytes positively secrete eNAMPT, which is enzymatically twice as active as iNAMPT¹¹. We speculated that a post-translational modification was likely responsible for the altered enzymatic activity and the secretion of eNAMPT. During our intensive search for modifications on the NAMPT protein, we found that iNAMPT was acetylated in brown and white adipose tissue (BAT and WAT, respectively) (Figure 1A). Interestingly, acetylation levels of iNAMPT decreased by ~50% in response to 48-hr fasting (Figure 1A). To recapitulate the alteration in iNAMPT acetylation in a cell culture system, we used differentiated HIB-1B brown adipocytes, which express a very high level of iNAMPT and secrete eNAMPT into culture supernatants. In cell extracts from HIB-1B adipocytes, relatively low levels of acetylated iNAMPT were detected (Figure 1B, lane M). Acetylation levels significantly increased when treating cells with trichostatin A (TSA) and nicotinamide, inhibitors of class I and II deacetylases and class III NAD-dependent deacetylases, respectively (Figure 1B, right two T+N lanes). In this condition, iNAMPT protein levels did not change in cell extracts, whereas secreted eNAMPT protein levels in culture supernatants decreased by ~60% (Figure 1C), implicating that the acetylation status of iNAMPT might predispose the protein to secretion. Because fasting decreased acetylation levels of iNAMPT in adipose tissue, we examined the effects of low glucose in media on iNAMPT acetylation and eNAMPT secretion in HIB-1B cells. The detection of decreased iNAMPT acetylation turned out to be technically difficult due to relatively low levels of acetylated iNAMPT in HIB-1B cells.

Nonetheless, lowering glucose dramatically enhanced eNAMPT secretion 3.5 to 5.5-fold in differentiated HIB-1B cells and 3T3-L1 white adipocytes (Figure 1D). Furthermore, nicotinamide completely inhibited the enhancement of eNAMPT secretion by low glucose (Figure 1D), suggesting that deacetylation of iNAMPT by nicotinamide-sensitive sirtuin family members might be responsible for the low glucose-induced enhancement of eNAMPT secretion.

SIRT1 regulates eNAMPT secretion by physically interacting with and deacetylating iNAMPT

It has been well known that the enzymatic activity of Sirtuins is effectively inhibited by nicotinamide in culture¹⁶. Among them SIRT1 is the direct homologue of the yeast Sir2, the first member of the Sirtuin family, having a broad range of targets^{17,18}. Therefore, we hypothesized that SIRT1 might regulate eNAMPT secretion in adipose tissue. To address this possibility, we examined whole-body *Sirt1* knockout (*Sirt1*^{-/-}) mice in the FVB background. Different from other *Sirt1*^{-/-} mouse lines in the B6 or 129 backgrounds, these FVB *Sirt1*^{-/-} mice do not die postnatally and can grow into adulthood¹⁹. In *Sirt1*^{+/+} mice, plasma eNAMPT levels showed moderate, but significant increases in response to 48-hr fasting (Figure 2A). However, these increases were completely abrogated in *Sirt1*^{-/-} mice (Figure 2A). Intriguingly, iNAMPT significantly accumulated in the WAT of *Sirt1*^{-/-} mice compared to *Sirt1*^{+/+} mice, whereas the iNAMPT protein levels did not differ in the liver between *Sirt1*^{+/+} and *Sirt1*^{-/-} mice (Figure 2B). Given that *Nampt* mRNA levels were indistinguishable in WAT between *Sirt1*^{+/+} and *Sirt1*^{-/-} mice (Figure 2C), this abnormal accumulation of iNAMPT in *Sirt1*^{-/-} WAT is likely associated with the defect in

eNAMPT secretion in *Sirt1*^{-/-} mice.

To further examine the connection between SIRT1 and eNAMPT secretion, we infected differentiated HIB-1B adipocytes with adenoviruses carrying either *Sirt1* or *Gfp* expression vectors and measured eNAMPT secretion. Overexpression of SIRT1 enhanced eNAMPT secretion 2.3-fold compared to GFP controls in differentiated HIB-1B cells (Figure 3A). We further confirmed this result by introducing both NAMPT and SIRT1 into HEK293 cells. Again, overexpression of SIRT1 enhanced eNAMPT secretion, and the effect was much more dramatic in HEK293 cells (~11-fold) compared to that in differentiated HIB-1B cells (Figure 3B). In this condition, we assessed the acetylation status of iNAMPT. Acetylated iNAMPT was detected only in the presence of TSA and nicotinamide, and iNAMPT acetylation levels significantly decreased by SIRT1 overexpression (Figure 3C). These results, in combination with the results from *Sirt1*^{-/-} mice, suggest that SIRT1-mediated deacetylation of iNAMPT predisposes the protein to be secreted from differentiated adipocytes.

Because SIRT1 tends to physically interact with its deacetylation targets, we also examined whether SIRT1 and iNAMPT physically interact in differentiated adipocytes. Indeed, SIRT1 and iNAMPT did interact in differentiated HIB-1B adipocytes (Figure 3D). Interestingly, the interaction between SIRT1 and iNAMPT appeared to be enhanced by low glucose (Figure 3D, right two lanes). Although SIRT1 is usually considered as a nuclear sirtuin, we found that a considerable amount of SIRT1 was localized in the cytoplasmic fractions from differentiated HIB-1B and 3T3-L1 cells (Figures 3E and S1). iNAMPT was primarily localized in the cytoplasm of these adipocytes (Figures 3E and S3). Therefore, these results suggest that SIRT1 physically

interacts with and deacetylates iNAMPT in the cytoplasm of differentiated adipocytes, promoting the secretion of eNAMPT.

Deacetylation of lysine 53 on iNAMPT enhances eNAMPT secretion

We next attempted to determine which acetylated residues of iNAMPT are important for the regulation of eNAMPT secretion. We established HEK293 and differentiated HIB-1B cells expressing C-terminally FLAG-tagged iNAMPT, and FLAG-tagged iNAMPT and eNAMPT proteins were purified from those cell extracts and culture supernatants, respectively. These purified NAMPT proteins, as well as the bacterially produced recombinant NAMPT protein, were subjected to a mass spectrometric analysis of protein modification. Five lysines, K53, K79, K107, K331, and K369, were found to be acetylated on iNAMPT, whereas only K369 was acetylated on eNAMPT (Figures 4A and S2). Surprisingly, four out of the five lysines were also acetylated on bacterially produced recombinant NAMPT, although it did not have acetylated K107 but acetylated K339 (Figure 4A), implying that the regulation of NAMPT acetylation might be conserved from bacteria to mammals. Among these acetylated lysines, the location of K53 on the crystal structure of iNAMPT is particularly interesting. NAMPT is a dimeric type II phosphoribosyltransferase, and K53, which protrudes from each monomer, is nicely aligned along the “cleft” of the dimer and located very close to the catalytic sites (Figure 4B). Contrarily, K79 is located along the other cleft on the opposite side of the dimer to the one containing K53 (Figure 4B). The other acetylated lysines are located on surrounding α -helices on both sides of the dimer. Therefore, we decided to introduce the deacetylation-mimicking K-to-R mutation into K53 and/or K79 and examined the

acetylation levels of each mutant iNAMPT, in the presence or absence of SIRT1, compared to that of the wild-type NAMPT protein in HEK293 cells. Whereas the wild-type and K79R mutant iNAMPT proteins showed SIRT1-dependent deacetylation, the K53R and K53/79R mutant iNAMPT proteins displayed reduced acetylation levels and did not show further reduction in acetylation levels by SIRT1 (Figure 4C), suggesting that K53 is the SIRT1-dependent acetylation site on iNAMPT. We then examined the enzymatic activity and the secretion of this K53R mutant, as well as another mutant K53A and the wild-type NAMPT protein in differentiated HIB-1B adipocytes that express FLAG-tagged versions of these proteins. The enzymatic activity of both K53R and K53A mutants did not differ from that of the wild-type protein (Figure 4D). However, the secretion of these mutant proteins was 2.5 to 3-fold higher than that of the wild-type protein (Figure 4E), strongly suggesting the importance of this particular lysine and its deacetylation for the regulation of eNAMPT secretion. Conversely, the introduction of the acetylation-mimicking K-to-Q mutation into K53 significantly decreases the enzymatic activity and the secretion of the protein (Figures 4F and 4G), suggesting that acetylation of lysine 53 suppresses NAMPT enzymatic activity and also prevents the protein from being secreted. Taken together, these results demonstrate that eNAMPT secretion is regulated by SIRT1 through the deacetylation of lysine 53 in differentiated adipocytes.

DISCUSSION

In our previous study, we have shown that eNAMPT is positively secreted by fully differentiated adipocytes through an unidentified non-classical secretory pathway. We have also shown that eNAMPT possesses significantly higher enzymatic activity compared to iNAMPT, implying that the secretion and the enzymatic activity of eNAMPT might be regulated in a coordinated manner. Our present study clearly demonstrates that the secretion and the enzymatic activity of eNAMPT are regulated by SIRT1-dependent deacetylation in adipocytes. First, iNAMPT is acetylated in WAT and BAT, and its acetylation levels decrease in response to fasting. Second, in differentiated adipocyte cultures, lowering glucose increases eNAMPT secretion, and nicotinamide, an inhibitor of SIRT1 enzymatic activity, completely abrogates the low glucose-induced increase in eNAMPT secretion. Third, *Sirt1*^{-/-} mice fail to show fasting-induced increases in plasma eNAMPT levels and show abnormal accumulation of iNAMPT in WAT. Fourth, in differentiated adipocytes, SIRT1 decreases iNAMPT acetylation levels and increases eNAMPT secretion through its physical interaction with NAMPT, whereas treatment with nicotinamide and trichostatin A increases iNAMPT acetylation and decreases eNAMPT secretion. Lastly, lysine 53, which is located close to the catalytic sites of dimeric NAMPT, is the SIRT1-sensitive acetylation site. Deacetylation-mimetic K-to-R mutation of this particular lysine increases eNAMPT secretion, whereas acetylation-mimetic K-to-Q mutation decreases the secretion and the enzymatic activity of eNAMPT in differentiated adipocytes. Whether eNAMPT is positively secreted or is produced simply due to cell lysis or cell death has been a serious debate. However, in this present study, our results provide compelling evidence that eNAMPT secretion is a

highly regulated process in adipose tissue in response to changes in nutritional availability.

Our and other groups have previously demonstrated that SIRT1 and NAMPT comprise a novel transcriptional-enzymatic feedback loop that produces a circadian oscillation of NAD in peripheral tissues^{20,21}. Our present study has revealed that SIRT1 and NAMPT comprise another NAD-regulatory feedback loop through the regulation of eNAMPT secretion in adipose tissue. In this new mechanism, SIRT1-dependent deacetylation of iNAMPT at lysine 53 predisposes the protein to secretion. The deacetylation event seems to occur in the cytoplasm of differentiated adipocytes, and approximately 0.5% of iNAMPT per hour is estimated to be secreted as eNAMPT in differentiated HIB-1B adipocytes (data not shown), suggesting that a very specific fraction of iNAMPT is destined to enter this SIRT1-dependent secretory machinery. Experiments with K-to-R and K-to-Q mutants of lysine 53 demonstrate that the acetylation status of lysine 53 is critical to determine the fate of iNAMPT. Because the K53A mutation also significantly increases eNAMPT secretion, lysine 53 *per se* appears to play an important role in determining the fate of iNAMPT, possibly providing a docking site to an unidentified factor that might interact with acetylated lysine 53 of iNAMPT and prevent it from secretion (Figure 5). Interestingly, it has been reported that in monocytes and macrophages activated by inflammatory stimuli, High Mobility Group protein 1 (HMGB1), a highly conserved chromatin architectural protein, is hyperacetylated and secreted as a proinflammatory cytokine²². In the case of HMGB1, hyperacetylation triggered by inflammatory stimuli redirects the protein from the nucleus to the cytoplasm and then to secretory lysosomes. Given that NAMPT has also been

reported to be nuclear, acetylation on specific lysines might be important to keep iNAMPT in the cytoplasmic compartment, sequestering it from secretion and nuclear transport.

Acetylation is also important to regulate the enzymatic activity of NAMPT. We identified five acetylation sites on iNAMPT, and four out of these five sites are deacetylated on eNAMPT. Interestingly, the enzymatic activity of iNAMPT is 2-fold lower than that of eNAMPT, and the K53Q mutant can recapitulate this acetylation-dependent reduction in the enzymatic activity. Lysine 53 is distinguished from other lysine residues because it is located at the “cleft” that contains the catalytic sites, although the other lysines might have other functions in different biological contexts. These results suggest that acetylation/deacetylation might induce a conformational change in the NAMPT structure and regulate its enzymatic activity. It will be of great interest to examine what effects the acetylation of lysine 53 makes on the structure of the catalytic sites and dimer formation of NAMPT. Because NAD drives SIRT1 activity in a circadian oscillatory manner, it is also likely that the deacetylation and the secretion of eNAMPT follow circadian oscillation. Indeed, plasma eNAMPT levels appear to show diurnal oscillation in mice, although it is still unclear whether this oscillation is produced by an intrinsic clock mechanism (Yoon and Imai, unpublished observation). Although where exactly NMN is synthesized by eNAMPT still remains unsolved, our findings provide an interesting possibility that the intimate interplay between SIRT1 and NAMPT contributes to multi-layered feedback loops regulating the dynamics of NAD biosynthesis within and between tissues and organs.

In conclusion, our finding that adipose tissue actively regulates the secretion

and the enzymatic activity of eNAMPT in an NAD/SIRT1-dependent manner provides strong support to the idea that adipose tissue functions as a critical determinant for the spatial and temporal coordination of NAD biosynthesis throughout the body. This systemic coordination of NAD biosynthesis might play an important role in orchestrating metabolic responses in multiple tissues and maintaining metabolic homeostasis against nutritional and environmental perturbations. In this highly coordinated systemic network, adipose tissue modulates the functions of remote tissues through the NAD/SIRT1-dependent regulation of eNAMPT secretion. This model also predicts that having an optimal amount of adipose tissue might be beneficial to maximize the robustness of the physiological system through the regulation of a proper amount of eNAMPT secretion. Further investigation of the dynamics of NAD on a systemic level will provide further insight into the role of adipose tissue as a critical modulator for the regulation of systemic NAD biosynthesis and metabolic regulation.

EXPERIMENTAL PROCEDURES

Detection of intracellular NAMPT and SIRT1 in tissues, and of extracellular NAMPT in plasma

Mice fed *ad libitum* or fasted for 48 hours were euthanized by carbon dioxide asphyxiation. Organs were immediately collected, homogenized in 1X Laemmli's sample buffer using a Polytron (Kinematica, Switzerland), and boiled for 5 minutes. Samples were then centrifuged at 16000g and protein concentrations were measured by the Bradford assay (Bio-Rad, CA). Before euthanization, plasma from mice fed *ad libitum* or fasted for 48 hours was collected by centrifuging blood at 3200g for 5 minutes at 4°C and immediately boiled for 5 minutes in 1X Laemmli's sample buffer. Tissue extracts and plasma samples were analyzed by Western blotting with anti-NAMPT (Bethyl Laboratories, TX) or anti-SIRT1 (Sigma, MO) antibodies.

Detection of acetylated NAMPT in adipose tissue and differentiated HIB-1B cells

WAT or BAT collected from mice was homogenized in 1X RIPA buffer (50 mM Tris-HCl, pH 8.0, 150 mM NaCl, 1% Igepal CA630, 0.5% Sodium deoxycholate, 0.1% SDS, 1 mM EDTA, 1 mM NaF, 10 µM trichostatin A, 10 mM nicotinamide, 0.5 mM DTT, protease inhibitor cocktail (Roche, Germany)). Cell extracts were immunoprecipitated with anti-acetyl lysine conjugated beads (ImmuneChem, Canada) overnight. Immunoprecipitates were eluted with 1X Laemmli's sample buffer, boiled for 5 minutes, and analyzed by Western blotting with anti-Nampt antibody (OMNI379, Enzo Life Science, NY). Fully differentiated HIB-1B cells were homogenized in NAMPT-IP buffer (PBS [pH 7.4], 0.5% NP-40, 1 mM EDTA, 1 mM NaF, 10 µM TSA, 10 mM

nicotinamide, 0.5 mM DTT, protease inhibitor cocktail (Roche, Germany)) in a similar way, except that anti-acetyl lysine antibody (Cell signaling, MA) and protein A agarose (Sigma, MO) were used for immunoprecipitation.

RNA isolation and analysis

Total RNA from WAT and BAT was isolated using the RNeasy lipid tissue mini-kit (Qiagen, CA). Total RNA from all other tissues was isolated using the RNeasy mini-kit (Qiagen, CA). cDNA was synthesized using the High-Capacity cDNA Reverse Transcription Kit (Applied Biosystems, CA) with random primers. Quantitative real-time PCR was performed using the 7500 Fast Real-Time PCR system (Applied Biosystems, CA). Relative expression levels were determined based on the CT values and normalized to *Gapdh*.

Differentiation of 3T3L1 and HIB-1B preadipocyte cell lines

All cell lines were cultured in Dulbecco's modified Eagle's medium supplemented with 10% fetal bovine serum and antibiotics. Confluent cultures of HIB-1B brown pre-adipocytes were differentiated by adding 0.5 mM isobutylmethylxanthine (IBMX), 1 mM dexamethasone, 5 mg/ml insulin, and 1 nM triiodothyronine (T3) for 2 days and then changing to the media containing 5 mg/ml insulin and 1 nM T3 every other day for 6 more days. 3T3-L1 white pre-adipocytes were differentiated similarly, except that T3 was absent in the media through the whole differentiation process. All chemicals were purchased from Sigma.

Generation of HIB-1B cells stably expressing wild type or mutant Nampt-FLAG

A C-terminally FLAG-tagged Nampt (Nampt-FLAG) was created and cloned into the mammalian expression vector pCXN2 as described previously ¹¹(Revollo et al., Cell Metabolism, 6:363). Each lysine mutant Nampt-FLAG was generated using the QuikChange II Site-Directed Mutagenesis Kit (Stratagene, CA) according to the manufacturer's protocol. To create HIB-1B cells expressing Nampt-FLAG or mutant Nampt-FLAG, HIB-1B cells were transfected (Superfect, QIAGEN, CA) with pCXN2-Nampt-FLAG or pCXN2-mutant Nampt-FLAG. Transfected HIB-1B cells were selected by incubating with 500 µg/ml of G418 (Invitrogen, CA) for 2 weeks. Before the secretion assay and the enzymatic reactions, HIB-1B cells were fully differentiated as described above.

MS analysis of acetylated lysine sites on NAMPT

Recombinant mouse NAMPT was expressed and prepared as described previously ⁴. iNAMPT and eNAMPT was immunoprecipitated from HEK293 cells and from media of differentiated HIB-1B cells expressing Nampt-FLAG, respectively, as described above. Each protein was resolved by 10% SDS/PAGE and visualized by Coomassie blue staining. The bands of protein were excised and subjected to MS analysis provided by the Taplin Biological Mass Spectrometry Facility at Harvard Medical School.

eNAMPT secretion assay

3T3L1 or HIB-1B cells were differentiated as described above. To detect endogenous iNAMPT or eNAMPT, cell extracts or culture supernatant were collected, respectively,

immunoprecipitated as described previously ¹¹, and analyzed by Western blotting with anti-NAMPT antibody (Bethyl Laboratories, TX). HEK293 cells transfected with Nampt-FLAG and HIB-1B cells stably expressing Nampt-FLAG were processed in the same way, except that anti-FLAG beads (M2, Sigma, MO) were used for immunoprecipitation. eNAMPT secretion levels were calculated by measuring and quantifying the amount of iNAMPT and eNAMPT by Western blotting.

Enzymatic reactions

Nampt enzymatic reactions were conducted as previously described ¹¹. For immunoprecipitation of intracellular Nampt-FLAG, whole cell extracts were prepared with NAMPT-IP buffer and mixed with anti-FLAG-M2 conjugated beads (Sigma, MO) for 2-3 hours at 4°C. For immunoprecipitation of extracellular Nampt-FLAG, HIB-1B culture supernatants were collected after incubating differentiated HIB-1B cells overnight with DMEM without fetal bovine serum but supplemented with 5 mg/ml insulin and 1 nM triiodothyronine, centrifuged at 3000 rpm for 2 min at 4°C, concentrated 8 to 10 fold with Amicon Ultra-15 columns (Milipore, MA), and mixed with anti-FLAG beads for 2-3 hours at 4°C. Immunoprecipitates were washed twice with IP-buffer and twice with PBS.

Immunoprecipitates on anti-FLAG beads were incubated in enzymatic reaction buffer (50 mM Tris-HCl, pH 8.5, 100 mM NaCl, 0.25 mM nicotinamide, 10 mM MgSO₄, 1.5% ethanol, 0.5 mM phosphoribosyl pyrophosphate (PRPP), 2 mM ATP) for 55 min at 37°C. After this reaction, mouse recombinant NMNAT and yeast alcohol dehydrogenase were added at a final concentration of 10 mg/ml each, and the mixture was incubated for 5 min at 37°C. Supernatants were collected by spinning down anti-FLAG beads, and

auto-fluorescence of NADH was measured in a PerkinElmer LS 50B fluorometer (340 nm excitation, 460 nm emission). NADH auto-fluorescence values were converted to the amount of NMN using a standard curve drawn with known amounts of NMN. Immunoprecipitates bound on anti-FLAG beads were extracted with 1X Laemmli's buffer, boiled for 5 min, and analyzed by Western blotting with anti-Nampt antibody. The amounts of Nampt used for enzymatic reactions were quantitated compared to the standards of mouse recombinant NAMPT. *Kcat* values were calculated based on the molar amount of NMN generated per molar amount of immunoprecipitated Nampt-FLAG proteins per unit time.

Subcellular protein fractionation

Cytoplasmic and nuclear protein fractions were separated and prepared using the Subcellular Protein Fractionation Kit (Thermo Scientific, IL) according to the manufacturer's protocol.

Statistical Analysis

Differences between two groups were assessed using the Student's *t* test. Comparisons among several groups were performed using one-way ANOVA with the Fisher's LSD *post-hoc* test. *p* values less than 0.05 were considered statistically significant.

FIGURE LEGENDS

Figure 1. iNAMPT acetylation status in adipose tissue regulates eNAMPT secretion.

- (A) iNAMPT acetylation levels in brown adipose tissue (BAT) and white adipose tissue (WAT) of FVB WT mice. The right panel represents the average value of two independent experiments. Each value is normalized to the fed values.
- (B) iNAMPT acetylation levels in differentiated HIB-1B cells.
- (C) Reduction of eNAMPT levels after TSA and Nicotinamide treatment in differentiated HIB-1B cells. eNAMPT secretion levels were calculated as (eNAMPT levels/iNAMPT levels)/the amount of total protein in cell lysates after quantifying Western blotting results.
- (B and C) Cells were treated with TSA and nicotinamide for 3 hours. T= TSA (5 mM); N= nicotinamide (5 mM); M= Mock (Ethanol)
- (D) Changes in eNAMPT secretion levels in differentiated HIB-1B cells and 3T3L1 cells. Cells were incubated with high glucose (H, 25 mM) or low glucose (L, 5 mM) media in the presence or absence of nicotinamide (N, 5 mM) for 3 hours. eNAMPT secretion levels were calculated as eNAMPT levels / (iNAMPT levels/ACTIN)/the amount of total protein in cell lysates by quantifying Western blotting results.
- (C and D) The bottom panels represent the average value of three independent experiments. Each value is normalized to the mock (C) or to the high glucose condition (D) values.

Data were analyzed by the Student's *t* test and one-way ANOVA with Fisher's LSD *post-hoc* test. All values are presented as mean \pm SEM. **p* < 0.05; ***p* < 0.01; ****p* < 0.005.

Figure 2. eNAMPT secretion is increased during fasting in a SIRT1 dependent manner.

- (A) Plasma eNAMPT levels from fed or fasted (48 hours) *Sirt1*^{+/+} and *Sirt1*^{-/-} mice (n= 7-12). The bottom panel represents eNAMPT levels of each condition normalized to the fed *Sirt1*^{+/+} level.
- (B) iNAMPT and SIRT1 protein levels in the WAT and the liver of *Sirt1*^{+/+} and *Sirt1*^{-/-} mice. iNAMPT levels were normalized to TUBULIN. The right panel represents each condition normalized to the fed values.
- (C) Quantitative RT-PCR results for *Nampt* mRNA expression in the WAT of *Sirt1*^{+/+} and *Sirt1*^{-/-} mice (n= 4).

Data were analyzed by the Student's *t* test and one-way ANOVA with the Fisher's LSD *post-hoc* test. All values are presented as mean \pm SEM. **p* < 0.05; ***p* < 0.01; ****p* < 0.005.

Figure 3. SIRT1 regulates eNAMPT secretion by deacetylating iNAMPT.

- (A and B) Increase of eNAMPT secretion by SIRT1 overexpression in differentiated HIB-1B cells (A) and in HEK293 cells (B), respectively. eNAMPT secretion levels were calculated as (eNAMPT levels/iNAMPT levels)/ the amount of total protein in cell lysates (A) or as (eNAMPT levels/ACTIN levels)/the amount of

total protein in cell lysates (B) by quantifying Western blotting results. The right panels represent the average value of three independent experiments. Each value is normalized to the GFP (A) or to the NAMPT (B) values.

(C) Decrease of iNAMPT acetylation by SIRT1 overexpression in HEK293 cells.

Cells were incubated in the absence or presence of TSA (T, 5 mM) and nicotinamide (N, 5 mM) overnight prior to cell lysis. Acetylation levels are normalized to iNAMPT levels. The right panel represents iNAMPT acetylation levels of each condition normalized to the fed values.

(D) Interaction between SIRT1 and iNAMPT in differentiated HIB-1B cells.

(E) iNAMPT and SIRT1 expression after subcellular fractionation of differentiated HIB-1B cells. Expression of GAPDH and TBP were used for the cytoplasmic and nuclear markers, respectively.

(D and E) Cells were incubated with media containing high glucose (H, 25mM) or low glucose (L, 5 mM) overnight (D) or for 3 hours (E).

Data were analyzed by the Student's *t* test. All values are presented as mean \pm SEM.

p* < 0.05; *p* < 0.01; ****p* < 0.005.

Figure 4. Lysine 53 acetylation status on iNAMPT is important in regulating eNAMPT secretion and enzymatic activity.

(A) NAMPT lysine acetylation sites. iNAMPT and eNAMPT were prepared from cell lysate of HEK293 and culture supernatant of differentiated HIB-1B cells, respectively, overexpressing Nampt-FLAG. HEK293 cells overexpressing

Nampt-FLAG were treated with TSA (5 mM) and nicotinamide (5 mM) overnight prior to cell lysis. Recombinant NAMPT was prepared from bacteria.

(B) NAMPT structure with K53 and K79 acetylation sites shown (arrows).

Monomers are indicated by orange and green, NMN bound to the catalytic site is shown in blue.

(C) Changes in WT or mutant iNAMPT acetylation status by SIRT1 overexpression in HEK293 cells. Cells were treated with TSA (5 mM) and nicotinamide (5 mM) overnight prior to cell lysis.

(D and F) The relative enzymatic activity of WT and NAMPT mutants in differentiated HIB-1B cells. The enzymatic activity was calculated as the amount of nicotinamide mononucleotide (NMN) synthesis measured using the enzyme-coupled fluourometric assay divided by the amount of immunoprecipitated NAMPT quantified by western blotting (data not shown). Values of WT or each NAMPT mutant were normalized to the WT enzyme activity value.

(E and G) Comparison of eNAMPT secretion between WT and mutant NAMPT. eNAMPT secretion levels were calculated as (eNAMPT levels/iNAMPT levels)/the amount of total protein in cells lysates. eNAMPT and iNAMPT levels were measured by quantifying Western blotting results. Each value was normalized to the WT value.

Each panel represents the average value of three independent experiments. Data were analyzed by the Student's *t* test and one-way ANOVA with the Fisher's LSD *post-hoc* test. All values are presented as mean \pm SEM. **p* < 0.05; ***p* < 0.01; ****p* < 0.005.

Figure 1

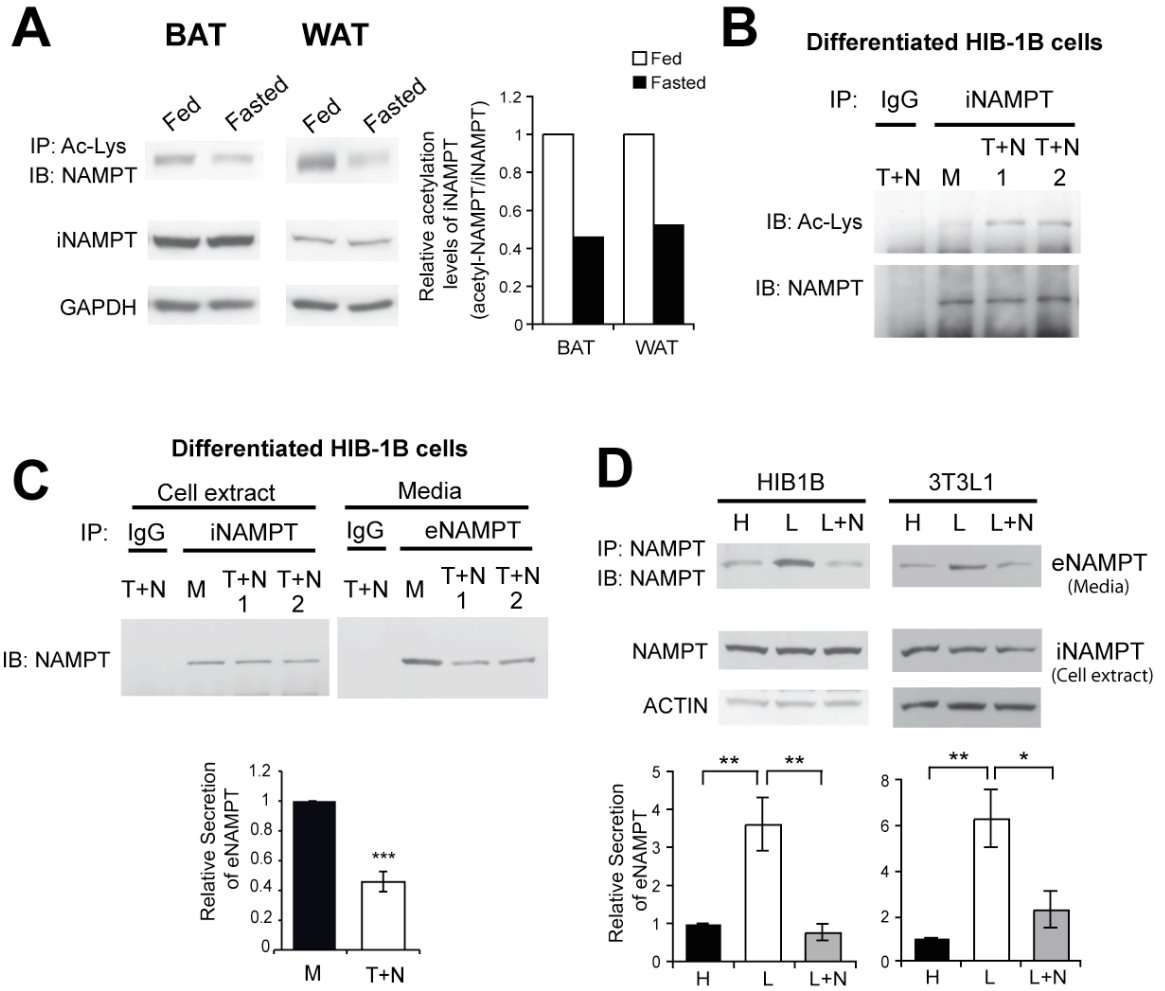


Figure 2

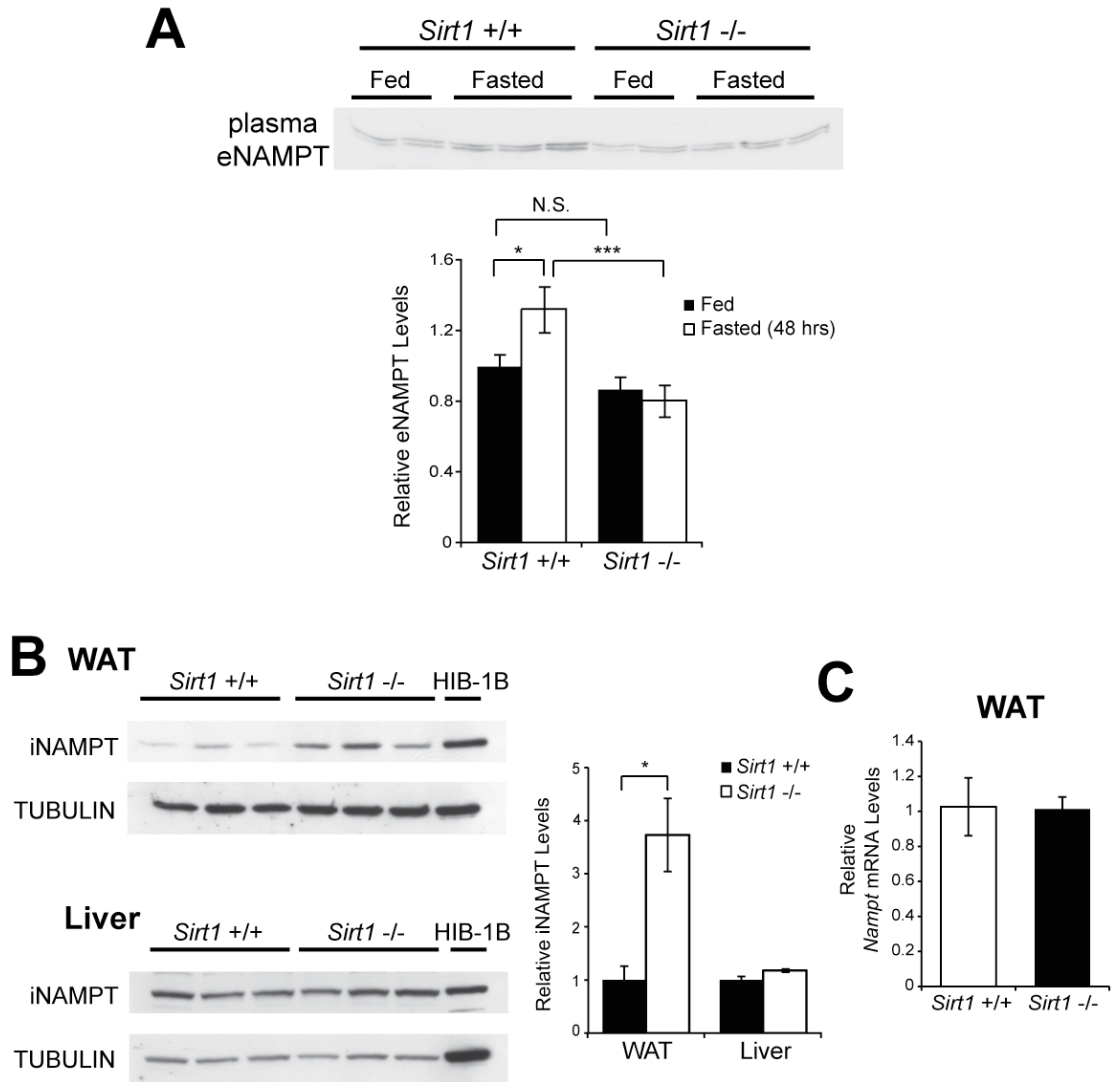


Figure 3

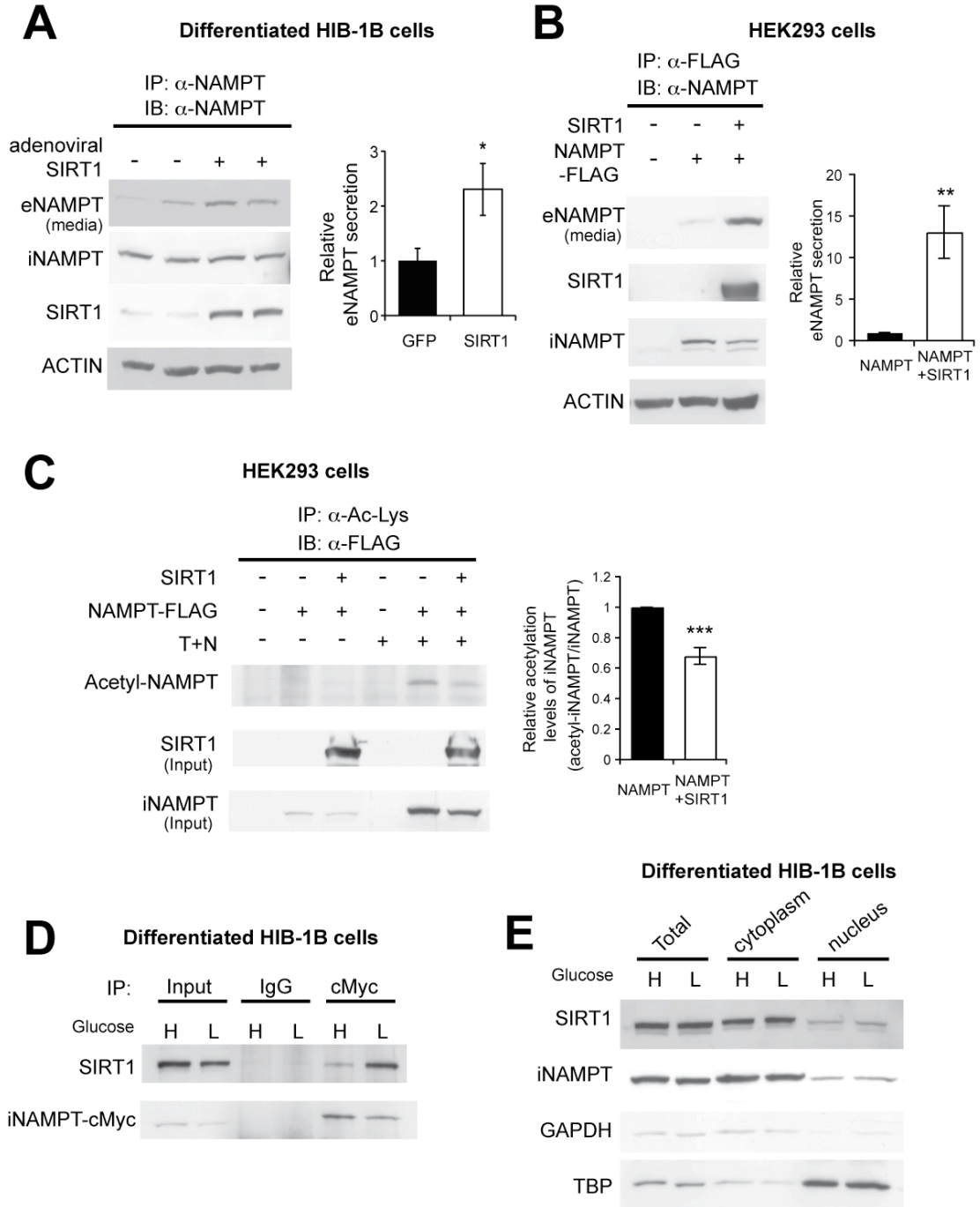
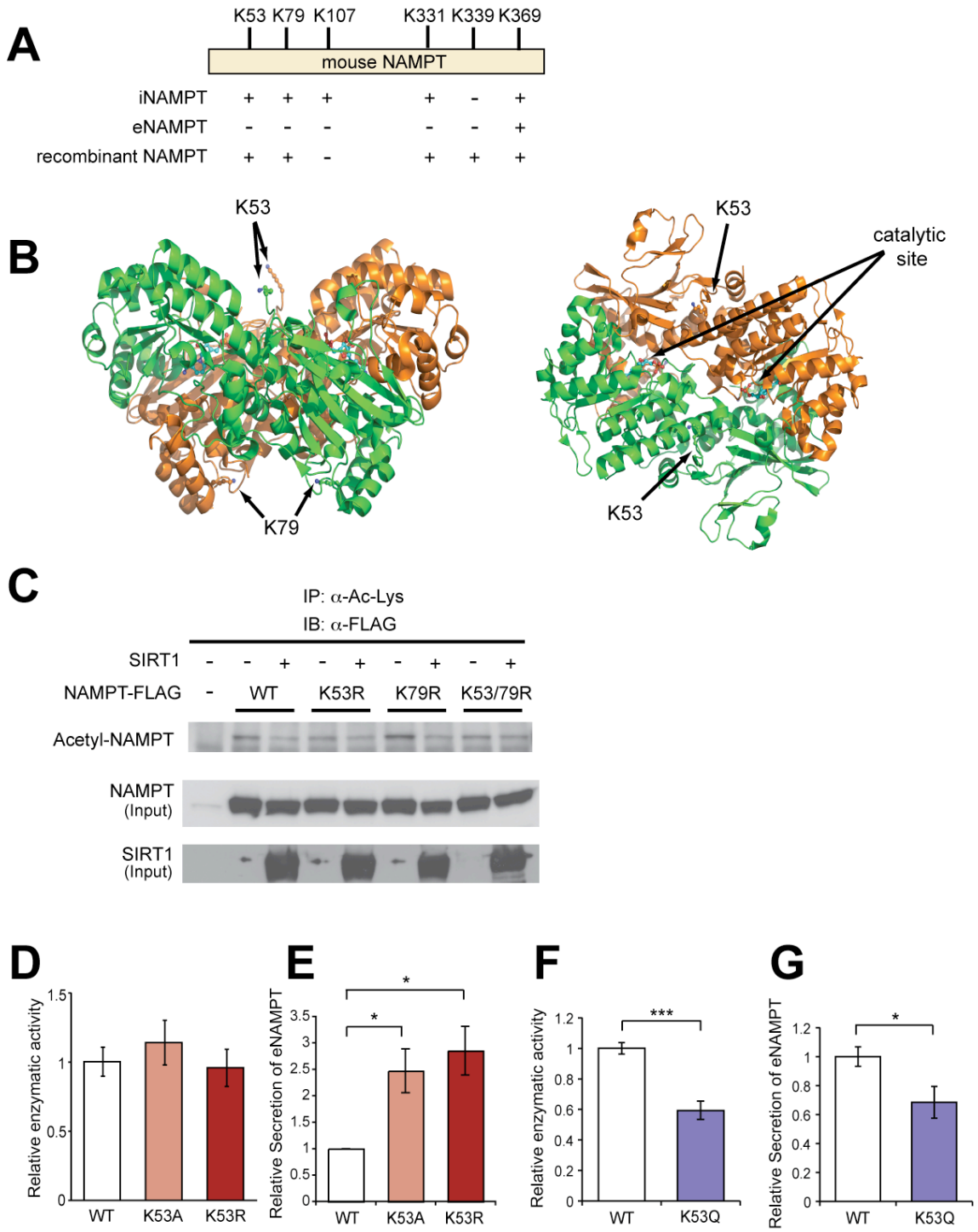


Figure 4



REFERENCES

1. Belenky, P., Bogan, K.L. & Brenner, C. NAD⁺ metabolism in health and disease. *Trends Biochem Sci* **32**, 12-19 (2007).
2. Bogan, K.L. & Brenner, C. Nicotinic acid, nicotinamide, and nicotinamide riboside: a molecular evaluation of NAD⁺ precursor vitamins in human nutrition. *Annu Rev Nutr* **28**, 115-130 (2008).
3. Magni, G., Amici, A., Emanuelli, M., Raffaelli, N. & Ruggieri, S. Enzymology of NAD⁺ synthesis. *Adv Enzymol Relat Areas Mol Biol* **73**, 135-182, xi (1999).
4. Revollo, J.R., Grimm, A.A. & Imai, S. The NAD biosynthesis pathway mediated by nicotinamide phosphoribosyltransferase regulates Sir2 activity in mammalian cells. *J Biol Chem* **279**, 50754-50763 (2004).
5. Martin, P.R., Shea, R.J. & Mulks, M.H. Identification of a plasmid-encoded gene from *Haemophilus ducreyi* which confers NAD independence. *J Bacteriol* **183**, 1168-1174 (2001).
6. Miller, E.S., *et al.* Complete genome sequence of the broad-host-range vibriophage KVP40: comparative genomics of a T4-related bacteriophage. *J Bacteriol* **185**, 5220-5233 (2003).
7. Kim, M.K., *et al.* Crystal structure of visfatin/pre-B cell colony-enhancing factor 1/nicotinamide phosphoribosyltransferase, free and in complex with the anti-cancer agent FK-866. *J Mol Biol* **362**, 66-77 (2006).
8. Wang, T., *et al.* Structure of Nampt/PBEF/visfatin, a mammalian NAD⁺ biosynthetic enzyme. *Nat Struct Mol Biol* **13**, 661-662 (2006).
9. Samal, B., *et al.* Cloning and characterization of the cDNA encoding a novel human

- pre-B-cell colony-enhancing factor. *Mol Cell Biol* **14**, 1431-1437 (1994).
10. Fukuhara, A., *et al.* Visfatin: a protein secreted by visceral fat that mimics the effects of insulin. *Science* **307**, 426-430 (2005).
 11. Revollo, J.R., *et al.* Nampt/PBEF/Visfatin regulates insulin secretion in beta cells as a systemic NAD biosynthetic enzyme. *Cell Metab* **6**, 363-375 (2007).
 12. Jia, S.H., *et al.* Pre-B cell colony-enhancing factor inhibits neutrophil apoptosis in experimental inflammation and clinical sepsis. *J Clin Invest* **113**, 1318-1327 (2004).
 13. Moschen, A.R., *et al.* Visfatin, an adipocytokine with proinflammatory and immunomodulating properties. *J Immunol* **178**, 1748-1758 (2007).
 14. Ognjanovic, S., Ku, T.L. & Bryant-Greenwood, G.D. Pre-B-cell colony-enhancing factor is a secreted cytokine-like protein from the human amniotic epithelium. *Am J Obstet Gynecol* **193**, 273-282 (2005).
 15. Li, Y., *et al.* Extracellular Nampt promotes macrophage survival via a nonenzymatic interleukin-6/STAT3 signaling mechanism. *J Biol Chem* **283**, 34833-34843 (2008).
 16. Neugebauer, R.C., Sippl, W. & Jung, M. Inhibitors of NAD⁺ dependent histone deacetylases (sirtuins). *Curr Pharm Des* **14**, 562-573 (2008).
 17. Liang, F., Kume, S. & Koya, D. SIRT1 and insulin resistance. *Nat Rev Endocrinol* **5**, 367-373 (2009).
 18. Brooks, C.L. & Gu, W. How does SIRT1 affect metabolism, senescence and cancer? *Nat Rev Cancer* **9**, 123-128 (2009).
 19. Satoh, A., *et al.* SIRT1 promotes the central adaptive response to diet restriction through activation of the dorsomedial and lateral nuclei of the hypothalamus. *J Neurosci* **30**, 10220-10232 (2010).

20. Ramsey, K.M., *et al.* Circadian clock feedback cycle through NAMPT-mediated NAD⁺ biosynthesis. *Science* **324**, 651-654 (2009).
21. Nakahata, Y., Sahar, S., Astarita, G., Kaluzova, M. & Sassone-Corsi, P. Circadian control of the NAD⁺ salvage pathway by CLOCK-SIRT1. *Science* **324**, 654-657 (2009).
22. Bonaldi, T., *et al.* Monocytic cells hyperacetylate chromatin protein HMGB1 to redirect it towards secretion. *EMBO J* **22**, 5551-5560 (2003).

Figure S1

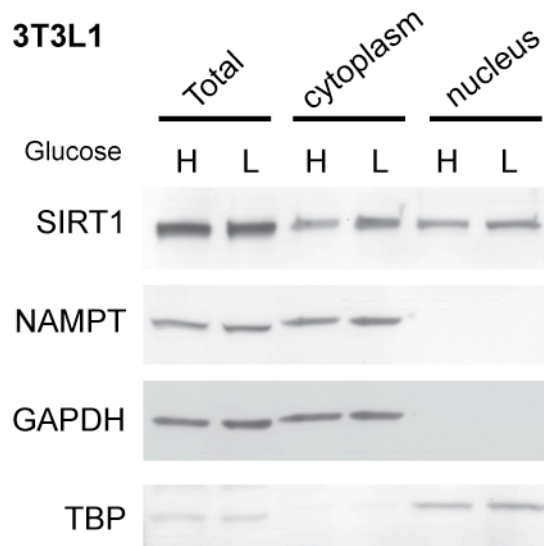


Figure S1. SIRT1 is expressed in both the cytoplasm and nucleus of differentiated 3T3 L1 cells.

Fully differentiated 3T3L1 cells were incubated with the media containing high glucose (H, 25mM) or low glucose (L, 5 mM) for 3 hours. Expressions of GAPDH and TBP were used for the cytoplasm and nucleus marker, respectively.

Figure S2

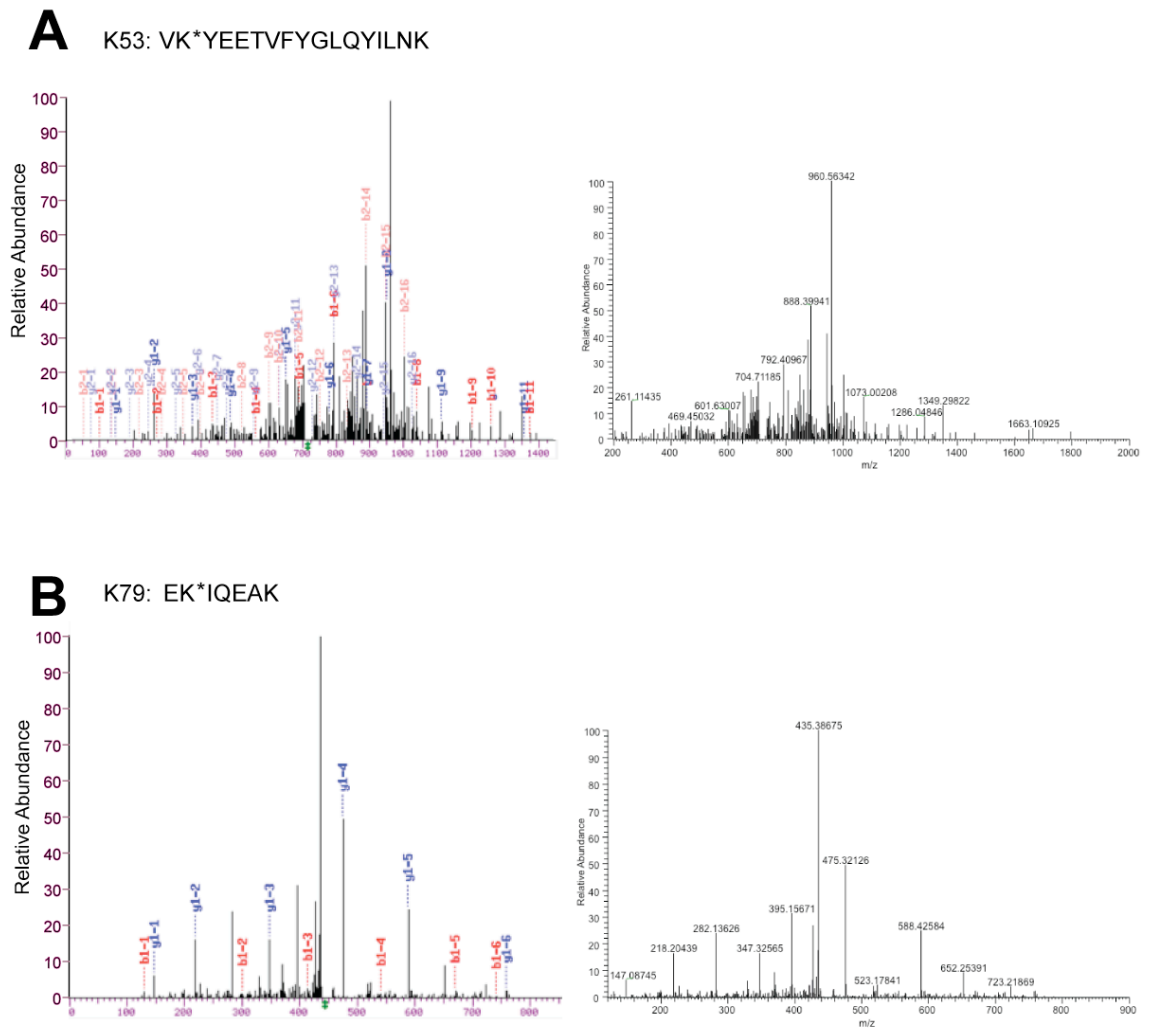


Figure S2. Acetylation on K53 and K79 of NAMPT are identified through MS/MS analysis.

MS/MS analysis of the peptide including K53 (A) and K79 (B) from mouse NAMPT. K*

indicates acetylated lysine. Left panels are the display from the search algorithm. Labels b and y designate the N- and C-terminal fragments, respectively, of the peptide produced by breakage at the peptide bond in the mass spectrometer. The number represents the number of N- or C- terminal residues present in the peptide fragment. Right panels are the raw data of the spectra.

Chapter 4.

**eNAMPT secreted from adipose tissue
regulates glucose homeostasis in mice**

ABSTRACT

Adipose tissue functions as an endocrine organ secreting a variety of humoral factors, called adipokines. Through the secretion of adipokines, adipose tissue regulates glucose and lipid metabolism and controls energy homeostasis at a systemic level. Nicotinamide phosphoribosyltransferase (NAMPT), the rate-limiting enzyme in NAD biosynthesis in mammals, has two different forms, intracellular and extracellular NAMPT (iNAMPT and eNAMPT, respectively), and eNAMPT is secreted from adipose tissue as one of the adipokines. Previously, we demonstrated that eNAMPT secretion is actively regulated by SIRT1 in response to nutrient availability, however, the function underlying the secretion of eNAMPT from adipose tissues is not fully understood yet. In an effort to address this question, we generated adipocyte-specific *Nampt* KO (ANKO) mice. We first confirmed that female ANKO mice show significant reductions in plasma eNAMPT levels. Interestingly, female ANKO show reduction of NAD levels not only in white and brown adipose tissue but also in the hypothalamus compared to control *Nampt*^{flox/flox} mice, suggesting that loss of *Nampt* only in adipose tissues could also influence hypothalamic function, including governing glucose homeostasis by lowering NAD levels in this tissue. Consistent with this notion, female ANKO exhibit severely impaired glucose tolerance and glucose-stimulated insulin secretion accompanied by hyperinsulinemia. Administration of NMN partially restores insulin sensitivity, but almost completely ameliorates the responsiveness of pancreatic β cells to glucose and hyperinsulinemia *in vivo*. Taken together, our results suggest the new possibility that adipose tissues play an important role in maintaining glucose homeostasis by controlling eNAMPT secretion and eNAMPT-mediated NAD biosynthesis at a systemic level.

INTRODUCTION

The adipocytes are highly specialized cells playing critical roles in energy regulation and homeostasis in that one organelle, the lipid droplet, encompasses greater than 95% of the entire cell body ¹. Adipocytes store energy in the form of triglycerides when energy intake exceeds expenditure and release it in the form of free fatty acids during starvation. Hence, the adipose tissue has been long considered as a passive and inactive organ that is primarily involved in energy storage. However, it is now clear that adipose tissue has additional roles in energy regulation via endocrine, paracrine, and autocrine signals. It has an exceptionally active secretory pathway whose function is not only to release lipids but also to secrete many endocrine and paracrine factors such as leptin, resistin, and TNF α , commonly referred to as adipokines ¹. Through release and circulation of these adipokines, adipose tissue has a role in regulating metabolism systemically, signaling to peripheral tissues such as liver and muscle and to the central nervous system through the hypothalamus, as well as to neighboring adipocytes and other local cell types within adipose tissue such as macrophages ¹⁻³.

Nicotinamide phosphoribosyltransferase (NAMPT), originally identified as the product of the gene that confers the capability of synthesizing NAD from nicotinamide in *Haemophilus ducreyi* ⁴, has two different forms in mammals: intra- and extracellular NAMPT (iNAMPT and eNAMPT, respectively). iNAMPT protein is expressed in almost all tissues although its expression levels is tissue dependent, ⁵ and only a few tissues, including adipose tissue, are able to secrete eNAMPT ^{6,7}. While the function of iNAMPT has been firmly established as the rate-limiting enzyme to synthesize NAD from nicotinamide in mammals, physiological relevance and function of eNAMPT has

still been controversial. For instance, eNAMPT had been suggested to have insulin-mimetic properties by directly binding to the insulin receptor, but this function has not been confirmed yet ⁸. In addition, a number of studies implicate that eNAMPT might function as a proinflammatory cytokine, although the enzymatic activity appears to be still required in some cases ⁹⁻¹². Since we demonstrated that eNAMPT also functions as an NAD biosynthetic enzyme using an *in vitro* culture system, we have been investigating the function of eNAMPT *in vivo* using genetically engineered mice. In pancreatic β cell-specific Sirt1 overexpressing (BESTO) mice, Sirt1 significantly promotes glucose-stimulated insulin secretion and improves glucose tolerance *in vivo* ¹³. However, Sirt1 activity is significantly reduced in aged β cells, which leads aged BESTO mice to completely lose all phenotypes of enhanced β cell function ¹⁴. This seems to be due to a reduction in plasma NMN levels over age, and consistent with this notion, administration of nicotinamide mononucleotide (NMN) restores enhanced glucose-stimulated insulin secretion and improved glucose tolerance in aged BESTO mice. Along the same lines, female *Nampt*^{+/-} mice, which have reduced plasma eNAMPT compared to WT, exhibit impaired glucose tolerance due to a defect in glucose-stimulated insulin secretion ⁶. Primary female *Nampt*^{+/-} islets also show a defect in NAD biosynthesis and glucose-stimulated insulin secretion, and, remarkably, administration of NMN can completely ameliorate this glucose-stimulated insulin secretion defect in female *Nampt*^{+/-} mice. These data clearly suggest that NAMPT-mediated NAD biosynthesis is necessary to maintain normal glucose-stimulated insulin secretion in pancreatic β cells. However, these results still do not answer the question whether plasma eNAMPT protein itself is required to maintain normal levels of NAD biosynthesis in pancreatic β cells over age in

order to prevent age-related decline in glucose-stimulated insulin secretion.

In the previous chapter, I showed that the secretion and the enzymatic activity of eNAMPT are regulated by SIRT in adipose tissue in response to nutritional changes. These findings suggest the possibility that adipose tissue plays a critical role in the maintenance of metabolic homeostasis by regulating eNAMPT secretion and NAD biosynthesis at a systemic level. Then what is the function of plasma eNAMPT specifically secreted and regulated by adipose tissue? In an effort to address this question, we generated adipose tissue-specific *Nampt* knockout (ANKO) mice. Consistent with our previous findings, female ANKO mice show significant reductions in plasma eNAMPT levels and NAD levels not only in white and brown adipose tissue but also in the hypothalamus, resulting in severe impairments in insulin sensitivity and glucose-stimulated insulin secretion. Interestingly, treatment with NMN completely restores the normal responsiveness of pancreatic β cells to glucose *in vivo*, while the restoration of insulin sensitivity is partial, suggesting that pancreatic β cell function is supported by adipose tissue, likely through the extracellular NMN supply mediated by eNAMPT. These findings open a new possibility that adipose tissue functions as a critical modulator for systemic NAD biosynthesis through the NAD/SIRT1-dependent regulation of the secretion and the enzymatic activity of eNAMPT.

RESULTS

ANKO mice exhibit reduced plasma eNAMPT levels and defects in NAD biosynthesis not only in adipose tissue but also in remote tissues

Given that the secretion and enzymatic activity of eNAMPT are highly regulated by SIRT1-dependent deacetylation in differentiated adipocytes (Chapter 3), eNAMPT secreted by adipose tissue likely has physiological relevance as an extracellular NAD biosynthetic enzyme. To address this hypothesis, we generated adipose tissue-specific Nampt knockout (ANKO) mice by crossing floxed Nampt ($Nampt^{flox/flox}$) mice and adiponectin-Cre driver mice (See Experimental Procedures). ANKO mice were born following the Mendelian ratio and looked overtly normal. As expected, ANKO mice showed a complete lack of iNAMPT expression in visceral WAT and BAT, although trace amounts of iNAMPT remained in subcutaneous WAT (Figure 1A). Consistent with the lack of iNAMPT, NAD levels were dramatically reduced to 7-28% of the control $Nampt^{flox/flox}$ mice in ANKO WAT and BAT (Figure 1B), demonstrating that NAMPT functions as a major NAD biosynthetic enzyme in adipose tissues. This dramatic reduction in NAD levels did not seem to affect the gross structure and development of adipose tissue. Mean adipocyte diameter, and body weight and body composition in ANKO mice were not significantly different from those in the control $Nampt^{flox/flox}$ mice (Figures S1A-C). However, we found that plasma eNAMPT levels significantly decreased by 30-40% in both fed and fasted conditions in ANKO females compared to those in control $Nampt^{flox/flox}$ mice (Figure 1C), demonstrating that adipose tissue significantly contributes to the production of circulating eNAMPT in female mice. Contrarily, ANKO male mice did not show such decreases in plasma eNAMPT levels

(data not shown). These results are consistent with the previously reported finding that Nampt-deficient heterozygous females exhibit a reduction in plasma eNAMPT levels, whereas Nampt-deficient heterozygous males do not ⁶. Interestingly, while other tissues such as the liver and skeletal muscle did not show any change in NAD levels (Figure 1B), there were a couple of tissues that showed moderate but significant decreases in NAD levels in ANKO females. For example, the hypothalamus, but not the hippocampus, showed a significant decrease in NAD levels in ANKO mice compared to controls (Figure 1D). mRNA expression levels of *Nampt* and other NAD biosynthetic enzymes showed no decrease in ANKO hypothalami (Figure S1D), indicating that the reduction in NAD levels detected in ANKO hypothalami was not due to intrinsic defects in their NAD biosynthetic machineries. Consistently, mRNA expression of *Ox2r*, a SIRT1 target gene in the brain, was also significantly decreased in hypothalamus of ANKO females, but not in hippocampus (Figure 1E), suggesting that NAD-dependent SIRT1 activity is lower in female ANKO hypothalamus. Taken together, these results demonstrate that the adipose tissue-specific deficiency of NAMPT causes the reduction in NAD levels not only in WAT and BAT but also in the hypothalamus where the NAD biosynthetic machineries are intact.

ANKO female mice show severe impairments in insulin sensitivity and glucose-stimulated insulin secretion

We found that ANKO female mice had higher blood glucose levels than control *Nampt*^{flox/flox} mice in both fed and fasted conditions (Figure 2A). ANKO females also showed severe hyperinsulinemia compared to *Nampt*^{flox/flox} and adiponectin-Cre females

in the fed condition (Figure 2B). Intraperitoneal glucose tolerance tests (IPGTTs) demonstrated that ANKO females had impaired glucose tolerance (Figure 2C). During IPGTTs, ANKO females also showed significant hyperinsulinemia compared to control $Nampt^{flox/flox}$ mice (Figure 2D, left panel). With this, ANKO females were able to enhance insulin secretion only ~2-fold in response to glucose, whereas control $Nampt^{flox/flox}$ mice showed ~5-fold increase in glucose-stimulated insulin secretion (Figure 2D, right panel), suggesting that glucose-stimulated insulin secretion is seriously hampered in ANKO females. Because pancreatic islets in ANKO females looked normal compared to those in control $Nampt^{flox/flox}$ females (Figure 2E), this defect of β cell responsiveness to glucose in ANKO females is likely not due to structural defects in pancreatic islets. Insulin tolerance tests (ITTs) demonstrated that ANKO females also developed severe insulin resistance (Figure 2F). HOMA-IR values, calculated from fasting glucose and insulin levels, also confirmed insulin resistance in ANKO females (ANKO 4.76 ± 0.82 , $Nampt^{flox/flox}$ 0.70 ± 0.15). Different from these ANKO females, ANKO male mice did not show any obvious metabolic defects, except for moderate increases in insulin levels in fed and fasted conditions (Figures S2A-E). This remarkable sex difference in ANKO mice is consistent with that previously observed in $Nampt^{+/-}$ mice⁶. Given that $Nampt^{+/-}$ females also display reduced plasma eNAMPT levels and impaired β cell function, we expected to see lower NAD levels in pancreatic β cells of female ANKO compared to control $Nampt^{flox/flox}$ mice, but it was not the case (date not shown).

Considering that hypothalamus also plays a critical role in glucose homeostasis by regulating pancreatic β cell function, it is likely that the adipose tissue-specific

deficiency of NAMPT independently affects both insulin secretion and action, resulting in complex combinatory phenotypes in glucose metabolism in ANKO females. Indeed, female ANKO mice exhibit induction of adipose tissue inflammation marked by increased macrophage infiltration which could blunt insulin signaling in peripheral tissues by increasing secretion of pro-inflammatory cytokines from adipose tissues¹⁵. Gene expression for markers of M1-like macrophages that secrete a characteristic signature of pro-inflammatory cytokines such as TNF α and IL-6 were increased, whereas those of M2-like macrophages that secrete anti-inflammatory cytokines such as IL-10 and IL-1 were decreased in female ANKO compared to control *Nampt*^{fl α /fl α} mice even under regular diet condition (Figure S4A). Consistently, the macrophage population was more polarized to type M1 in visceral adipose tissue in female ANKO mice compared to female *Nampt*^{fl α /fl α} mice. ANKO females displayed an increase in the relative proportion of adipose CD11b⁺ CD11c⁺ pro-inflammatory M1 macrophages (16.1%), but a decrease of adipose CD11b⁺ CD11c⁻ anti-inflammatory M2 macrophages (56.6%), compared to WT (M1; 7.39%, M2; 70.2%) (Figure S4B). These data indicate that female ANKO mice show severe insulin resistance and impaired glucose-stimulated insulin secretion due to the defects in multiple organs including adipose tissues and the hypothalamus.

Treatment with NMN restores normal responsiveness of pancreatic β cells to glucose and improves insulin sensitivity in ANKO female mice

NMN is the product of the NAMPT enzymatic reaction and a key NAD intermediate in mammals. It has been demonstrated that systemic administration of NMN is able to

enhance NAD biosynthesis *in vivo* and dramatically improve metabolic complications in different genetic and disease models in which NAMPT-mediated NAD biosynthesis is seriously compromised^{6,14,16}. Therefore, we anticipated that NMN administration might be able to ameliorate the metabolic defects in ANKO female mice. We administered NMN once a day at the dose of 500 mg/kg body weight/day for up to four weeks to a cohort of ANKO female mice. As a control, we injected PBS into another cohort of ANKO female mice and control *Nampt*^{flox/flox} mice.

Four-week NMN treatment increased NAD levels in the WAT and BAT of ANKO females (Figure 3SA), although they did not reach the levels detected in control *Nampt*^{flox/flox} tissues (Figure 1B). In accordance with these NAD increases in WAT and BAT, fed glucose and insulin levels decreased considerably in NMN-treated ANKO females (Figures 3A and B). However, results from IPGTTs showed that the improvement of glucose tolerance in NMN-treated ANKO females was minimal compared to that in PBS-treated ANKO females (Figure 3C). During IPGTTs, the absolute insulin levels in response to glucose were significantly lower in NMN-treated ANKO females compared to those in PBS-treated ANKO females (Figure 3D, left panel). Importantly, the fold increase in glucose-stimulated insulin secretion was completely restored in NMN-treated ANKO females to the level observed in control *Nampt*^{flox/flox} mice (Figures 3D and 2D, right panels), suggesting that the responsiveness of pancreatic β cells to glucose was fully recovered by NMN treatment. On the other hand, results from ITTs showed that NMN-treated ANKO mice still had insulin resistance, although there was a significant improvement in insulin sensitivity compared to PBS-treated ANKO females (Figure 3E). HOMA-IR values also confirmed this trend (PBS-treated

ANKO 5.38 ± 0.76 , NMN-treated ANKO 2.25 ± 0.41 , PBS-treated *Nampt*^{flox/flox} 0.97 ± 0.10). It seemed that in NMN-treated ANKO females, β cell function to secrete insulin in response to glucose was fully restored by NMN, whereas the restoration of WAT and BAT functions might only be partial. Indeed, we found that the levels of leptin, manufactured primarily in adipose tissues, were not fully restored in NMN-treated ANKO females (Figure 3F). In addition, according to gene expression profiles, M1 macrophages as well as M2 macrophages are increased in NMN-treated ANKO mice (Figure S4D), indicating that NMN administration did not fully restore the function of adipose tissues in female ANKO mice. These data could raise the possibility that improvement of β cell function sensing glucose and in turn secreting insulin could be separated from the partial restoration of WAT and BAT function by NMN treatment in female ANKO. Taken together, these results from NMN treatment strongly suggest that defects in NAD biosynthesis detected in adipose tissue and hypothalamus, which are caused by the adipose tissue-specific deficiency of NAMPT, essentially contribute to the impairments in insulin sensitivity and insulin secretion in ANKO female mice.

DISCUSSION

In our previous study in chapter 3, we clearly demonstrated that the secretion and the enzymatic activity of eNAMPT are regulated by SIRT1-dependent deacetylation in adipocytes in response to nutrient availability. Here we demonstrated why adipose tissue secretes eNAMPT into blood circulation using this sophisticated mechanism. We have obtained important clues as to the function of eNAMPT using adipose tissue-specific Nampt knockout (ANKO) mice. ANKO females, but not males, show significant decreases in plasma eNAMPT levels. A surprising finding is that the adipose tissue-specific deficiency of NAMPT causes significant reduction in NAD levels not only in WAT and BAT but also in the hypothalamus. Because the hypothalamus in ANKO females does not have any obvious defects in the NAD biosynthetic machineries, the reduction in NAD levels detected in this remote tissue is likely attributed to the NAMPT deficiency in adipose tissue. Furthermore, the defect appears to be very specific to hypothalamus because other tissues and organs, including the liver, skeletal muscle, and the hippocampus that is located close to the hypothalamus, do not show any reduction in NAD. Female ANKO mice exhibit severely impaired glucose tolerance and glucose-stimulated insulin secretion, even though they have hyperinsulinemia. Although where exactly NMN is synthesized by eNAMPT still remains a critical question, these results from ANKO mice open a novel paradigm for the systemic regulation of NAD biosynthesis and metabolism through the regulation of the secretion and enzymatic activity of eNAMPT from adipose tissue.

The results from ANKO mice reveal a surprising connection between adipose tissue and another remote tissue, the hypothalamus. The fact that the adipose tissue-

specific deficiency of NAMPT causes such severe metabolic complications is remarkable, supporting the importance of NAMPT-mediated NAD biosynthesis in adipose tissue for the systemic regulation of glucose metabolism. It is possible that the severe insulin resistance observed in ANKO females might be caused by functional defects in multiple tissues, particularly the hypothalamus and adipose tissues, both of which show significant reduction in NAD levels. For example, the hypothalamus regulates glucose metabolism through the melanocortin system which senses systemic hormonal and nutritional changes and in turn governs appetite and energy expenditure via leptin, ghrelin and Agouti-related protein (AgRP)^{17,18}. The hypothalamus also directly controls insulin secretion from pancreatic β cell by signaling through the autonomous nervous system and hypothalamic hormones¹⁹⁻²¹. Considering those, it is likely that decreased NAD in the hypothalamus could cause a defect in hypothalamic function for the regulation of glucose homeostasis, contributing to insulin resistance. In addition, inflammation in adipose tissues, induced by infiltration of large numbers of macrophages as shown in female ANKO mice, has a key role in systemic insulin resistance, impaired glucose tolerance and the development of metabolic syndrome and type 2 diabetes¹⁵. Given that reducing SIRT1 expression in lean animals is sufficient to activate NF- κ B, a key protein upregulated in immune response, resulting in macrophage infiltration in adipose tissues similar to that seen in obesity²², this female ANKO phenotype could also be at least partly due to inactivation of SIRT1 caused by reduction of NAD levels in adipose tissues since NAD is required for SIRT1 deacetylase reaction. However, the hypothalamus might also remotely control macrophage infiltration in adipose tissue. Indeed, loss of autophagy only in POMC neurons in the hypothalamus has been shown to

cause an increase in the proportion of M1 macrophages in adipose tissue²³.

Interestingly, NMN treatment almost completely restores the defect in glucose-stimulated insulin secretion in ANKO female mice with a significant improvement of hyperinsulinemia, but only partially improves glucose tolerance and insulin sensitivity in these animals. For instance, HOMA-IR indices calculated for PBS-treated *Nampt*^{flox/flox}, PBS-treated ANKO, and NMN-treated ANKO mice are 0.97, 5.38, and 2.25, respectively, showing approximately a 60% improvement in insulin sensitivity by NMN treatment. This partial improvement in insulin sensitivity appears to be due to the incomplete restoration of NAD levels in adipose tissue after NMN treatment. Consistent with this notion, plasma leptin levels as well as adipose tissue macrophages in NMN-treated ANKO mice are not fully brought back to the levels in control *Nampt*^{flox/flox} mice. One likely explanation is that adipose tissue has higher NAD turnover compared to other tissues so that more frequent or continuous NMN administration might be necessary to achieve full NAD restoration. Further investigation will be required to flesh out the detailed mechanism of the severe insulin resistance caused by the deficiency of NAMPT in adipose tissue.

eNAMPT produces NMN in blood, which is then distributed to specific remote tissues like the hypothalamus and influences its function. Considering that plasma eNAMPT levels are significantly reduced in ANKO mice, one plausible explanation to describe the ANKO phenotype is that lower levels of eNAMPT result in lower NMN production in blood, which then limits the NMN distributed to tissues throughout the body. Insufficient NMN could disturb the regular function of remote tissues, including the hypothalamus. A recent study argues against this possibility, claiming that NAMPT

is unable to synthesize NMN in blood circulation²⁴. However, caution is required to extrapolate the results from this study to the *in vivo* environment for the following reasons. First, this study used bacterially produced recombinant NAMPT in all assays. As shown in our present study, bacterially produced recombinant NAMPT carries acetylated lysines similar to iNAMPT, but completely different from eNAMPT. Second, the equilibrium of the NAMPT reaction must be shifted constantly to the production of NMN in blood circulation because NMN is swiftly transported into tissues, as previously reported¹⁶, suggesting that detecting low steady-state concentrations of NAMPT substrates in plasma does not necessarily mean that NAMPT is unable to synthesize NMN in the blood. Indeed, this study reports that when adding NAMPT and its substrates to blood, NMN biosynthesis can clearly occur. Therefore, it is critically important to examine the *in vivo* kinetics of NMN biosynthesis in both tissues and blood circulation, which is still a significant technical challenge. The study to address this key question is currently underway.

Our previous findings that adipose tissue actively regulates the secretion and enzymatic activity of eNAMPT in an NAD/SIRT1-dependent manner suggest the possibility that adipose tissue functions as a critical determinant for the spatial and temporal coordination of NAD biosynthesis throughout the body. Our present findings in chapter 4 show that ANKO females, having lower plasma eNAMPT levels compared to *Nampt*^{flox/flox} mice, display significant reduction of NAD levels in the hypothalamus. This finding supports the idea that the systemic coordination of NAD biosynthesis via eNAMPT might play an important role in orchestrating metabolic responses in multiple tissues and maintaining metabolic homeostasis against nutritional and environmental

perturbations. However, there are a couple of questions that remain to be investigated. For instance, we still do not fully understand exactly where eNAMPT-mediated NAD biosynthesis occurs. The detailed molecular mechanism underlying the impaired glucose tolerance and attenuated β cells function in female ANKO mice is also still unclear. Further studies may soon give us a more complete understanding of the mechanism by which eNAMPT-mediated NAD biosynthesis regulates glucose homeostasis, and thus give us the potential to design effective therapies for metabolic diseases such as type 2 diabetes.

EXPERIMENTAL PROCEDURES

Generation of ANKO mice

Nampt^{flox/flox} mice and Adiponectin-Cre mice were generated as described previously and generously provided to us^{25,26}. Adiponectin-Cre mice were mated with Nampt^{flox/flox} mice, and cohorts were established by mating F1 Nampt^{flox/+};Cre to Nampt^{flox/flox} mice. Nampt^{flox/flox};Cre and Nampt^{flox/flox};+ were considered as ANKO and WT, respectively.

Detection of intracellular NAMPT in tissues, and of extracellular NAMPT in plasma

Mice fed ad libitum were euthanized by carbon dioxide asphyxiation. Organs were immediately collected, homogenized in 1X Laemmli's sample buffer, and boiled for 5 minutes. Samples were then centrifuged at 16000g and protein concentrations of supernatant were measured by the Bradford assay (Biorad, CA). Plasma from mice fed ad libitum or fasted for 48 hours was collected by centrifuging blood at 3200g for 5 minutes at 4°C and immediately boiled for 5 minutes in 1X Laemmli's sample buffer. Tissue extracts and plasma samples were analyzed by Western blotting with anti-NAMPT (Bethyl Laboratories, TX) or anti-ACTIN (Sigma, MO) antibodies.

NAD⁺ measurements

Frozen tissues were extracted in perchloric acid and neutralized in K₂CO₃ on ice as described previously (Ramsey et al., Science, 324:651). NAD⁺ levels were determined using an HPLC system (Shimadzu, Japan) with a Supelco LC-18-T column (15 cm x 4.6

cm; Sigma, MO). The HPLC was run at a flow rate of 1 ml/min with 100% buffer A (50 mM phosphate buffer, pH 7.4) from 0-5 min, a linear gradient to 95% buffer A /5% buffer B (100% methanol) from 5-6 min, 95% buffer A /5% buffer B from 6-11 min, a linear gradient to 85% buffer A /15% buffer B from 11-13 min, 85% buffer A /15% buffer B from 13-23 min, and a linear gradient to 100% buffer A from 23-24 min. NAD⁺ is eluted at about 11 min. NAD⁺ levels were quantitated based on the peak area compared to a standard curve and normalized to the weight of the frozen tissue or to the number of primary islets.

RNA isolation and analysis

Total RNA from WAT and BAT was isolated using an RNeasy lipid tissue mini-kit (QIAGEN, CA). Total RNA from the other tissues was isolated using RNeasy mini-kit (QIAGEN, CA). cDNA was synthesized using the High-Capacity cDNA Reverse Transcription Kit (Applied Biosystems, CA) with random primers. Quantitative real-time PCR was performed using the 7500 Fast Real-Time PCR system (Applied Biosystems, CA). Relative expression levels were determined based on the CT values and normalized to *Gapdh*.

Animal experimentation

Mice were maintained on a standard diet (PicoLab 5053 Rodent Diet 20 [Lab Diets, St.Louis, MO, USA]) with free access to food and water under a 12 hour light/ dark cycle

at constant temperature (22°C). For IPGTT experiments, mice were fasted for 16 hours, and 50% dextrose (2g/kg body weight) was injected intraperitoneally. Blood was collected from the tail vein at 0, 15, 30, 60, and 120 minutes. Blood glucose levels were determined using an Accu-Chek II glucometer (Roche Diagnostics), and plasma insulin levels were determined using the Singulex Erenna immunoassay system at the Washington University Core Laboratory for Clinical Studies. For ITT experiments, mice were fasted for 4 hours before they were injected with human insulin (0.75U/kg body weight; Lilly). Blood glucose levels were measured at 0, 15, 30, 45, and 60 minutes after insulin injections. Lipid, cholesterol, and triglyceride levels were measured using reagents from Thermo Electron Corporation (Waltham, WA), while non-esterified free fatty acid levels were measured using reagents from Wako (Richmond, VA) at the Washington University Animal Model Research Core associated with the Nutrition Obesity Research Center (NORC) and the Diabetes Research and Training Center (DRTC). Plasma leptin levels were measured using a mouse leptin ELISA kit (Milipore, MA) at the Washington University Core Laboratory for Clinical Studies. For body composition analysis, mice were subjected to magnetic resonance imaging (EchoMRI, TX). For synchronization of female estrus cycle, female mice were exposed to bedding from male cages for 3 days. Synchronized females were used in all mouse experiments.

Statistical analysis

Differences between two groups were assessed using the Student's *t* test. Comparisons among several groups were performed using one-way ANOVA with the Fisher's LSD *post-hoc* test. *p* values less than 0.05 were considered statistically significant.

FIGURE LEGENDS

Figure 1. ANKO mice have lower plasma eNAMPT and NAD⁺ levels in the hypothalamus and adipose tissue.

- (A) iNAMPT levels in visceral WAT, subcutaneous WAT, BAT, brain, liver, and muscle from 2-month-old female $\text{Nampt}^{\text{flox/flox}}$ and ANKO mice.
- (B) Plasma eNAMPT levels from 5-6-month-old female $\text{Nampt}^{\text{flox/flox}}$ and ANKO mice. Plasma was collected from mice fed or fasted for 48 hours. Bottom panels represent eNAMPT levels from each genotype normalized to $\text{Nampt}^{\text{flox/flox}}$ (n = 8-10).
- (C) Tissue NAD⁺ levels in visceral WAT, subcutaneous WAT, BAT, liver, and skeletal muscle from 3-4-month-old female $\text{Nampt}^{\text{flox/flox}}$ and ANKO mice (n = 4-8).
- (D) Tissue NAD⁺ levels in hypothalamus and hippocampus from 3-4-month-old female $\text{Nampt}^{\text{flox/flox}}$ and ANKO mice (n = 4-8), and in pancreatic islet NAD⁺ levels from 5-6-month-old female $\text{Nampt}^{\text{flox/flox}}$ and ANKO mice.
- (E) Quantitative RT-PCR results for Ox2r mRNA expression in hypothalamus of 3-4-month-old fed female $\text{Nampt}^{\text{flox/flox}}$ and ANKO mice (n = 4).

Data were analyzed by the Student's *t* test. All values are presented as mean ± SEM.

*p < 0.05; **p < 0.01; ***p < 0.001

Figure 2. ANKO mice have impaired glucose metabolism and hyperinsulinemia.

- (A) Fed or fasted (48 hours) plasma glucose levels in 3-4-month-old female $\text{Nampt}^{\text{flox/flox}}$ and ANKO mice (n = 7-9).

- (B) Fed plasma insulin levels in 3-4-month-old female $Nampt^{flox/flox}$, ANKO, and adiponectin-Cre mice (n = 5-10).
- (C) Glucose tolerance in 3-4-month-old female $Nampt^{flox/flox}$ (dotted line) and ANKO (solid line) mice (n = 4-5). The area under the curve (AUC) is presented next to the glucose tolerance curves.
- (D) Plasma insulin levels in 3-4-month-old female $Nampt^{flox/flox}$ and ANKO mice during IPGTT. The right panel represents insulin normalized to the basal level at 0 min.
- (E) Representative hematoxylin and eosin staining of paraffin-embedded pancreas section from 3-4-month-old fed $Nampt^{flox/flox}$ and ANKO mice.
- (F) Insulin tolerance in 3-4-month-old female $Nampt^{flox/flox}$ (dotted line) and ANKO (solid line) mice (n = 6).

Data were analyzed by the Student's *t* test and one-way ANOVA with the Fisher's LSD *post-hoc* test. All values are presented as mean \pm SEM. **p* < 0.05; ***p* < 0.01; ****p* < 0.001.

Figure 3. NMN administration improves hyperinsulinemia and glucose metabolism in 7-8 month-old female ANKO mice compared to wild-type.

- (A) Fed plasma glucose levels after PBS or NMN treatment (n = 9).
- (B) Fed plasma insulin levels after PBS or NMN treatment (n = 9).

(C) Glucose tolerance after PBS (solid line) or NMN (dotted line) treatment (n = 9) in female ANKO mice. The area under the curve (AUC) is presented next to the glucose tolerance curves.

(D) Plasma insulin levels during IPGTT. The right panel represents insulin normalized to the basal level at 0 min.

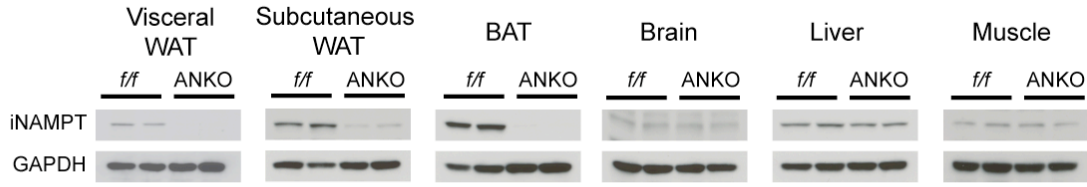
(E) Insulin tolerance test after PBS (solid line) or NMN (dotted line) treatment (n = 9) in female ANKO mice.

(F) Plasma leptin levels after PBS or NMN treatment.

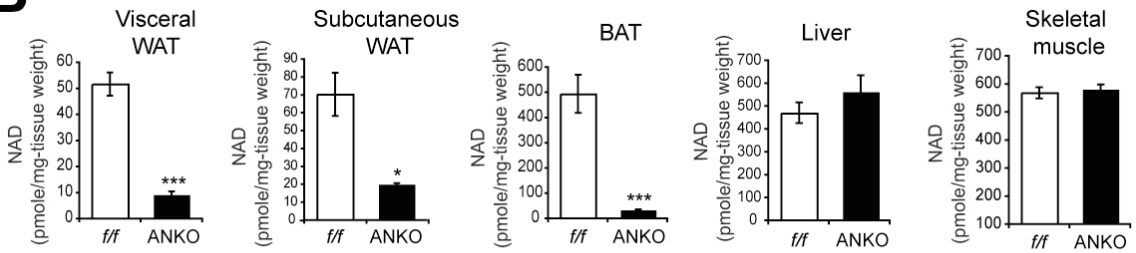
NMN (500 mg/kg body weight/day) was administered for 4 weeks. ITTs were conducted several days before IPGTTs. Data were analyzed by the Student's *t* test and one-way ANOVA with the Fisher's LSD *post-hoc* test. All values are presented as mean \pm SEM. **p* < 0.05; ***p* < 0.01; ****p* < 0.001.

Figure 1

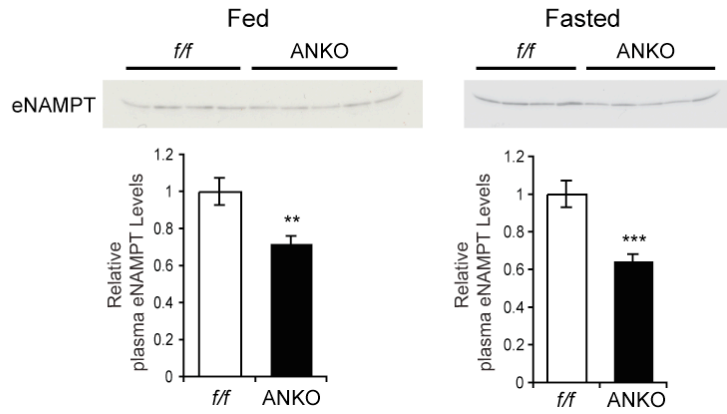
A



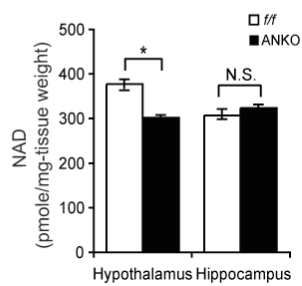
B



C



D



E

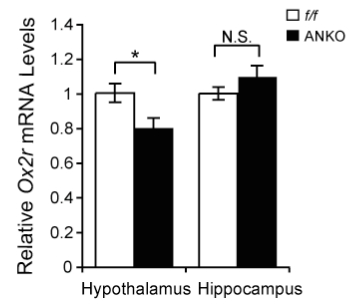


Figure 2

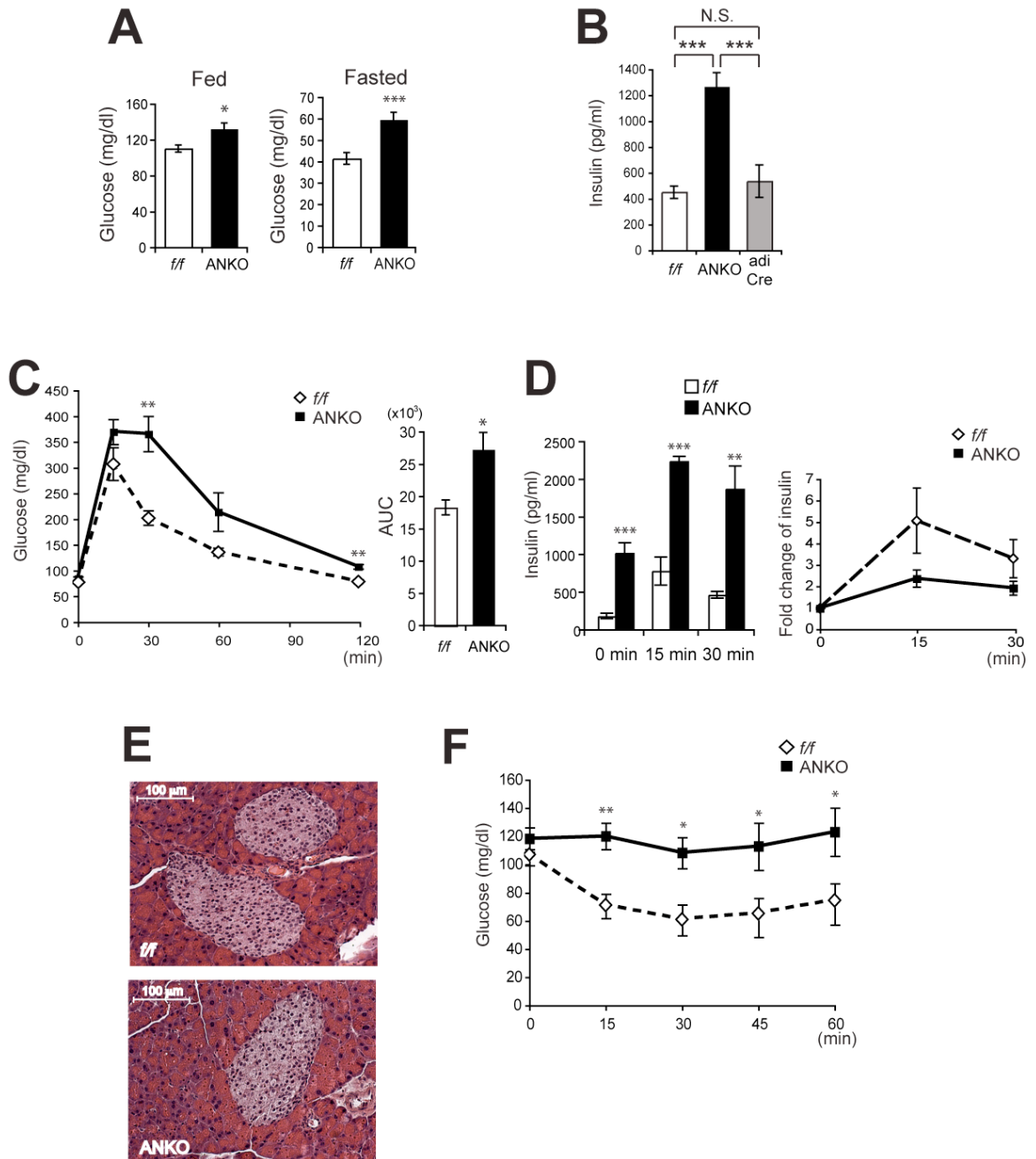
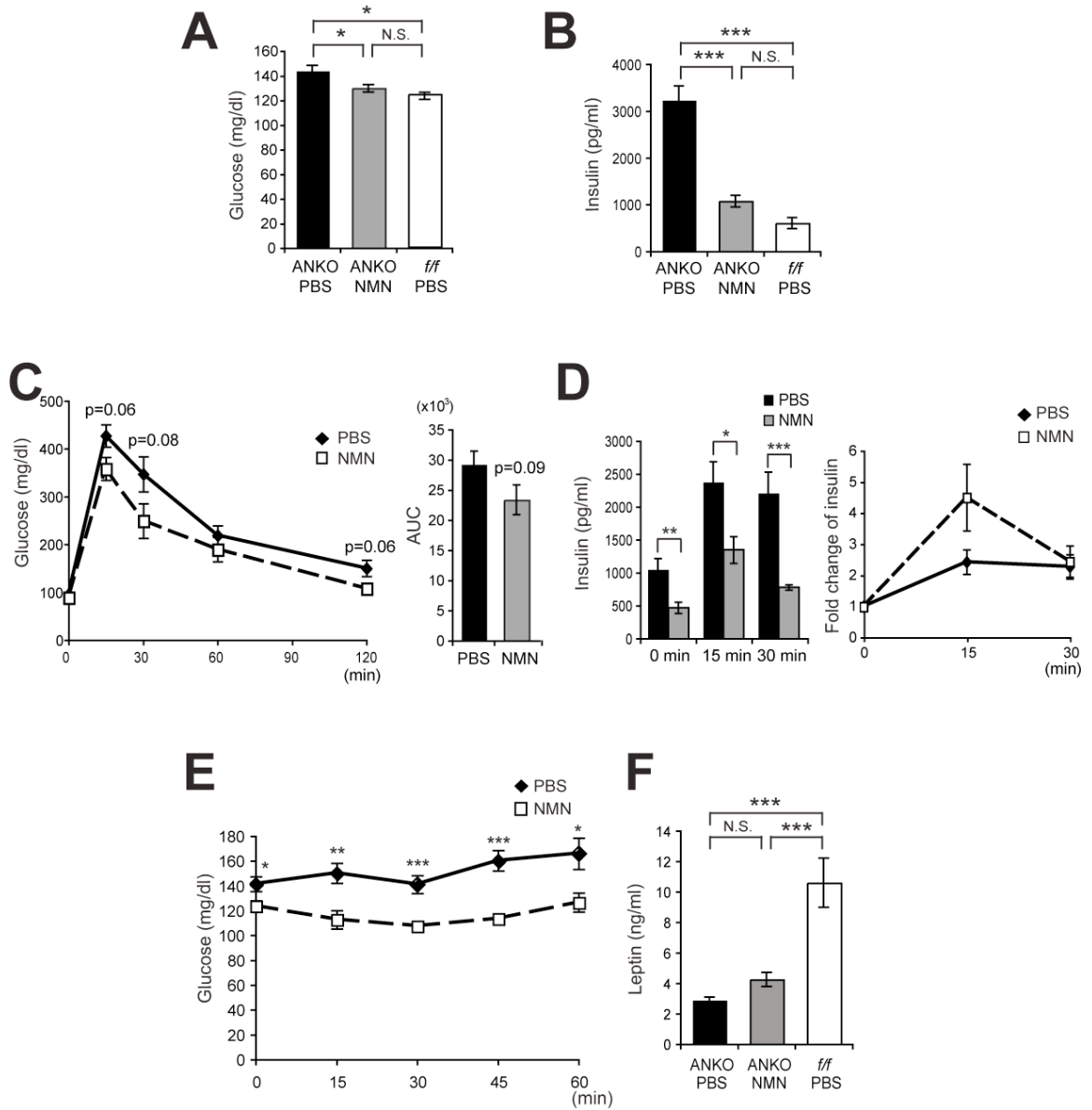


Figure 3



REFERENCES

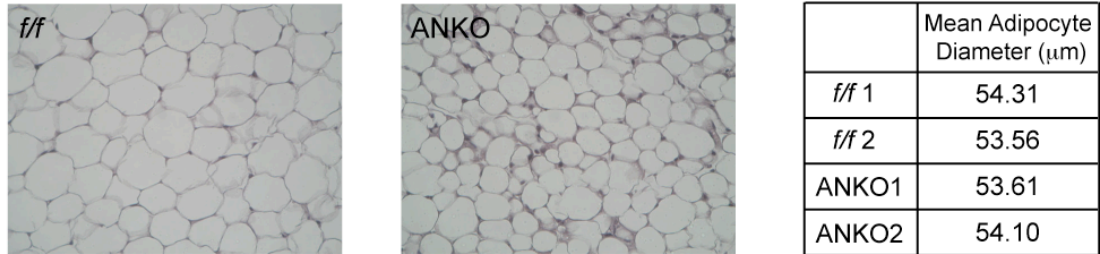
1. Trujillo, M.E. & Scherer, P.E. Adipose tissue-derived factors: impact on health and disease. *Endocr Rev* **27**, 762-778 (2006).
2. Horvath, T.L. The hardship of obesity: a soft-wired hypothalamus. *Nat Neurosci* **8**, 561-565 (2005).
3. Osborn, O. & Olefsky, J.M. The cellular and signaling networks linking the immune system and metabolism in disease. *Nat Med* **18**, 363-374 (2012).
4. Martin, P.R., Shea, R.J. & Mulks, M.H. Identification of a plasmid-encoded gene from *Haemophilus ducreyi* which confers NAD independence. *J Bacteriol* **183**, 1168-1174 (2001).
5. Kitani, T., Okuno, S. & Fujisawa, H. Growth phase-dependent changes in the subcellular localization of pre-B-cell colony-enhancing factor. *FEBS Lett* **544**, 74-78 (2003).
6. Revollo, J.R., *et al.* Nampt/PBEF/Visfatin regulates insulin secretion in beta cells as a systemic NAD biosynthetic enzyme. *Cell Metab* **6**, 363-375 (2007).
7. Tanaka, M., *et al.* Visfatin is released from 3T3-L1 adipocytes via a non-classical pathway. *Biochem Biophys Res Commun* **359**, 194-201 (2007).
8. Fukuhara, A., *et al.* Retraction. *Science* **318**, 565 (2007).
9. Jia, S.H., *et al.* Pre-B cell colony-enhancing factor inhibits neutrophil apoptosis in experimental inflammation and clinical sepsis. *J Clin Invest* **113**, 1318-1327 (2004).
10. Li, Y., *et al.* Extracellular Nampt promotes macrophage survival via a nonenzymatic interleukin-6/STAT3 signaling mechanism. *J Biol Chem* **283**,

- 34833-34843 (2008).
11. Moschen, A.R., *et al.* Visfatin, an adipocytokine with proinflammatory and immunomodulating properties. *J Immunol* **178**, 1748-1758 (2007).
 12. Skokowa, J., *et al.* NAMPT is essential for the G-CSF-induced myeloid differentiation via a NAD(+)-sirtuin-1-dependent pathway. *Nat Med* **15**, 151-158 (2009).
 13. Moynihan, K.A., *et al.* Increased dosage of mammalian Sir2 in pancreatic beta cells enhances glucose-stimulated insulin secretion in mice. *Cell Metab* **2**, 105-117 (2005).
 14. Ramsey, K.M., Mills, K.F., Satoh, A. & Imai, S. Age-associated loss of Sirt1-mediated enhancement of glucose-stimulated insulin secretion in beta cell-specific Sirt1-overexpressing (BESTO) mice. *Aging Cell* **7**, 78-88 (2008).
 15. Olefsky, J.M. & Glass, C.K. Macrophages, inflammation, and insulin resistance. *Annu Rev Physiol* **72**, 219-246 (2010).
 16. Yoshino, J., Mills, K.F., Yoon, M.J. & Imai, S. Nicotinamide mononucleotide, a key NAD(+) intermediate, treats the pathophysiology of diet- and age-induced diabetes in mice. *Cell Metab* **14**, 528-536 (2011).
 17. Gantz, I. & Fong, T.M. The melanocortin system. *Am J Physiol Endocrinol Metab* **284**, E468-474 (2003).
 18. Cone, R.D. Anatomy and regulation of the central melanocortin system. *Nat Neurosci* **8**, 571-578 (2005).
 19. Calegari, V.C., *et al.* Inflammation of the hypothalamus leads to defective pancreatic islet function. *J Biol Chem* **286**, 12870-12880 (2011).

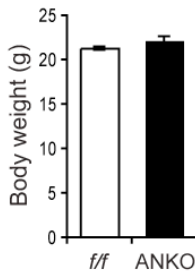
20. Schmid, J., *et al.* Modulation of pancreatic islets-stress axis by hypothalamic releasing hormones and 11beta-hydroxysteroid dehydrogenase. *Proc Natl Acad Sci U S A* **108**, 13722-13727 (2011).
21. Kaushik, S., *et al.* Autophagy in hypothalamic AgRP neurons regulates food intake and energy balance. *Cell Metab* **14**, 173-183 (2011).
22. Gillum, M.P., *et al.* SirT1 regulates adipose tissue inflammation. *Diabetes* **60**, 3235-3245 (2011).
23. Kaushik, S., *et al.* Loss of autophagy in hypothalamic POMC neurons impairs lipolysis. *EMBO Rep* **13**, 258-265 (2012).
24. Hara, N., Yamada, K., Shibata, T., Osago, H. & Tsuchiya, M. Nicotinamide phosphoribosyltransferase/visfatin does not catalyze nicotinamide mononucleotide formation in blood plasma. *PLoS One* **6**, e22781 (2011).
25. Rongvaux, A., *et al.* Nicotinamide phosphoribosyl transferase/pre-B cell colony-enhancing factor/visfatin is required for lymphocyte development and cellular resistance to genotoxic stress. *J Immunol* **181**, 4685-4695 (2008).
26. Eguchi, J., *et al.* Transcriptional control of adipose lipid handling by IRF4. *Cell Metab* **13**, 249-259 (2011).

Figure S1

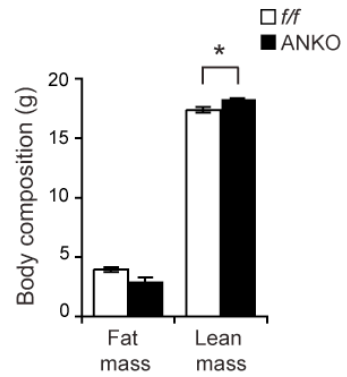
A



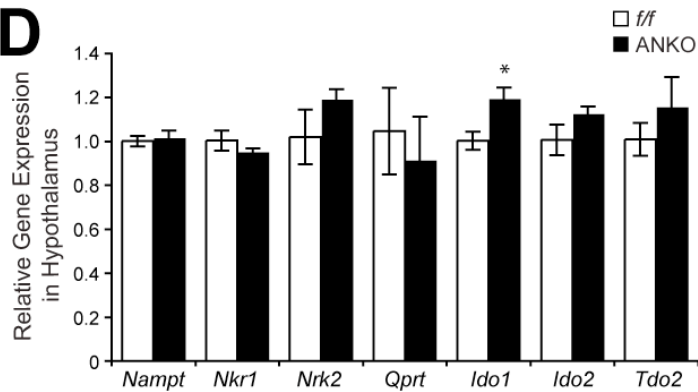
B



C



D



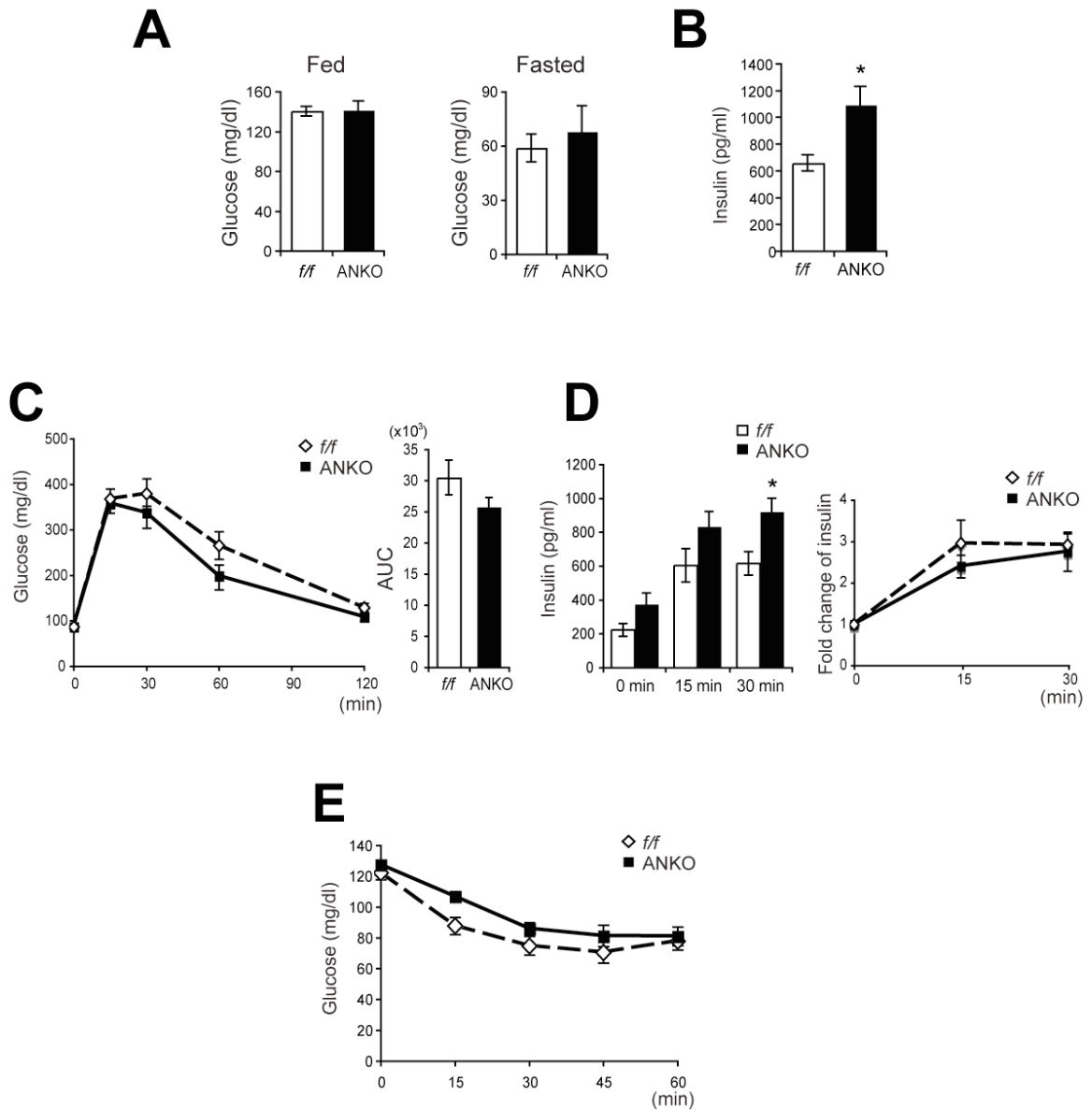
Supplementary Figure 1. Female ANKO mice have normal adipose tissue morphology and gene expression profiles in the hypothalamus.

- (A) Representative hematoxylin and eosin staining of paraffin-embedded visceral WAT section from 3-4-month-old fed female WT and ANKO mice. The right panel shows the mean adipocyte diameter from 3-4-month-old fed female WT and ANKO mice (n=2).
- (B) Body weights of 4-month-old female WT and ANKO mice on a standard diet (n = 9-11).
- (C) Body composition analysis of 4-month-old female WT and ANKO mice on a standard diet (n= 2-4).
- (D) Quantitative RT-PCR results for genes representative of NAD⁺ biosynthesis in hypothalamus of 3-4-month-old fed female WT and ANKO mice (n = 4).

Data were analyzed by the Student's *t* test. All values are presented as mean \pm SEM.

p* < 0.05; *p* < 0.01; ****p* < 0.001.

Figure S2

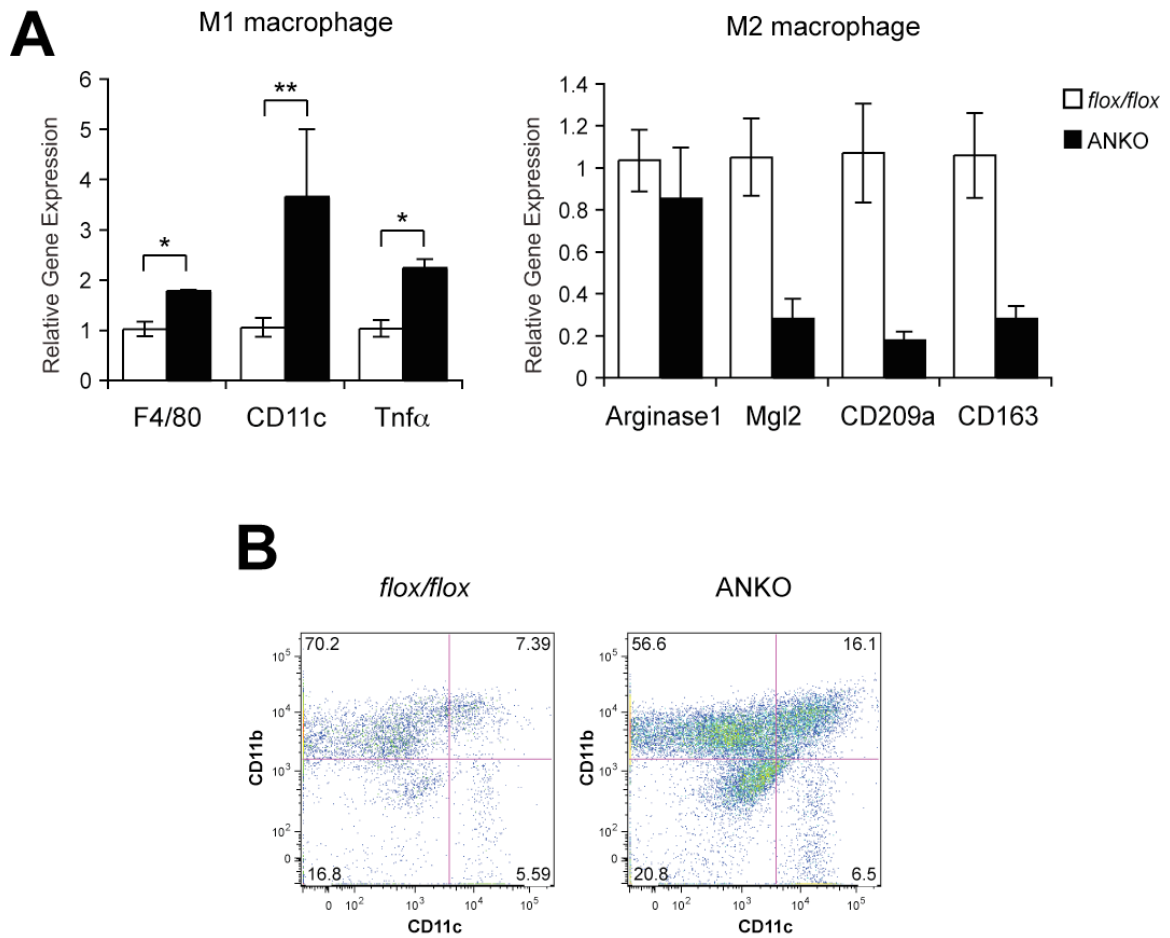


Supplementary Figure 2. Male ANKO mice have normal glucose metabolism and insulin secretion compared to wild type.

- (A) Fed or fasted (48 hours) plasma glucose levels in 3-4-month-old male $\text{Nampt}^{\text{flox/flox}}$ and ANKO mice (n = 7).
- (B) Fed plasma insulin levels in 3-4-month-old male $\text{Nampt}^{\text{flox/flox}}$ and ANKO mice (n = 6).
- (C) Glucose tolerance in 3-4-month-old male WT and ANKO mice (n = 6-7). The area under the curve (AUC) is presented next to the glucose tolerance curves.
- (D) Plasma insulin levels in 3-4-month-old male WT and ANKO mice during IPGTT. The right panel represents insulin normalized to the basal level at 0 min.
- (E) Insulin tolerance in 3-4-month-old male WT and ANKO (n = 6-7).

Data were analyzed by the Student's *t* test and one-way ANOVA with the Fisher's LSD *post-hoc* test. All values are presented as mean \pm SEM. **p* < 0.05; ***p* < 0.01; ****p* < 0.001.

Figure S3



Supplementary Figure 3. Female ANKO mice exhibit increased macrophage infiltration polarized to M1 in adipose tissue compared to wild type.

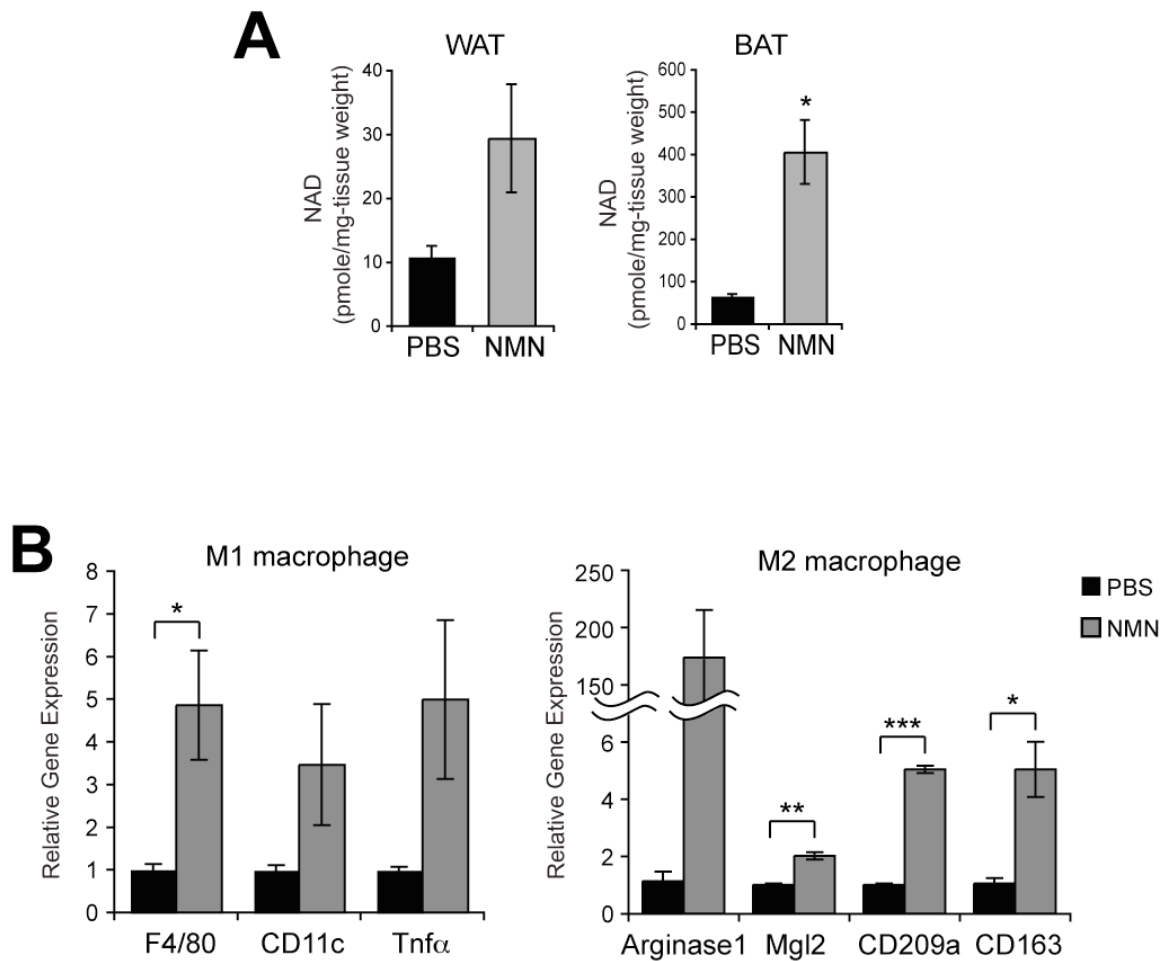
(A) Quantitative RT-PCR results for genes representative of M1 and M2 macrophages in adipose tissue of 3-4-month-old fed female *Nampt*^{flox/flox} and ANKO mice (n = 2-4).

(B) Adipose tissue macrophages (ATM) from the stromal vascular fraction analyzed by flow cytometry. The percentage of Cd11c⁺ (upper right quadrant; M1) and Cd11c⁻ (upper left quadrant; M2) cells within the Cd11b⁺ ATM population is shown.

Data were analyzed by the Student's *t* test. All values are presented as mean ± SEM.

p* < 0.05; *p* < 0.01.

Figure 4S



Supplementary Figure 4. NMN administration to ANKO mice does not fully restore NAD⁺ levels in adipose tissue to that of WT and does not significantly alter adipose tissue macrophages

(A) Tissue NAD⁺ levels in visceral WAT and BAT from 7-8-month-old female ANKO mice after PBS or NMN treatment for 4 weeks (n = 3).

(B) Quantitative RT-PCR results for genes representative of M1 and M2

macrophages in adipose tissue of 7-8 month old female ANKO mice after PBS or NMN treatment for 4 weeks (n = 3).

Data were analyzed by the Student's *t* test. All values are presented as mean \pm SEM.

* $p < 0.05$; ** $p < 0.01$; *** $p < 0.001$.

SUPPLEMENTAL EXPERIMENTAL PROCEDURES

Adipocyte size measurement

10-50 mg of white adipose tissue was fixed for at least 30 days in a solution containing 0.2 M Osmium Tetroxide and 50 mM Collidine-HCL buffer. After fixation, samples were collected onto a 10 micron screen and then washed with saline for 24 hours. After washing, samples were again collected onto a 10 micron screen and then incubated for 3-4 days in 8 M Urea in saline to further dissociate the tissue. After urea treatment, samples were filtered through a 250 micron screen and collected onto a 10 micron screen. Free, fixed adipocytes were removed from the filter and stored in saline (0.154 M NaCl with 0.01% Triton) at 4°C until Multisizer analysis. Analysis was performed at the Washington University Nutrition Obesity Research Center (NORC). For the analysis, samples were processed on a Beckman MultisizerTM 3 Coulter Counter (Beckman Coulter, CA). For each sizing run, microsphere beads in sizes 50, 100, and 150 mm were run to confirm proper calibration. Data was analyzed using the Multisizer 3 software (Beckman Coulter, CA).

Isolation of stromal vascular cells and flow cytometry.

The epididymal fat pad was removed from mice and minced into small pieces (~1 mm). The minced tissue was transferred to tubes containing 30 µg/ml Liberase TM (Roche, Germany) and 1.5% BSA in KRH buffer (4.8 mM KCl, 2.5 mM CaCl₂, 1.2 mM MgSO₄, 118 mM NaCl, 20 mM HEPES) and shaken vigorously at 37°C for 20~30 min. The digested tissue was strained through a 250 µM nylon mesh and centrifuged at 100g for 5

min. The pellet was washed twice with KRH buffer + 1.5% BSA, incubated in ACK lysis buffer (150 mM NH₄Cl, 10 mM KHCO₃, 0.1 mM EDTA) to remove erythrocytes, and finally resuspended in PBS supplemented with 1% BSA and 2 mM EDTA.

The isolated stromal vascular cells were blocked with mouse BD Fc Block™ (BD Pharmingen, CA) for 15 min and stained with antibodies to CD45, CD11b, and CD11c (BD Pharmingen, CA) to identify M1 (CD11b⁺, CD11c⁺) and M2 (CD11b⁺, CD11c⁻) macrophage populations. 7-AAD (BD Pharmingen, CA) was used to exclude dead cells. FACS data was collected and analyzed with a FACSCantoII flow cytometer (BD Biosciences, CA) and FlowJo (Treestar, OR).

Chapter 5.

Summary, Discussion, and Future Direction

Summary

In this thesis work, I provided biochemical and physiological evidence that shows how NAMPT is regulated in response to both alterations in nutrient conditions and the aging process in cellular and systemic levels, and how glucose homeostasis is affected through these regulations. First, iNAMPT levels and NAMPT-mediated NAD^+ biosynthesis are decreased in metabolically active tissues, specifically adipose tissue and liver, under high fat diet and with age contributing to the pathogenesis of type 2 diabetes. Second, administration of NMN, an enzymatic product of NAMPT, ameliorated impaired glucose tolerance in high fat diet- or age- induced type 2 diabetic mice by restoring normal NAD^+ levels and in turn enhancing SIRT1 activity. This resulted in either improved insulin sensitivity or insulin secretion. Third, SIRT1 deacetylates iNAMPT, which causes increases in both eNAMPT secretion and its enzymatic activity in adipose tissue, when nutrient availability is limited. Fourth, knocking out *Nampt* specifically in mouse adipose tissue displays a phenotype of impaired glucose tolerance and reduced glucose-stimulated insulin secretion in pancreatic β cells. This is presumably due to lower NAD^+ levels in remote metabolic tissues such as the hypothalamus, and these phenotypes can be corrected by the administration of NMN.

The findings presented here provide the first evidence that NAMPT protein levels and NAMPT-mediated NAD^+ biosynthesis is compromised by high fat diet and aging, contributing to the pathogenesis of type 2 diabetes. Additionally, we present the first proof of concept that promoting NAD^+ biosynthesis by administration of NMN, a key NAD^+ intermediate, can be an effective intervention to treat the pathophysiology of diet- and age- induced type 2 diabetes. We also demonstrated that eNAMPT secretion is

positively regulated by SIRT1 in response to nutrient availability in adipose tissues. By deacetylating K53 on NAMPT, SIRT1 controls not only eNAMPT secretion from adipocytes but also its enzymatic activity, comprising a new positive feed back loop. Furthermore, by using female adipose tissue-specific *Nampt* knock out (ANKO) mice, we revealed that NAMPT in adipose tissue contributes to the maintenance of whole body glucose homeostasis regulating remote tissues through its enzymatic activity and presumably also through its secretion. In this chapter, I will further discuss my findings of the function and regulation of eNAMPT in the context of the current knowledge. I will also discuss the questions that still remain or have newly arisen from my thesis work.

Do NAMPT and SIRT1 compose a new feedback loop?

The biological significance of the NAD^+ biosynthetic pathway in the regulation of the enzymatic activity of Sirtuins has been highlighted. In particular, NAMPT, the rate-limiting enzyme in the mammalian NAD^+ biosynthetic pathway, has recently been shown to have important roles related to sirtuin biology, metabolism, cancer, and the immune response. However, how NAMPT itself and NAMPT-mediated NAD^+ biosynthesis are regulated has not been comprehensively studied yet. Recently, it has been reported that NAMPT and NAD^+ levels display circadian oscillations that are regulated by the core clock machinery in mice ^{28,29}. This genetic mechanism involves the heterodimeric CLOCK/BMAL1 complex, a key structure of circadian transcription factors that control the circadian oscillation of NAMPT and its metabolite NAD^+ levels by inducing *Nampt* transcription. This loop is closed by feedback from the NAD^+ -dependent deacetylase SIRT1. SIRT1 is a component of the CLOCK/BMAL1 transcription complexes and acts

as a negative transcriptional regulator, thus comprising a novel circadian clock feedback loop involving NAMPT/NAD⁺ and SIRT1/CLOCK/BMAL1.

Nampt transcription also seems to be positively regulated by SIRT1 depending on the nutrient condition or cell type. Tao et al., have demonstrated that both *Nampt* gene expression and NAMPT-dependent NAD⁺ biosynthesis in hepatocytes are controlled by Forkhead box protein Os (FOXOs), whose activity is increased by SIRT1 through their deacetylation^{30,31}. Combinatorially with SIRT1, FOXOs protect against fatty liver disease by increasing *Nampt* transcription, and in turn NAD⁺ biosynthesis in hepatocytes³⁰. In human colorectal cancer cells, SIRT1 enhances *Nampt* transcription by stabilizing c-MYC, which binds to a region encompassing the noncanonical E-box in the *Nampt* promoter, resulting in suppression of senescence and apoptosis in cells, and presumably contributing to the development and maintenance of tumors in the context of deregulated c-MYC³².

In chapter 3, we proposed a new mechanism in which NAMPT is also regulated by SIRT1 on a post-translational level. We found that iNAMPT is acetylated in adipose tissue and that the acetylation level of iNAMPT is decreased during fasting, partly by SIRT1. By deacetylating lysine 53 on iNAMPT, SIRT1 increases both enzymatic activity and secretion of eNAMPT from adipocytes. NAMPT is undoubtedly an important regulator of Sirtuins, including NAD⁺-dependent SIRT1, because of its role in converting Nicotinamide into NMN, a crucial NAD⁺ precursor in mammals. Considering this, an increase in eNAMPT secretion by SIRT1 from adipose tissue could enhance NAD⁺ biosynthesis systemically, resulting in activation of Sirtuins in remote tissues, which generates a new positive feedback loop involving NAMPT/NAD⁺ and SIRT1.

How is eNAMPT secreted?

Soluble secretory proteins typically contain N-terminal signal peptides that direct them to the translocation apparatus of the endoplasmic reticulum (ER). Following vesicular transport from the ER via the Golgi to the cell surface, luminal proteins are released into the extracellular space by fusion of Golgi-derived secretory vesicles with the plasma membrane. This pathway of protein export from eukaryotic cells is known as the classical, or ER/Golgi-dependent secretory pathway. However, Nampt does not possess an appropriate cleavable signal sequence², and the mechanism that mediates the secretion of eNAMPT from adipocytes has remained poorly understood. We have previously found though that eNAMPT is not released simply because of cell lysis or cell death, but that it is actively secreted from adipocytes³. In this study, we established HIB-1B cell lines constitutively expressing FLAG-tagged Nampt or FLAG-tagged preprolactin (Ppl), which is secreted through the ER/Golgi secretory system. When these cells were treated with brefeldin A, an inhibitor of protein transport from the ER to the Golgi, which led to protein accumulating inside of the ER, the secretion of eNAMPT was not affected while Ppl secretion was completely inhibited³. It has been proposed that many other proteins including Fibroblast growth factor 1 (FGF-1), and FGF-2, Thioredoxin, Interleukin 1 α (Il1 α), and Il1 β , gelectin-1 and -3, and High Mobility Group Protein 1 (HMGB1), are exported by a mechanism that is independent of the classical secretory pathway, and many of them are known to directly accumulate at specific spots and form microvesicles in the cells⁴, indicating that NAMPT secretion might be secreted through an unconventional microvesicle-dependent protein secretion pathway. Tanaka et al. clearly ruled out this possibility through subcellular fractionation analysis showing

that NAMPT is exclusively localized in cytoplasm, but not in the membrane or in vesicles². Taken together, these data suggested that eNAMPT is secreted through a non-classical secretory pathway independent of the ER/Golgi or microvesicle secretory system.

In an effort to elucidate a more detailed secretion mechanism of eNAMPT, I proposed that acetylation status is an important factor to regulate eNAMPT secretion from adipocytes. Through mass-spectrometry analysis, I observed that the acetylation status of iNAMPT was different from that of eNAMPT. Five acetylation sites were found on iNAMPT in mammalian cells, while only 4 out of 5 acetylation sites that were found on iNAMPT were deacetylated on eNAMPT, implying that acetylation condition differentiates eNAMPT from iNAMPT. We also found that the levels of acetylation on iNAMPT in adipocytes were decreased in adipocytes of fasted mice compared to an ad lib condition, but plasma eNAMPT levels were increased in the same conditions. Interestingly, plasma eNAMPT levels were unchanged in fasted *Sirt1* KO mice, suggesting that SIRT1 is involved in deacetylating iNAMPT and increasing eNAMPT secretion into plasma in response to changes in nutritional conditions. Through *in vitro* biochemistry experiments using differentiated brown and white adipocytes and HEK293 cells, we also have confirmed that SIRT1 induces eNAMPT secretion by deacetylating lysine 53 on iNAMPT in adipocytes. Taken together, we conclude that acetylated iNAMPT stays in the cells while deacetylated iNAMPT, by SIRT1 during fasting, is predisposed to an undefined secretory mechanism and transmitted out of adipocytes.

Unfortunately, the detailed molecular mechanism of eNAMPT secretion upon acetylation is still in mystery. So far, there has been only one report showing that

acetylation status of the protein is involved in its secretion. Gardella et al., showed that activation of monocytes results in the accumulation of HMGB1, which also lacks a secretory signal peptide and does not traverse the ER-Golgi system, into cytoplasmic vesicles that display the features of secretory lysosomes⁵. In the following study, Bonaldi et al, demonstrated that monocytes and macrophages increase acetylation levels of HMGB1 extensively upon activation with lipopolysaccharide. This results in relocalization of HMGB1 to the cytosol to be secreted through a secretory lysosome, which is also used for other cytokines such as IL-1 β and IL-18⁶. Interestingly, acetylation promotes the secretion of HMGB1, whereas deacetylation promotes the secretion of eNAMPT. In addition, it is already well recognized that eNAMPT is secreted through non-classical secretory mechanism^{2,3}. Based on these findings, it would be possible that eNAMPT secretion, dependent upon its acetylation status, requires the presence of specific transporters or organelles. According to the NAMPT protein dimer structure, the lysine 53 acetyl groups that are deacetylated by SIRT1 are located close to the enzymatic core domain of the NAMPT dimer and project from NAMPT like antennas (Chapter 3, Figure 4b). Therefore, the acetylated lysine 53 residues could serve as docking sites for binding partners responsible for sequestering iNAMPT from secretory machinery, and in turn, iNAMPT deacetylated by SIRT1 could be released from a binding partner and translocated to a particular transporter or organelle upon appropriate stimulation. To clarify this hypothesis in the future, it would be interesting and also important to find iNAMPT binding partners by performing MS analysis of proteins that are co-immunoprecipitated with iNAMPT from adipocytes and analyze their roles in controlling eNAMPT secretion.

Is adipose tissue the only source of eNAMPT?

It has not been studied whether adipose tissue is the only source for eNAMPT in mammals, or if there are other organs or tissues that are capable of releasing significant amounts of eNAMPT into plasma. To answer this question, I successfully generated adipose tissue-specific *Nampt* knock out (ANKO) mice by breeding adiponectin-Cre mice to *Nampt*^{flox/flox} mice. While ANKO mice showed almost complete knock out of *Nampt* expression in several adipose tissue depots, eNAMPT levels in plasma were only reduced by 30-40%, depending on nutritional condition compared to WT, indicating that there are other sources that supply plasma eNAMPT other than adipose tissue. *Nampt* was originally identified from a human peripheral blood lymphocyte cDNA library as a presumptive cytokine ⁷. In addition, its expression widely found in the immune system is induced by inflammatory stimuli in cells engaging in innate immunity, specifically within neutrophils, monocytes, and macrophages, as well as in epithelial and endothelial cells ^{7,8}. Based on these findings, it has been proposed that these immune cells could be a major source of plasma eNAMPT. In an effort to prove this hypothesis, Friebe and his colleagues have evaluated which leukocyte subpopulations account for the high eNAMPT production ⁹. They have found that *Nampt* mRNA expression was higher in granulocytes and monocytes compared to lymphocytes, and that granulocytes released enzymatically active eNAMPT protein into cell culture supernatant fractions significantly more than other cell types ⁹. These findings indicate that granulocytes may be the major source for plasma eNAMPT. However, this seems not to be the case. In *Nampt* knock out mice specifically in myeloid cell lines such as monocytes, mature macrophages, and granulocytes, made by using *Nampt*^{flox/flox} mice and lysM-Cre mice, plasma eNAMPT did

not change compared to $\text{Nampt}^{\text{flox/flox}}$ control mice (M.J. Yoon, D. MacDuff, and H. W. Virgin, unpublished data). A healthy typical adult has a blood volume of approximately 4.7 to 5 liters, and the number of leukocytes is normally between 4×10^9 and 1.1×10^{10} which makes up approximately only 1% of blood in a healthy adult. Considering this, leukocytes could supply only a small fraction of plasma eNAMPT compared to other sources even though leukocytes secrete significant amount of eNAMPT.

Recent studies show that eNAMPT levels in serum are lower in patients with non-alcoholic steatohepatitis than in patients with simple steatosis or obese healthy control ¹⁰, and that plasma eNAMPT levels are dramatically decreased in patients with liver cirrhosis ¹¹. This raised the possibility that hepatocytes could play an important role in maintaining plasma levels of eNAMPT. In line with these two recent papers, Garten et al. demonstrated that eNAMPT was released from HepG2 cells as well as primary rat and human hepatocytes ¹². The separation of HepG2 supernatants according to molecular weight using size exclusion chromatography revealed that a greater amount of eNAMPT was present as the potentially enzymatically active dimer and a minor portion as the monomer, indicating that hepatocytes may release enzymatically active eNAMPT into the plasma as adipocytes do. However, while adipocytes actively regulate eNAMPT secretion depending on nutritional condition (Chapter 3), eNAMPT secretion from hepatocytes seems not to be influenced by glucose, but released in a more constitutive fashion. These results suggest that although both adipocytes and hepatocytes secrete enzymatically active eNAMPT into plasma, adipocytes possess a particular mechanism to sense environmental changes and control eNAMPT secretion,

Even though the mechanism regulating eNAMPT secretion in hepatocytes differs from that in adipocytes, hepatocytes are likely able to compensate for any lack of function of adipocytes to secrete eNAMPT. For example, in the fed condition, ANKO mice did not show abnormal protein expression of iNAMPT in any tissues, compared to control *Nampt*^{flox/flox} mice. However, in the fasted condition, when eNAMPT secretion from adipocytes was increased, ANKO mice exhibited increased iNAMPT expression in liver, but not in muscle, which does not contain any eNAMPT secretion capacity. Consistent with this, fasted liver NAD⁺ levels increased by 30% compared to WT. This implies that there might be crosstalk between the liver and adipose tissue to compensate for each other's eNAMPT secretion capabilities, especially when more eNAMPT is required. Our colleague, Dr. David Rudnick at Washington University in St. Louis, is generating Liver-specific *Nampt* knock out mice using *Nampt*^{flox/flox} and albumin-CRE mice. Using them would be of great interest to compare the effects of glucose metabolism on eNAMPT secreted from liver to that from adipose tissue, and to examine if any communication exists between the two tissues that controls physiological requirements of eNAMPT in response to nutritional conditions.

What is the function of eNAMPT, cytokine or NAD⁺-biosynthetic enzyme?

eNAMPT has been suggested to possess three different activities. First, eNampt was identified as a cytokine that enhances the maturation of B cell precursors in the presence of IL-7 and stem cell factor ⁷. Second, eNampt was described as a new visceral fat-derived hormone named visfatin, possessing insulin-mimetic effects by directly binding to insulin receptor ¹³. Finally, we identified eNampt to be the rate-limiting NAD⁺

biosynthetic enzyme in mammals^{14,15}. Subsequent studies have produced conflicting results regarding the physiological significance for the first two functions, and the lack of a putative receptor challenges the claim that eNAMPT is a cytokine or insulin-mimetic hormone. Despite the conflicts, we have clearly demonstrated that eNAMPT exhibits robust NAD⁺ biosynthesis enzymatic activity similar to iNAMPT, and that eNAMPT does not exert insulin-mimetic effects *in vitro* or *in vivo*^{3,15}.

Recently, one group has questioned the function of eNAMPT as a NAD⁺ biosynthetic enzyme, especially in plasma¹⁶. Hara et al., have claimed that eNAMPT cannot participate in NMN formation in plasma due to a lack of ATP, the activator of NAMPT, in extracellular spaces¹⁶. However, a significant amount of NMN was able to be produced when they added PRPP and ATP for the reaction in plasma. Based on this result, it is possible that extracellular concentrations of ATP might rise high enough to support NMN synthesis under specific conditions, such as in spleen where old red blood cells are destroyed and recycled and in the microenvironment of damaged cells. ATP is important as a source of adenosine, but also deleterious due to its intrinsic activity in the tumor microenvironment. For instance, ATP itself has pro-inflammatory activity that modulates inflammation by triggering IL-1 maturation and release¹⁷. In addition, ATP causes the release of metalloproteases (MMP9) and induction of indoleamine oxygenase in dendritic cells. Both of these activities may be very relevant for tumor progression as MMP9 release facilitates tumor invasion while indoleamine oxygenase has immunosuppressive activity¹⁸. Considering those aforementioned activities of ATP, removing extracellular ATP as soon as possible is necessary. eNAMPT synthesizing plasma NMN could simultaneously play an important role in inhibiting tumorigenesis by

removing extracellular ATP. It is critically important to investigate the *in vivo* kinetics of NMN biosynthesis and the environment required for NMN biosynthesis, particularly in the blood stream.

In female ANKO mice, not only WAT and BAT but also the hypothalamus exhibit significant reductions in NAD^+ levels, causing severe impairments of systemic insulin sensitivity and glucose-stimulated insulin secretion. There have been multiple pieces of evidence that show how the hypothalamus is a major integration site for information received from neuronal, hormonal, and nutritional cues. In turn, it regulates glucose homeostasis by altering hepatic and skeletal muscle glucose fluxes as well as influencing insulin secretion from pancreatic β cells¹⁹. Collectively, these data support the idea that the adipose tissue-specific deficiency of NAMPT causes a functional defect in the hypothalamus by lowering its levels of NAD^+ . We still cannot, however, rule out the possibility that the reduction of NAD^+ biosynthesis itself in WAT and BAT could be the primary factor influencing the development of insulin resistance in female ANKO mice. We could clearly answer this question if we could increase hypothalamic NAD^+ biosynthesis by either overexpressing NAMPT or injecting NMN directly. If impaired glucose tolerance or glucose stimulated-insulin secretion in female ANKO mice is improved, we could claim that low hypothalamic NAD^+ is causative for these metabolic phenotype in female ANKO.

Do gender differences affect energy metabolism via NAMPT?

Gender exerts profound effects on metabolism and endocrine function of the adipose organ. Women have a higher percentage of body fat than men and tend to store

adipose tissue preferentially in the gluteal-femoral region, as opposed to the male pattern of obesity concentrated in the visceral and abdominal depots. Adipocyte metabolism in these depots also differs between genders²⁰⁻²². Interestingly, these differences disappear with menopause and may be the cause of weight gain in the abdominal region after menopause²³, suggesting that female sex hormones play a significant role in these gender depot differences, leading to differences in adipocyte metabolism. In addition, endocrine function of the adipose tissue also exhibits sexual dimorphism. For instance, serum levels of adiponectin, an adipocyte-derived hormone, are similar in newborn mice, but after sexual maturation, circulation levels of adiponectin are twice as high in female mice compared with male mice²⁴. Leptin also exhibits a similar sexual dimorphism²⁵. These studies imply that gender differences of metabolism and endocrine function of the adipose organ could result in the differences in whole body energy metabolism between genders.

Consistent to this notion, we also observed gender differences in metabolism in several lines of mouse models. An increased dosage of SIRT1 in pancreatic β cells enhanced glucose-stimulated insulin secretion and improved glucose tolerance in both male and female beta cell-specific Sirt1-overexpressing (BESTO) transgenic mice at 3 and 8 months of age²⁶. As this same cohort of BESTO mice reached 18-24 months of age, glucose-stimulated insulin secretion by Sirt1 through repression of Ucp2 was blunted in both male and female BESTO mice. However, NMN administration restored enhanced glucose-stimulated insulin secretion and improved glucose tolerance only in the aged BESTO females²⁷. Similarly, *Nampt*^{+/-} females, but not males, displayed decreased plasma levels of eNAMPT as well as impaired glucose tolerance and significantly

reduced glucose-stimulated insulin secretion, and these defects were completely restored by administration of NMN ³. ANKO mice also showed similar gender differences as *Nampt*^{+/-} mice did. Female ANKO, but not male ANKO, exhibited lower levels of plasma eNAMPT compared to *Nampt*^{flox/flox} control mice. They also showed severely impaired glucose tolerance and impaired glucose-stimulated insulin secretion accompanied with hyperinsulinemia, even though male ANKO also had mild hyperinsulinemia. Since both *Nampt*^{+/-} and ANKO females showed metabolic phenotypes different than males, I speculated that reduction in plasma eNAMPT could result in polycystic ovary syndrome (PCOS). To prove this hypothesis, I compared histology of ovary structure between 3-month old *Nampt*^{flox/flox} mice and age-matched female ANKO mice that show more severe impaired glucose tolerance with hyperinsulinemia similar to PCOS patients than *Nampt*^{+/-} mice. I did not observe any obvious differences between them, unfortunately, although ANKO females tended to have higher plasma estrogen levels compared to *Nampt*^{flox/flox} mice (data not shown). Even though administration of NMN successfully ameliorated the glucose tolerance and glucose-stimulated insulin secretion completely in *Nampt*^{+/-} and partially in ANKO mice, we still do not know if a reduction of eNAMPT protein itself is necessary for developing these abnormal metabolic phenotypes. It would be of great interest to investigate which tissues cause impaired glucose metabolism in ANKO mice and to see whether increasing eNAMPT in plasma by injecting NAMPT protein improves impaired glucose metabolism in ANKO mice.

Final comments

In my studies of the regulation and function of NAMPT in mammals, I attempted to shed light on the importance and the mechanism of NAMPT-mediated NAD⁺ biology underpinning type 2 diabetes. I have found that NAMPT and NAMPT-mediated NAD⁺ biosynthesis is dramatically reduced in metabolically active tissues of a diet- and age-induced type 2 diabetes mice model, resulting in a disturbance of glucose homeostasis. I have also demonstrated that eNAMPT secretion from adipocytes is regulated by SIRT1 through its deacetylase activity in response to nutrient condition. I have also demonstrated that *Nampt* knockout specifically in adipose tissues causes impaired glucose tolerance and functional defects in β cells secreting insulin, which is also observed in diet- and age- induced type 2 diabetes mice. Interestingly, because the phenotype of both diet and age-induced type 2 diabetes mice models, as well as female ANKO mice, can be corrected by injecting NMN, it is highly possible that NMN could be used as therapeutic agent to improved type 2 diabetes.

Although having biochemical evidence of the existence of this NAD⁺ biosynthetic enzyme decades ago, its biological significance is only starting to be understood. So far, many groups, including us, have unraveled many secrets of NAMPT including its biochemistry, structure, and role in physiology, but there are still many aspects that remain a mystery. This thesis project has allowed me to understand the detailed mechanism of modulating NAMPT expression as well as eNAMPT secretion from adipocytes that affect metabolic homeostasis. This thesis project has also led me to pay attention to new fields such as adipose tissue inflammation and sex differences and their affects upon metabolic phenotypes. I believe that understanding these questions will also contribute to finding more fascinating discoveries in the field of metabolism.

REFERENCES

1. Olefsky, J.M. & Glass, C.K. Macrophages, inflammation, and insulin resistance. *Annu Rev Physiol* **72**, 219-246 (2010).
2. Tanaka, M., *et al.* Visfatin is released from 3T3-L1 adipocytes via a non-classical pathway. *Biochem Biophys Res Commun* **359**, 194-201 (2007).
3. Revollo, J.R., *et al.* Nampt/PBEF/Visfatin regulates insulin secretion in beta cells as a systemic NAD biosynthetic enzyme. *Cell Metab* **6**, 363-375 (2007).
4. Nickel, W. The mystery of nonclassical protein secretion. A current view on cargo proteins and potential export routes. *Eur J Biochem* **270**, 2109-2119 (2003).
5. Gardella, S., *et al.* The nuclear protein HMGB1 is secreted by monocytes via a non-classical, vesicle-mediated secretory pathway. *EMBO Rep* **3**, 995-1001 (2002).
6. Bonaldi, T., *et al.* Monocytic cells hyperacetylate chromatin protein HMGB1 to redirect it towards secretion. *EMBO J* **22**, 5551-5560 (2003).
7. Samal, B., *et al.* Cloning and characterization of the cDNA encoding a novel human pre-B-cell colony-enhancing factor. *Mol Cell Biol* **14**, 1431-1437 (1994).
8. Luk, T., Malam, Z. & Marshall, J.C. Pre-B cell colony-enhancing factor (PBEF)/visfatin: a novel mediator of innate immunity. *J Leukoc Biol* **83**, 804-816 (2008).
9. Friebe, D., *et al.* Leucocytes are a major source of circulating nicotinamide phosphoribosyltransferase (NAMPT)/pre-B cell colony (PBEF)/visfatin linking obesity and inflammation in humans. *Diabetologia* **54**, 1200-1211 (2011).
10. Jarrar, M.H., *et al.* Adipokines and cytokines in non-alcoholic fatty liver disease. *Aliment Pharmacol Ther* **27**, 412-421 (2008).

11. de Boer, J.F., Bahr, M.J., Boker, K.H., Manns, M.P. & Tietge, U.J. Plasma levels of PBEF/Nampt/visfatin are decreased in patients with liver cirrhosis. *Am J Physiol Gastrointest Liver Physiol* **296**, G196-201 (2009).
12. Garten, A., *et al.* Nicotinamide phosphoribosyltransferase (NAMPT/PBEF/visfatin) is constitutively released from human hepatocytes. *Biochem Biophys Res Commun* **391**, 376-381 (2010).
13. Fukuhara, A., *et al.* Visfatin: a protein secreted by visceral fat that mimics the effects of insulin. *Science* **307**, 426-430 (2005).
14. Martin, P.R., Shea, R.J. & Mulks, M.H. Identification of a plasmid-encoded gene from *Haemophilus ducreyi* which confers NAD independence. *J Bacteriol* **183**, 1168-1174 (2001).
15. Revollo, J.R., Grimm, A.A. & Imai, S. The NAD biosynthesis pathway mediated by nicotinamide phosphoribosyltransferase regulates Sir2 activity in mammalian cells. *J Biol Chem* **279**, 50754-50763 (2004).
16. Hara, N., Yamada, K., Shibata, T., Osago, H. & Tsuchiya, M. Nicotinamide phosphoribosyltransferase/visfatin does not catalyze nicotinamide mononucleotide formation in blood plasma. *PLoS One* **6**, e22781 (2011).
17. Gu, B.J. & Wiley, J.S. Rapid ATP-induced release of matrix metalloproteinase 9 is mediated by the P2X7 receptor. *Blood* **107**, 4946-4953 (2006).
18. Marteau, F., Gonzalez, N.S., Communi, D., Goldman, M. & Boeynaems, J.M. Thrombospondin-1 and indoleamine 2,3-dioxygenase are major targets of extracellular ATP in human dendritic cells. *Blood* **106**, 3860-3866 (2005).

19. Sandoval, D., Cota, D. & Seeley, R.J. The integrative role of CNS fuel-sensing mechanisms in energy balance and glucose regulation. *Annu Rev Physiol* **70**, 513-535 (2008).
20. Blaak, E. Gender differences in fat metabolism. *Curr Opin Clin Nutr Metab Care* **4**, 499-502 (2001).
21. Fried, S.K., Leibel, R.L., Edens, N.K. & Kral, J.G. Lipolysis in intraabdominal adipose tissues of obese women and men. *Obes Res* **1**, 443-448 (1993).
22. Edens, N.K., Fried, S.K., Kral, J.G., Hirsch, J. & Leibel, R.L. In vitro lipid synthesis in human adipose tissue from three abdominal sites. *Am J Physiol* **265**, E374-379 (1993).
23. Rebuffe-Scrive, M., Andersson, B., Olbe, L. & Bjorntorp, P. Metabolism of adipose tissue in intraabdominal depots of nonobese men and women. *Metabolism* **38**, 453-458 (1989).
24. Combs, T.P., *et al.* Sexual differentiation, pregnancy, calorie restriction, and aging affect the adipocyte-specific secretory protein adiponectin. *Diabetes* **52**, 268-276 (2003).
25. Saad, M.F., *et al.* Sexual dimorphism in plasma leptin concentration. *J Clin Endocrinol Metab* **82**, 579-584 (1997).
26. Moynihan, K.A., *et al.* Increased dosage of mammalian Sir2 in pancreatic beta cells enhances glucose-stimulated insulin secretion in mice. *Cell Metab* **2**, 105-117 (2005).
27. Ramsey, K.M., Mills, K.F., Satoh, A. & Imai, S. Age-associated loss of Sirt1-mediated enhancement of glucose-stimulated insulin secretion in beta cell-specific Sirt1-overexpressing (BESTO) mice. *Aging Cell* **7**, 78-88 (2008).

28. Nakahata, Y., Sahar, S., Astarita, G., Kaluzova, M. & Sassone-Corsi, P. Circadian control of the NAD⁺ salvage pathway by CLOCK-SIRT1. *Science* **324**, 654-657 (2009).
29. Ramsey, K.M., *et al.* Circadian clock feedback cycle through NAMPT-mediated NAD⁺ biosynthesis. *Science* **324**, 651-654 (2009).
30. Tao, R., *et al.* Hepatic FoxOs regulate lipid metabolism via modulation of expression of the nicotinamide phosphoribosyltransferase gene. *J Biol Chem* **286**, 14681-14690 (2011).
31. Daitoku, H., *et al.* Silent information regulator 2 potentiates Foxo1-mediated transcription through its deacetylase activity. *Proc Natl Acad Sci U S A* **101**, 10042-10047 (2004).
32. Menssen, A., *et al.* The c-MYC oncoprotein, the NAMPT enzyme, the SIRT1-inhibitor DBC1, and the SIRT1 deacetylase form a positive feedback loop. *Proc Natl Acad Sci U S A* **109**, E187-196 (2012).